gp130 Cytokines Stimulate Tyrosine Hydroxylase Proteasomal Degradation and Activity in Sympathetic Neurons

by

Xiao Shi

A DISSERTATION

Presented to the Department of Physiology & Pharmacology
and the Oregon Health & Science University
School of Medicine
in partial fulfillment of
the requirements for the degree of

Doctor of Philosophy

December 2012

School of Medicine

Oregon Health & Science University

CERTIFICATE OF APPROVAL

This is to certify that the Ph.D. dissertation of

Xiao Shi

has been approved

_____
Mentor/Advisor: Beth A. Habecker, Ph.D.

_____
Committee Chair/Member: Dennis Koop, Ph.D.

_____
Member: Philip Stork, M.D.

_____
Member: William Woodward, Ph.D.

_____
Member: Aaron Janowsky, Ph.D.

Table of Contents

LIST OF FIGURES

Chapter 1: Introduction

Chapter 2: Manuscript 1

Chapter 3: Manuscript 2

Chapter 4: Discussion and Future Directions

Chapter 5: Methods

Chapter 6: Appendices

LIST OF ABBREVIATIONS

AAADC	aromatic amino acid decarboxylase
AP-1	activating protein 1
BH_4	tetrahydrobiopterin
CAMPK II	calcium/calmodulin dependent protein kinase II
Cdk5	cyclin-dependent kinase 5
CIS	cytokine-induced SH2 protein
CLC	cardiotrophin-like cytokines
CNTF	ciliary neurotrophic factor
ChAT	choline acetyl transferase
CRE	cAMP response element
CREB	cAMP response element binding protein
CT-1	cardiotrophin-1
DA	dopamine
DBH	dopamine-β-hydroxylase
DUBs	deubiquitinating enzymes

E1	ubiquitin activating enzyme
E2	ubiquitin conjugating enzyme
E3	ubiquitin ligase
ERK	extracellular signal regulated kinase
gp130	glycoprotein130
KIR	kinase inhibitory region
IL-6	interleukin-6
IL-11	interleukin-11
JAK	Janus kinase
L-DOPA	3, 4-dihydroxyphenylalanine
LIF	Leukemia inhibitory factor
LIFR	Leukemia inhibitory factor receptor
MAKPAPK 1 and 2	MAKP-activated protein kinase 1 and 2
MEK	mitogen-activated protein kinase kinase
MSK 1	mitogen and stress-activated protein kinase 1
NE	norepinephrine

NET	NE transporter
NGF	nerve growth factor
OSM	oncostatin-M
OSMR	oncostatin-M receptor
PD	Parkinson’s disease
PI3K	phosphoinositide-3-kinase
PKA	cyclic AMP-dependent protein kinase
PKC	protein kinase C
PKG	protein kinase G
PNMT	phenylethanolamine- N – methyl transferase
PRAK	p38-regulated/activated kinase
Rpt	ATPase regulatory particles triple
Rpn	Non-ATPase regulatory particles
SH2	Src homology 2
SHP-2	Src homology-2 domain-containing protein tyrosine phosphatase

SOCS	suppressor of cytokine signaling
STAT	signal transducers and activators of transcription
TH	tyrosine hydroxylase
TNF	tumor necrosis factor
VAChT	vesicular acetylcholine transporter
VIP	vasoactive intestinal polypeptide
VMAT	vesicular monoamine transporter

Acknowledgement

It is a pleasure to thank the many people who made this thesis possible.

I would like to thank the members of my Thesis Advisory Committee/Exam Committee for their support and guidance over years: Dr. Dennis Koop, Dr. Philip Stork, and Dr. William Woodward. I really appreciate you sharing your experiences with me and providing valuable advice. I would also like to thank Dr. Aaron Janowsky for his willingness to serve on my Thesis Exam Committee.

Especially, I would like to thank Dr. Beth Habecker for her mentorship. I truly thank you for your training and guidance over years. Thank you for training me how design experiments and improve my communication skills. I would also like to thank her for her patience in reading countless poorly written drafts. Beth, you are not only a great mentor, but also a great friend.

I would also like to thank many students and friends. First, I would like to thank the members of the Habecker laboratory. Thank you to Diana Parrish, Ryan Gardner, Michael Pellegrino and former graduate student Christina Lorentz. Thank you all for your support and entertainment. All of you help me learn new things every day. I would like to extend special thanks to Diana Parrish. Thank you for spending the time to read my thesis and provide feedback. To Christina Lorentz: pigs do have wings. I would also like to thank the graduate students in department of Physiology and Pharmacology. Thank you for your support. I would like to thank Lisa Bleyle and Damani Bryant for technical help.

Lastly, I would like to thank my family. To Zheng: Thank you for your endless support and understanding. I love you. To Erin and Ariel: Thank you for giving mommy hugs when I get home. You make me brave and keep me going on. Finally, I would like to thank my parents. You always love me no matter what happens. I dedicate this thesis to them.

Abstract

Tyrosine hydroxylase is the rate-limiting enzyme in norepinephrine synthesis, and its expression and activity are regulated by growth factor, ischemia, nerve activity and inflammation. For example, inflammatory cytokines acting through the gp130 receptor cause the local depletion of TH in cardiac sympathetic nerves after myocardial infarction, without lowering TH gene expression. However, the mechanism of this cytokine-induced TH protein loss remains unknown.

In the first part of my thesis, I investigated whether cytokines increased TH degradation. Experiments in Chapter 2 showed for the first time that inflammatory cytokines can stimulate proteasomal degradation of TH in catecholaminergic neurons. I showed that gp130 cytokines decreased TH half-life in sympathetic neurons and neuroblastoma cells, suggesting an increase in TH protein turnover. I found that CNTF induced TH ubiquitination and stimulated TH proteasomal degradation. In addition, I also identified that ERK1/2 was required for CNTF-induced TH ubiquitination and the associated decrease in TH half-life.

Previous *in vivo* studies indicated that depleting the gp130 receptor in neurons prevented CNTF-induced loss of TH, but not the content of NE. This suggested that cytokines may affect TH enzyme activity. To examine this issue, I assayed TH activity in neurons in the presence or absence of cytokines. I

showed that CNTF increased the rate of L-DOPA production, suggesting an increase in TH specific activity.

Overall, cytokines influence not only the level of TH protein, but also the activity of the enzyme. These studies have important implications for local regulation of neurotransmission at the site of inflammation and contribute to understanding the dysfunction and degeneration of catecholaminergic neurons in neurologic diseases which are affected by inflammatory cytokines.

Chapter 1 Introduction

1.1 Sympathetic nervous system

The autonomic nervous system maintains homeostasis in living organisms by regulating blood pressure, respiration and metabolism. There are two major components of the autonomic nervous system: the sympathetic and the parasympathetic nervous system. These two components often have opposite effects in which one activates a physiological action and the other inhibits it. The sympathetic nervous system mediates the “fight-or-flight” response and is a major neuronal regulator of cardiovascular function. Activation of the sympathetic system results in an increase in heart rate and the force of contraction of the heart by releasing of norepinephrine (NE).

There are two kinds of neurons involved in sympathetic transmission: pre- and post- ganglionic neurons. Preganglionic neurons originate from the thoracolumbar region of the spinal cord. These short preganglionic neurons travel to paravertebral sympathetic ganglia and form synapses with postganglionic neurons. Preganglionic neurons release acetylcholine which activates nicotinic acetylcholine receptors on the postganglionic neurons. The long postganglionic neurons extend axons to peripheral target tissues throughout the body. Postganglionic sympathetic neurons arise from the thoracic and lumbar neural crest cells, which migrate ventrally from the dorsal neural tube to form

sympathetic ganglia near the dorsal aorta. The development of sympathetic neurons is initiated by bone morphogenetic protein (BMP)-2 and BMP-7 derived from the dorsal aorta, which stimulate expression of pan-neuronal markers and the NE synthetic enzymes, tyrosine hydroxylase (TH) and dopamine beta hydroxylase (DBH)(Sarkar and Howard 2006). Eventually, postganglionic sympathetic neurons extend axons to their peripheral target organs, and in response to simulation they release norepinephrine which activates adrenergic receptors on peripheral targets.

1.2 Plasticity of sympathetic nervous system

Sympathetic neurons are plastic in response to stimuli from the environment. Cultured sympathetic neurons decrease noradrenergic properties and acquire cholinergic features when they are grown in presence of non-neuronal cells or in conditioned medium from those cells (Furshpan *et al.* 1976;Patterson and Chun 1977). Leukemia inhibitory factor (LIF) was the first factor found to induce cholinergic differentiation in cultured sympathetic neurons (Yamamori *et al.* 1989). LIF is a member of the interleukin-6 (IL-6) type cytokine family which also includes IL-11, ciliary neurotrophic factor (CNTF), cardiotrophin-1 (CT-1), cardiotrophin-like cytokines (CLC) and oncostatin-M (OSM) (Heinrich *et al.* 2003). CNTF, LIF and CT-1 induce vasoactive intestinal peptide (VIP) and choline acetyltransferase (ChAT) expression in cultured

sympathetic neurons, while suppressing noradrenergic transmission (Li *et al.* 2003;Patterson and Chun 1977;Saadat *et al.* 1989). These studies in cultured neurons led to identification of cytokines as cholinergic differentiation factors.

One well-studied example of sympathetic plasticity *in vivo* is the neurotransmitter switch that occurs in during development of the sympathetic innervation of sweat glands. Most sympathetic neurons are noradrenergic. However, a subset of sympathetic neurons, including the neurons innervating the sweat gland, are cholinergic. When sympathetic axons first innervate the sweat gland during the development, they contain catecholamines and express TH and DBH (Landis 1983). Over several weeks catecholamines disappear, and noradrenergic properties decrease as the gland innervation matures. Instead, neurons develop cholinergic features such as choline acetyltransferase (ChAT), vesicular acetylcholine transporter (VAChT) and vasoactive intestinal peptide (VIP) (Landis and Keefe 1983;Schotzinger and Landis 1988).This results in functional cholinergic innervation of the sweat glands. The switch of transmitter phenotype is induced by interaction with the sweat glands, and studies using transgenic mice revealed that cytokines released from sweat gland cells were responsible for this transmitter switch (Stanke *et al.* 2006).

Similar changes also occur in adult neurons after injury (Rao *et al.* 1993;Sun *et al.* 1996). One example is the decreased expression of TH mRNA and production of NE after axotomy of sympathetic neurons in the superior cervical ganglion (Zigmond *et al.* 1996). Suppression of noradrenergic properties

in sympathetic neurons after axotomy is caused by inflammatory cytokines signaling through the glycoprotein130 (gp130) receptor (Habecker *et al.* 2009). Another example is heart failure, which is characterized by elevated inflammatory cytokines in the heart, including LIF, CT-1 and IL-6(Blum and Miller 1998). These inflammatory cytokines released from failing myocardium suppress noradrenergic transmission and induce cholinergic function in cardiac sympathetic neurons (Kanazawa *et al.* 2010).

1.3 gp130 Cytokines and signaling pathways

IL-6 type cytokines are involved in inflammatory and immunologic responses and play roles in haematopoiesis, liver and neuronal regeneration, embryonic development and cardiovascular physiology. The cytokines IL-6, IL-11, LIF, CNTF, OSM, CT-1, and CLC, which do not have similar amino acid sequences, all bind to plasma membrane receptor complexes which contain the common receptor subunit glycoprotein 130 (gp130) (Heinrich *et al.* 2003). Each receptor complex includes two signal transducing receptors, either a homodimer of gp130 or a heterodimer of gp130 with either the LIF receptor (LIFR) or the OSM receptor (OSMR) (Fig. 1.1) (Heinrich *et al.* 2003). IL-6, IL-11 and CNTF also require specific non-signaling α- receptors (IL-6 α- receptor, IL-11 α- receptor and CNTF α- receptor) for signal transduction. IL-6, IL-11 and CNTF first bind to their respective α- receptor subunit, and then the complex of cytokine and

α- receptor binds to the signaling receptors. IL-6 and IL-11 are the only cytokines of this family signaling through the gp130 homodimer. LIF, CNTF, CT-1, and CLC all signal through the LIF receptor and gp130 heterodimer, while OSM induces the heterodimerization of the OSM receptor and gp130.

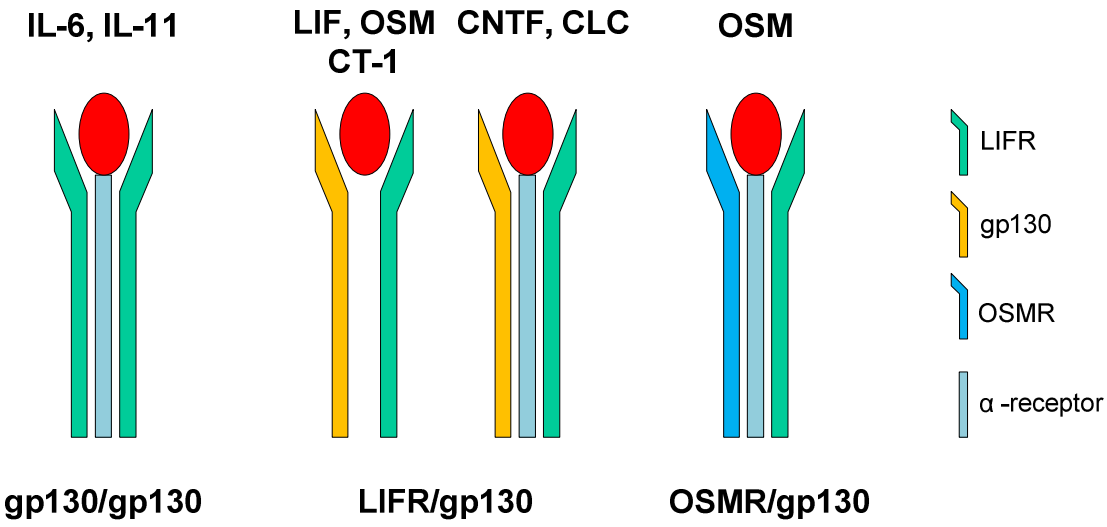

Figure 1.1 Receptor complexes of IL-6-type cytokines.

IL-6-type cytokines signal through different combinations of receptor subunits. IL-6 and IL-11 signal through the gp130 homodimer and a non-signaling α- receptor. OSM uses the OSM receptor (OSMR) and a gp130 heterodimer which also requires non-signaling α- receptors. The rest of the members signal through the LIF receptor (LIFR) and gp130 heterodimer with or without non-signaling α-receptors.

IL-6 type cytokines induce the activation of Janus kinase (Jak) family tyrosine kinases to stimulate signal transduction. Jaks are intracellular tyrosine kinases and are constitutively associated with the cytoplasmic regions of the receptor subunits. There are four members of the Jak family expressed in mammalian cells: Jak1, Jak2, Jak3, and Tyk2 (Heinrich *et al.* 1998). Jak3 is mainly expressed in cells with haematopoietic origins, whereas the rest are widely expressed (Heinrich *et al.* 1998). Jaks bind to receptors at the conserved membrane-proximal box1 region, a proline-rich motif, and the box2 region which is a cluster of hydrophobic amino acid residues followed by positively charged amino acid (Heinrich *et al.* 2003). Activated Jaks phosphorylate several conserved tyrosine residues on gp130, LIFR and OSMR. Those phosphorylated tyrosine residues provide the docking sites for the downstream signaling molecules.

Cytokines stimulate three major signaling pathways: Jak/STAT (signal transducers and activators of transcription), MEK (mitogen-activated protein kinase kinase) /ERK (extracellular signal regulated kinase), and PI3K (phosphoinositide-3-kinase) /Akt (Fig. 1.2) (Dziennis and Habecker 2003;Heinrich *et al.* 2003). Upon cytokine binding, Jak phosphorylates tyrosine residues on both gp130 and LIFR. Phosphorylation of Y765/812/904/914 on mouse gp130 and Y976/996/1023 of mouse LIFR provides docking sites for STAT proteins (Fischer and Hilfiker-Kleiner 2008). The pattern of phosphorylation is similar in the human receptors, with phosphorylation of Y767/814/905/915 of human gp130

and Y981/1001/1028 of human LIFR providing STAT docking sites (Ohtani *et al.* 2000). All IL-6 type cytokines potently activate STAT3 and to a minor extent STAT1. STAT1 and STAT3 bind to the activated receptor through their SH2 (Src homology 2) domains. Subsequent to receptor binding, STAT proteins are phosphorylated. The phosphorylated STAT proteins form either homo- or heterodimers and translocate to the nucleus where they induce transcription of target genes. Phosphorylation of the proximal tyrosine residue at Y757 on the cytoplasmic domain of mouse gp130 or Y969 on mouse LIFR is important for recruiting Src homology-2 domain-containing protein tyrosine phosphatase (SHP-2) which is required for activation of the MEK/ERK and PI3K/Akt signaling pathways. On human cytokine receptors, Y759 of gp130 or Y974 on LIFR are responsible for SHP-2 binding and activation of downstream signaling. Phosphorylated SHP-2 forms a complex with the growth factor receptor protein-2 associated binding protein1/2 and the p85 subunit of PI3K. This leads to activation of the Akt pathway.

Cytokines stimulate SOCS (suppressor of cytokine signaling) expression to inhibit cytokine signaling. The SOCS family has eight members: SOCS1-7 and cytokine-induced SH2 protein (CIS). SOCS1 and SOCS3 inhibit gp130 signaling. SOCS can inhibit cytokine signaling through several different mechanisms. First, SOCS binds to cytokine receptors to prevent STAT binding and activation (Palmer and Restifo 2009). Second, in addition to blocking STAT recruitment to the receptor, SOCS also can target cytokine receptors and Jaks for proteasomal

degradation. SOCS family members share an SH2 domain and a C-terminal SOCS box which can interact with ubiquitinating machinery enzymes and E2 ubiquitin transferase (Bullock *et al.* 2006) to target proteins for proteasomal degradation (Fig. 1.3). Finally, in addition to the functional domains shared across the SOCS family, SOCS1 and SOCS3 have a kinase inhibitory region (KIR). This KIR domain can bind to Jaks and inhibit Jak kinase activity directly (Kamura *et al.* 1998;Zhang *et al.* 2001).

Studies in non-neuronal cells have identified SOCS-dependent cross-talk between STAT3 and ERK1/2 signaling following activation of gp130 (Fischer and Hilfiker-Kleiner 2008;Lehmann *et al.* 2003). Tyrosine residue 757 within gp130 binds not only the SHP-2, which leads to activation of ERK1/2 and Akt, but also serves as a docking site for SOCS3 (Fig. 1.4). Cytokine activation of STAT3 stimulates SOCS3 expression in most cell types, and SOCS3 in turn blunts activation of ERK1/2 by competing with SHP2 for binding to tyrosine 757. This suggests that SHP2 is important for early signal modulation.

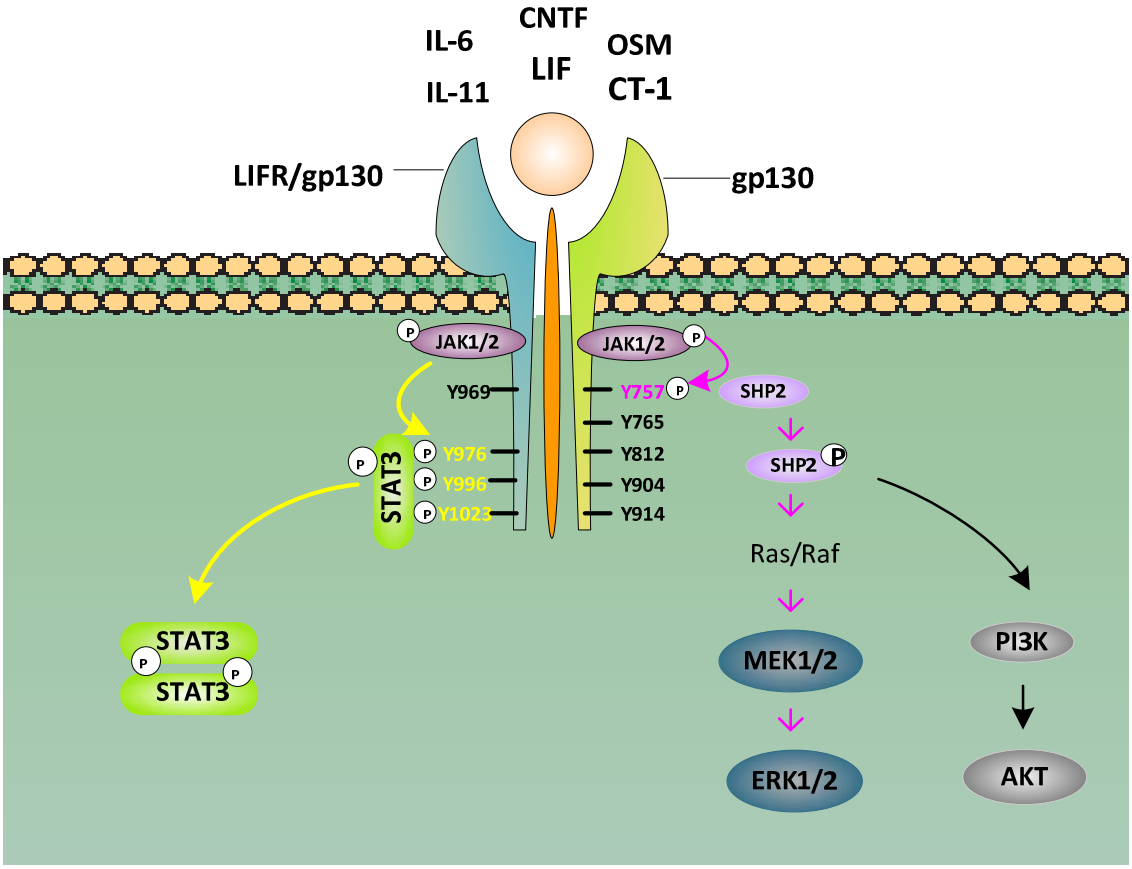

Figure 1.2 Signaling pathways of gp130 cytokines

The schematic diagram shows gp130 cytokines are signaling through a gp130 homodimer or LIFR/gp130 heterodimer. Binding of cytokines to their receptor leads to activation of associated JAKs. Activated JAKs phosphorylate the cytoplasmic domain of gp130 and LIFR which provide docking sites for down-stream signaling molecules. Subsequently, three major signaling pathways: JAK/STAT, MEK/ERK, and PI3K/Akt are triggered.

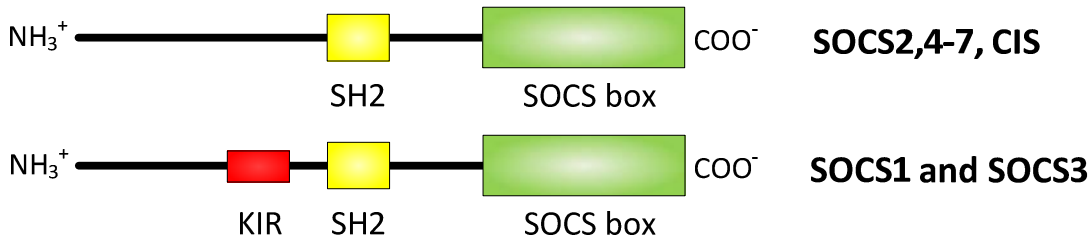

Figure 1.3 Structure of SOCS family.

The members of the SOCS family share a central SH2 domain (yellow) and a C-terminal SOCS box (green). In addition, SOCS1 and SOCS3 have a kinase inhibitory region (KIR, red) which serves as a pseudo-substrate for JAKs and block JAKs activity.

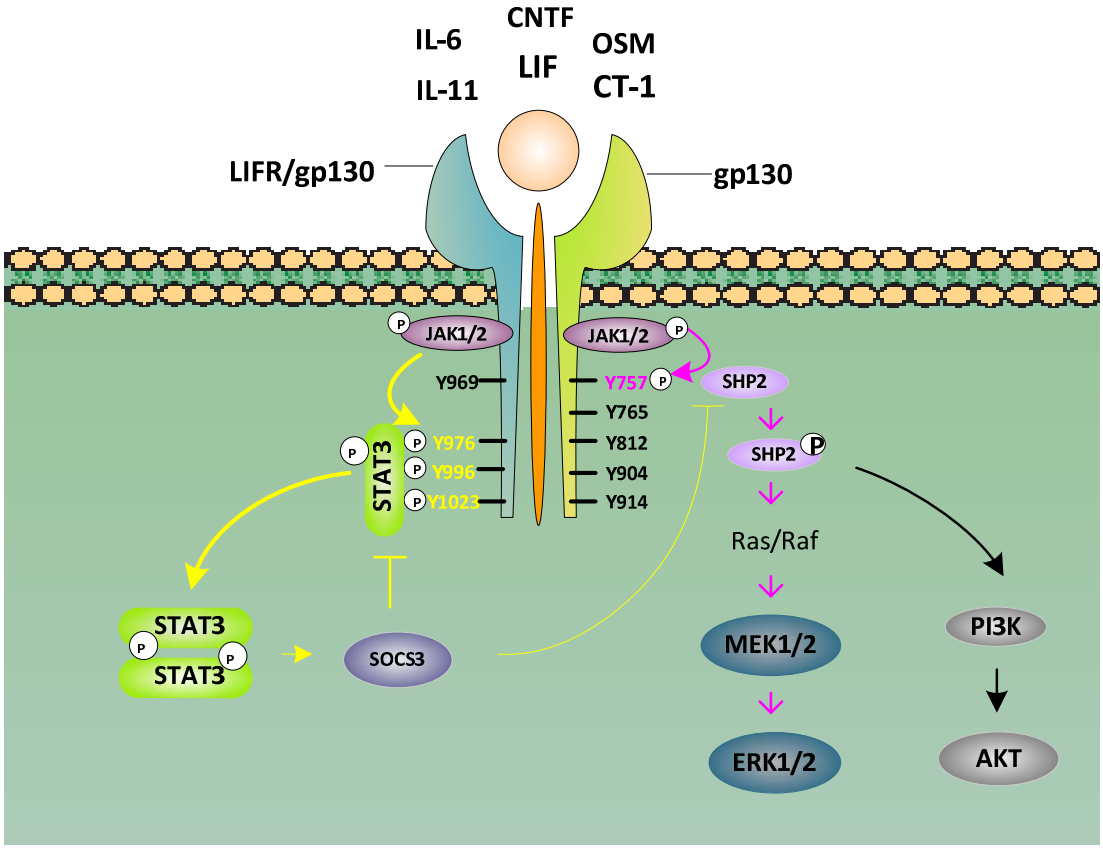

Figure 1.4 SOCS3 and SHP2 regulate gp130 signaling.

Phosphorylation at Y757 on the cytoplasmic domain of mouse gp130 recruits SHP-2 which is required for activation of the MEK/ERK and PI3K/Akt signaling pathways. Cytokine-induced SOCS3 competes with SHP2 binding at Y757 which leads to attenuation of the downstream signaling.

1.4 Catecholamine synthesis

The biogenic amines containing a catechol group (3, 4 – dihydroxyphenyl) are referred to as catecholamines. They include dopamine, norepinephrine and epinephrine. These catecholamines function primarily as neurotransmitters, but epinephrine is released from the adrenal medulla and serves as a hormone. Dopamine is one of the major neurotransmitters present in the central nervous system while NE is the major neurotransmitter of sympathetic neurons, and epinephrine is released from adrenal chromaffin cells.

Catecholamines are synthesized from the essential amino acid L-tyrosine. TH, the rate-limiting enzyme in catecholamine biosynthesis (Fig. 1.5), catalyzes the formation of L-DOPA (3, 4-dihydroxyphenylalanine) from L-tyrosine. L-DOPA is decarboxylated to form dopamine (DA) by L-aromatic amino acid decarboxylase. DA is then taken up into secretory vesicles by the vesicular monoamine transporter (VMAT) where it is converted to norepinephrine (NE) by dopamine-β-hydroxylase (DBH). NE is released at nerve terminals and the action of NE is terminated by uptake through the NE transporter (NET). NE taken back into nerve terminals is repacked into vesicles or metabolized by monoamine oxidase.

1.5 TH- rate limiting enzyme in NE synthesis

TH (tyrosine-3-monooxygenase) is the rate limiting enzyme in catecholamine biosynthesis. TH belongs to an aromatic amino acid hydroxylase genetic superfamily which also includes tryptophan hydroxylase and phenylalanine hydroxylase. All of these enzymes catalyze the conversion of aromatic amino acids by utilizing molecular oxygen, ferrous iron (Fe^{2+}) and tetrahydrobiopterin (BH_4) (Kumer and Vrana 1996). Each TH monomer consists of an N-terminal regulatory domain and a C-terminal catalytic domain. TH monomers form a tetramer, with a relative molecular weight of 240 KD, through an interaction at the C-terminal catalytic domain (Kumer and Vrana 1996). TH is found in a wide range of tissues, including the brain, gut, retina, the sympathetic nervous system and the adrenal medulla. TH is encoded by a single gene, and most species express only a single isoform of TH (Haycock 2002). In humans, alternative splicing of a single gene produces four different isoforms (hTH1-4) which differ in amino acid sequence of the N-terminus (Kumer and Vrana 1996). hTH1 is similar to TH found in other species while other isoforms (hTH2-4) all contain an insertion between exon1 and exon2 of the TH gene resulting in additional amino acids of those isoforms (Nagatsu and Ichinose 1991). All four isoforms of TH are expressed in the human brain and adrenal medulla but hTH1 and 2 are the major forms in these neuronal tissues.

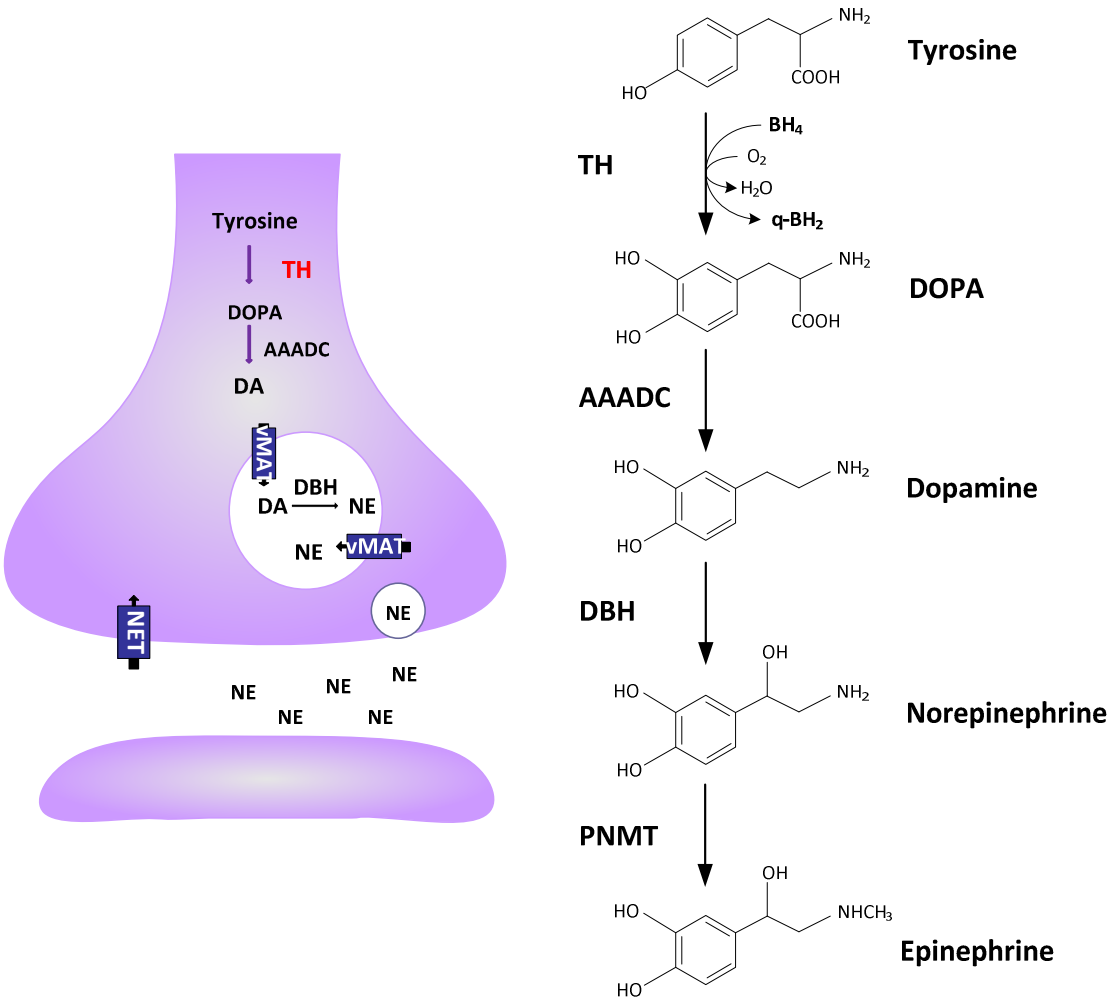

Figure 1.5 Catecholamine biosynthesis.

Catecholamines are synthesized from the amino acid tyrosine. TH, the rate-limiting enzyme, catalyzes L-DOPA formation from L-tyrosine. The rest of the steps are catalyzed by aromatic amino acid decarboxylase (AAADC), dopamine-β-hydroxylase (DBH), and phenylethanolamine- N – methyl transferase (PNMT). Dopamine (DA) is transported into vesicles by the vesicular monoamine

transporter (vMAT). In the vesicle, DBH converts DA to NE. NE, released at the nerve terminal, is taken back by the NE transporter (NET).

1.5.1 Regulation of TH

As TH catalyzes the rate-limiting step in catecholamine biosynthesis, its activity is regulated by a variety of mechanisms. This falls into two categories: short-term regulation and long-term regulation.

TH is subjected to several types of regulation in response to acute stimuli. One type of acute regulation is feedback inhibition by catecholamines. The binding of catecholamines to TH leads to a 78-90% inhibition of enzyme activity *in vitro* (Kumer and Vrana 1996). Normally, reduced pterin is the first substrate to bind to the enzyme. The binding of catecholamines to the free enzyme prevents pterin from binding to ferric iron at the catalytic site. This feedback inhibition by catecholamines is a form of competitive inhibition and can be overcome by increasing the concentration of pterin. A second type of acute regulation is phosphorylation of the enzyme. Acute regulation of catecholamine synthesis can occur by modulation of the phosphorylation states of TH. Various physiological stimuli can induce phosphorylation on four serine residues (Ser8, Ser19, Ser31 and Ser40) in the N-terminal regulatory domain of TH by activation of different protein kinases (Fig. 1.6) (Dunkley *et al.* 2004).

Phosphorylation on Ser40 by cyclic AMP-dependent protein kinase (PKA) is the best studied. In rat brain and bovine adrenal chromaffin cells, PKA is able to phosphorylate TH at Ser40. Agents including forskolin, 8-bromo cAMP, dibutryl cAMP and vasoactive intestinal polypeptide (VIP), signaling through the PKA

pathway, can increase phosphorylation on Ser40 (Dunkley *et al.* 2004). In addition, protein kinase C (PKC), calcium/calmodulin dependent protein kinase II (CAMPK II) , protein kinase G (PKG), MAKP-activated protein kinase 1 and 2 (MAKPAPK 1 and 2), p38-regulated/activated kinase (PRAK) and mitogen and stress- activated protein kinase 1 (MSK 1) also can phosphorylate TH at Ser40 (Dunkley *et al.* 2004). Phosphorylation at Ser40 increases the affinity of TH for its cofactor BH_4 and results in increased TH enzyme activity in situations where BH_4 is present at sub-saturating levels (Daubner *et al.* 1992;McCulloch *et al.* 2001).

Phosphorylation on Ser31 by extracellular signal regulated protein kinase 1/2 (ERK1/2) and cyclin-dependent kinase 5 (cdk 5) also regulates TH activity. Treating PC12 cells with NGF, bradykinin, muscarine, or ATP can increase TH phosphorylation at the Ser31 residue (Kumer and Vrana 1996). Phosphorylation of hTH3 at Ser31 *in vitro* increased TH activity by decreasing the K_M for BH_4 (Sutherland *et al.* 1993). This suggests that the effect of Ser31 phosphorylation by ERK is similar to phosphorylation on Ser40 by PKA. Cdk5 phosphorylation of TH on Ser31 stimulates TH activity by increasing TH protein stability (Moy and Tsai 2004).

Phosphorylation on Ser19 is stimulated by CAMPK II and MAPKAPK 2 *in vitro* and *in vivo*. Phosphorylation on Ser19 was found in all catecholamine cell groups in the rat brain (Dunkley *et al.* 2004) suggesting Ser19 was phosphorylated to a substantial level under resting conditions. There is little

evidence that phosphorylation at Ser19 plays a direct role modulating TH activity, but Ser19 and Ser31 can facilitate subsequent Ser40 phosphorylation which is critical in regulating TH activity (Lehmann *et al.* 2006). ERK1/2 and MAPKAPK 2 can phosphorylate TH on Ser8, but the physiological role of Ser8 phosphorylation is not clear (Dunkley *et al.* 2004).

TH is also subject to long-term regulation, including changes in TH gene transcription. TH gene expression is regulated by many physiological and pharmacological stimuli, including hormones, depolarization, cytokines and drugs. TH gene expression is stimulated during development by the transcription factors Hand2 and Gata3 (Muller and Rohrer 2002), and IL-6 family cytokines down-regulate TH mRNA in adult neurons by decreasing expression of Hand2 (Pellegrino *et al.* 2011). TH mRNA is increased during development and in adult neurons by nerve growth factor, depolarization, and nicotine (Kumer and Vrana 1996). The TH promoter has numerous regulatory sites, including a cAMP response element (CRE), activating protein 1 (AP-1) and NF-kB sites, which are involved in transcriptional regulation. The CRE plays an important role in cAMP and Ca^{2+} induced TH gene expression. Elevated cAMP stimulates PKA, resulting in phosphorylation of cAMP response element binding protein (CREB), and CREB binds to the CRE site to regulate both basal and inducible TH gene expression (Nagamoto-Combs *et al.* 1997;Piech-Dumas and Tank 1999). In addition to increasing transcription, cAMP also increases TH mRNA stability which elevates TH mRNA levels (Fossom *et al.* 1992).

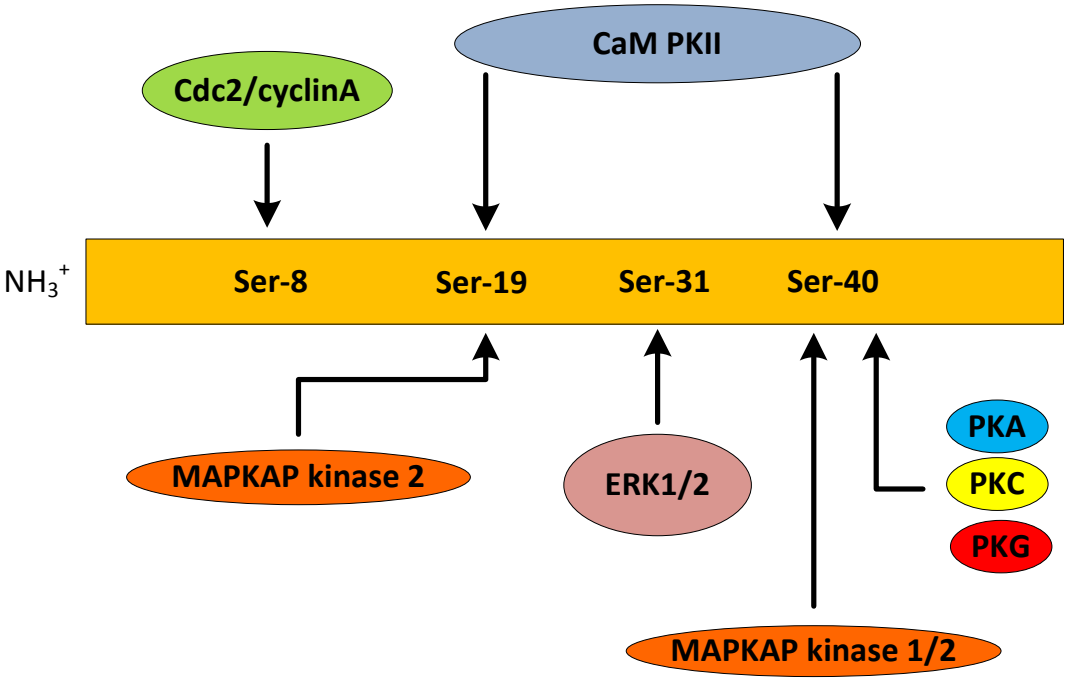

Figure 1.6 Sites of phosphorylation in the N-terminal regulatory domain of TH.

Four phosphorylation sites (Ser8, Ser19, Ser31 and Ser40) are within the first 40 amino acids of TH. Protein kinases are able to phosphorylate different serine residues.

1.5.2 TH protein turnover

Chronic exposure to physiological and pharmacological stimuli regulates TH protein levels in addition to effects on transcription. There are two major protein degradation pathways: the ubiquitin-proteasome pathway and the lysosome-endosome pathway. TH is a substrate of the ubiquitin-conjugating enzyme system (Doskeland and Flatmark 2002), and angiotensin (1-7) stimulates TH proteasomal degradation (Lopez Verrilli *et al.* 2009). These findings suggest that TH degradation through the ubiquitin-proteasome system may be stimulated by chronic exposure to physiological factors.

1.5.2.1 Ubiquitin- proteasome pathway

The ubiquitin-proteasome pathway plays a major role in selective protein degradation in eukaryotes. It also regulates various cellular events including cell cycle, transcription, DNA repair, signal transduction, and immune responses. The initial step of this protein degradation pathway is ubiquitination which is an ATP- dependent process (Fig. 1.7). Ubiquitin is first activated by the ubiquitin activating enzyme (E1). Activated ubiquitin then transfers to ubiquitin conjugating enzyme (E2), an ubiquitin carrier protein. The protein substrate and the E2 enzyme with ubiquitin both bind to a specific ubiquitin ligase (E3). The activated ubiquitin moiety is transferred to the protein substrate by E3. E2 and E3 can conjugate multiple ubiquitin moieties to the protein substrate and generate a polyubiquitin chain. This polyubiquitin chain functions as a signal to target the protein substrate to the 26s proteasome for degradation. Proteins are rapidly

degraded into small peptides. Following protein substrate degradation, ubiquitin is also released and the short peptides get reused.

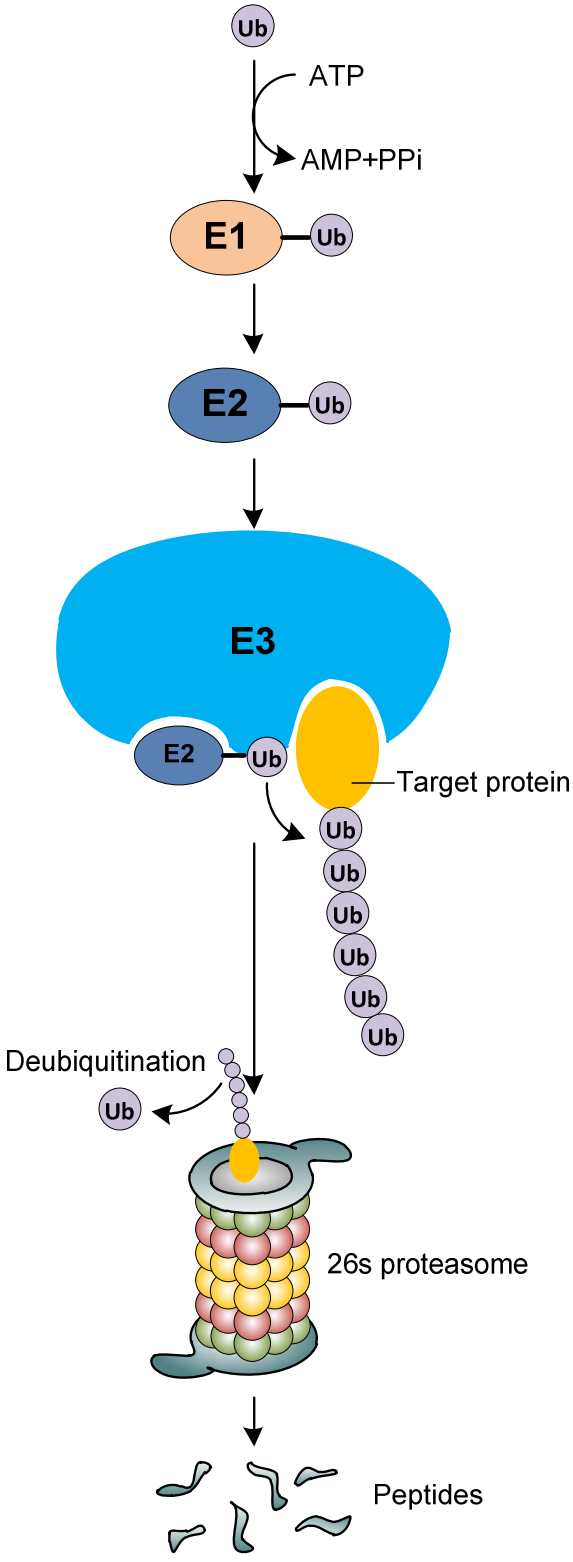
Ub
ATP
AMP+PPi
E1
Ub
E2
Ub
E3
E2
Ub
Target protein
Ub
Ub
Ub
Ub
Ub
Ub
Deubiquitination
Ub
26s proteasome
Peptides

Figure 1.7 Protein degradation through the ubiquitin-proteasome system. Ubiquitin is activated by the ubiquitin-activating enzyme (E1). Ubiquitin then transfers to a ubiquitin-conjugation enzyme (E2). The E2-ubiquitin complex and protein substrate both bind to the ubiquitin-protein ligase (E3) where the activated ubiquitin moiety is transferred to the protein substrate. Conjugating ubiquitin moieties to the protein substrate generates a polyubiquitin chain which is a signal target the protein to the 26S proteasome for degradation. Ubiquitin is removed by the deubiquitinating enzymes (DUBs) and reused. The protein substrate is hydrolyzed into short peptides.

1) Ubiquitination

Ubiquitin is a small regulatory protein with 76 amino acids. It is highly conserved and ubiquitously expressed in eukaryotic cells. Ubiquitination is a reversible post-translational modification. The C-terminal glycine of ubiquitin is covalently linked to a lysine side chain in the target protein through an isopeptide bond. The lysine side chain within ubiquitin is then linked to the C-terminal glycine of another ubiquitin, thereby forming a polyubiquitin chain through repetition of this reaction.

Protein substrates can be monoubiquitinated (a single ubiquitin on one lysine residue), multiubiquitinated (multiple single ubiquitins on several lysine residues), and polyubiquitinated (polyubiquitin chain) (Fig. 1.8) (Powell 2006). The ubiquitin also can link to a target protein at the amino terminus which is less common. Conjugating protein with different forms of ubiquitination generate different molecular weight products of the same protein substrate. This results in detecting ubiquitinated protein in a high molecular weight smear in immunoblots. Different types of ubiquitination can serve as signals for different cellular events. Polyubiquitination usually targets protein substrates for proteasome degradation (Ciechanover *et al.* 2000). Monoubiquitination at multiple sites is required for receptor tyrosine kinase endocytosis (Haglund *et al.* 2003).

Ubiquitin itself has seven lysine residues (K6, K11, K27, K29, K33, K48 and K63) with their specific functions. Activated ubiquitin can conjugate to any

one of these lysine residues of the previous ubiquitin to form a chain. Polyubiquitin chains linked through Lys48 are most common and target proteins to the 26S proteasome for degradation(Powell 2006). In addition to targeting proteins to the proteasome, Lys63-linked polyubiquitin chains are also involved in DNA repair and endocytosis (Tan *et al.* 2008;Wen *et al.* 2012). The functions of the other residues are not clear.

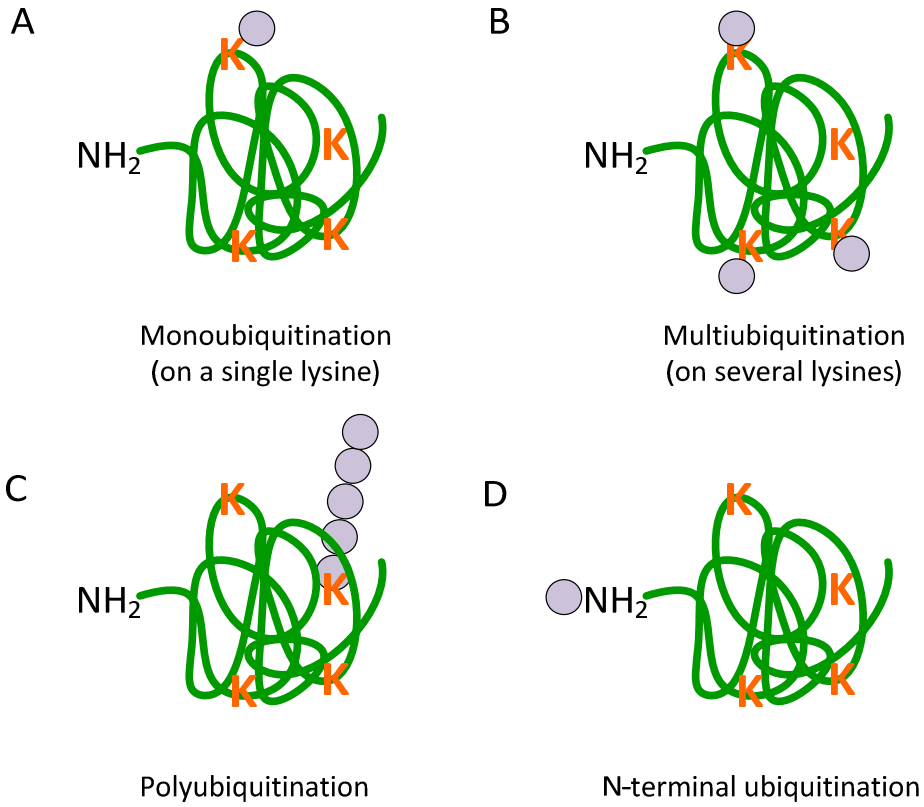

Figure 1.8 Types of ubiquitination.

Monoubiquitination refers to a single ubiquitin on a single lysine (A). Multiubiquitination is a single ubiquitin on several lysines (B). Proteins can be polyubiquintinated on one or more lysine residues (C). N-terminal ubiquintiantion refers to conjugation of ubiquitin to the α-NH_2 group at the N-terminus which is uncommon (D).

2) Proteasome

The proteasome is a large 26S multicatalytic protease complex. It degrades polyubiquitinated proteins to produce small peptide fragments. The 26S proteasome is composed of two sub-complexes: 20S, a catalytic core particle and 19S, a regulatory particle (Fig. 1.9) (Ciechanover 2005). The 19S particle, containing ubiquitin binding subunits, binds on both ends of the 20S barrel-like structure to form a 26S holoenzyme. The 19S regulatory particle consists of at least 17 proteins which form two sub-complexes, the lid and base. These proteins fall into two groups based on their function: the ATPase regulatory particles triple A (Rpt 1-6) and the non-ATPase regulatory particles (Rpn1-12) (Ciechanover 2005). The lid recognizes the polyubiquitin chain on the target protein with high fidelity. The base is made of six ATPase subunits (Rpt 1-6) and two non-ATPase subunits, Rpn1 and Rpn2. The base utilizes ATP to unfold the protein substrate and thread the protein into the narrow catalytic chamber of the 20s proteasome.

The 20S core particle has four stacked rings: two outer α-rings and two inner β-rings (Ciechanover *et al.* 2000;Myung *et al.* 2001). Each ring has seven subunits. The ring-structure forms a proteolytic chamber for protein degradation. The proteolytic activity of the 20S proteasome occurs within the inner β-subunits. The 20S proteasome has multiple catalytic activities which are ATP- independent. The proteolytic activities refer to cleave the peptide bond after a particular amino

acid such as a basic residue like trypsin. The main activities of the 20S proteasome are trypsin-like (basic group), chymotrypsin-like (large hydrophobic group) and post-glutamyl peptide hydrolyzing (acidic group) (Myung *et al.* 2001). In addition to these classic proteolytic activities, the 20S proteasome can also have branched-chain amino acid-preferring activity and small neutral amino acid-preferring activity (Ciechanover 2005). Different β-subunits correspond to the different catalytic activities.

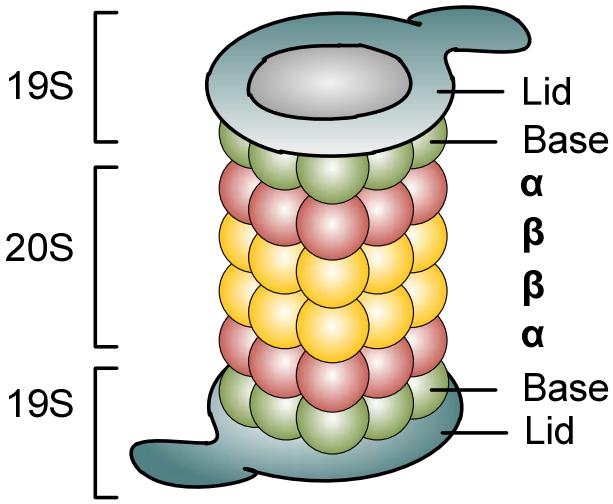

Figure 1.9 26S proteasome.

The 26S proteasome contains a 20S catalytic core and two 19S regulatory particles. The 20S proteasome is assembled with two outer (α subunits) and two inner (β subunits) rings to form a hollow structure where proteolysis occurs. The19S regulatory particle binds to both ends of the 20S proteasome, which gate the channel and unfold the protein substrates.

3) Proteasome inhibitors

Most available proteasome inhibitors directly target the core catalytic 20S proteasome. There are two categories: synthetic inhibitors and natural products. The synthetic inhibitors, which are peptide-based compounds with different pharmacophores, provide selective inhibition of proteasome activity. Peptide aldehydes were the first developed synthetic proteasome inhibitors and have been used as serine and cysteine protease inhibitors for a long time (Myung *et al.* 2001). MG132, Calpain inhibitor I and PSI belong to this class. MG-132 (Fig. 1.10) has been widely used in proteasome studies and selectively inhibits the chymotrypsin-like activity of the 20S proteasome.

In contrast to the synthetic analogs, natural products also provide selective inhibition of proteasome activity. Lactacystin, a *Streptomyces Lactacystinaeus* metabolite, is one of the proteasome inhibitors isolated from natural sources (Fig. 1.10). Lactacysin irreversibly modifies the amino terminal threonine of the β-subunit which inhibits 20S proteasome activity. The clasto-lactacystin β-lactone (Fig. 1.10) is an active component of lactacystin and reacts with the hydroxyl group of the amino terminal threonine to form an ester adduct.

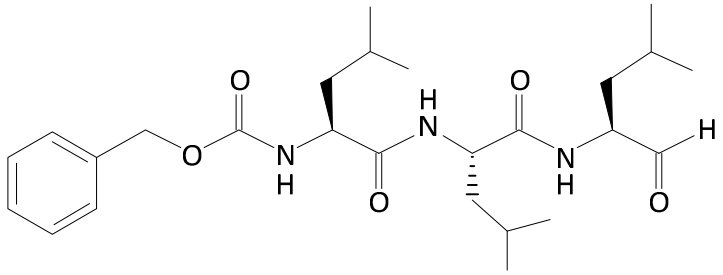

MG-132

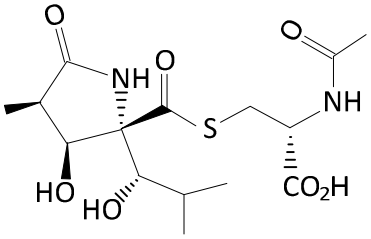

Lactacystin

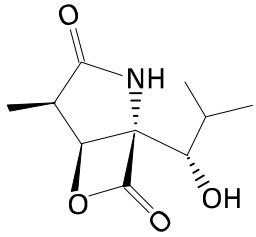

clasto-lactacystin β-lactone

Figure 1.10 Structure of proteasome inhibitors.

MG-132 is a synthetic proteasome inhibitor, which inhibits the chymotrypsin-like activity of the proteasome. Lactacysin is a natural proteasome inhibitor and targets the 20S proteasome by an irreversible modification of threonine residues. Clasto-lactacystin β-lactone is the active component of lactasystin.

4) Deubiquitination

The ubiquitin-conjugated protein is a dynamic complex. The process of ubiquitination is reversible by deubiquitinating enzymes (DUBs). Deubiquitinating enzymes are a large group of enzymes which can cleave ubiquitin from target proteins. Failure to add or remove the ubiquitin chain from a target protein can result in inappropriate degradation, affecting the protein half-life and steady state levels (Amerik and Hochstrasser 2004;Zhao *et al.* 2011).

1.5.2.2 Lysosomal degradation

The other main proteolysis pathway is lysosomal degradation. The lysosome is an intracellular vesicle which contains various hydrolytic enzymes including proteases. These enzymes function optimally at an acidic pH. In contrast to the ubiquitin-proteasome pathway, the lysosome system degrades not only intracellular proteins through autophagy, but also extracellular proteins which are taken in through endocytosis. For example, the LIF receptor is degraded through the lysosome system in response to tumor necrosis factor (TNF) stimulation (Yu *et al.* 2007). There is little evidence to support regulated TH degradation through the lysosomal pathway.

1.6 Purpose of thesis, hypothesis and summary of results

In vivo studies indicated TH protein levels were depleted in the peri-infarct left ventricle after myocardial infarction. But TH mRNA was elevated in the sympathetic neurons innervating the heart (Parrish *et al.* 2008). Inflammatory cytokines signaling through gp130 are responsible for the local depletion of TH (Parrish *et al.* 2010). However, the mechanism of cytokine-induced TH loss remains unknown.

Therefore, I hypothesize that cytokines regulate TH degradation and activity in sympathetic neurons.

To test this hypothesis, I measured TH protein half-life in both sympathetic neurons and SK-N-BE(2)M17 neuroblastoma cells. I found that cytokines, such as CNTF, decreased TH half-life, suggesting an increase in TH protein turnover. CNTF induced TH ubiquitination and stimulated TH proteasomal degradation. ERK1/2 was required for CNTF-induced TH ubiquitination and the associated decrease in TH half-life (Chapter 2).

Removing the neuronal gp130 receptor prevented the loss of TH in damaged left ventricle but did not restore NE levels (Parrish *et al.* 2010), suggesting the possibility that cytokines influence TH enzyme activity in addition to their effect on TH protein levels. To examine this issue, I measured TH activity in the presence or absence of CNTF. I found CNTF increased the rate of L-DOPA production per enzyme molecule, suggesting an increase in TH specific

activity. The specific activity of TH from cultured sympathetic neurons lacking the gp130 receptor was not increased by CNTF treatment. CNTF also increased the fraction of TH phosphorylated on Ser31, which may contribute to the increase in TH activity (Chapter 3).

Chapter 2

gp130 cytokines stimulate proteasomal degradation of tyrosine hydroxylase via extracellular signal regulated kinases 1 & 2

Xiao Shi and Beth A. Habecker

Department of Physiology and Pharmacology, Oregon Health & Science University, Portland, OR, 97239, USA

Corresponding Author: Beth A. Habecker, PhD,

Chapter 2 is a manuscript that appears as it was published in:

Journal of Neurochemistry, 2012, Volume 120, p. 239-247

Abstract

Injury-induced cytokines act through gp130 in sympathetic neurons to suppress expression of tyrosine hydroxylase (TH) and other genes associated with noradrenergic transmission. These cytokines also trigger the local loss of TH in peri-infarct sympathetic axons after myocardial infarction, but altered gene expression cannot explain the selective loss of TH enzyme in one region of the heart. We hypothesized that inflammatory cytokines, which are highest near the infarct, stimulated local degradation of TH protein. We used cultured sympathetic neurons and neuroblastoma cells to test this hypothesis. The cytokines ciliary neurotrophic factor (CNTF) and leukemia inhibitory factor (LIF) suppressed TH content in both neurons and neuroblastoma cells. CNTF suppressed TH in a gp130-dependent manner, and decreased the half-life of TH protein by approximately 50%. CNTF stimulated the ubiquitination of TH in both neurons and neuroblastoma cells, and the proteasome inhibitors MG-132 and lactacystin prevented the CNTF-induced loss of TH protein. Inhibiting activation of extracellular signal regulated kinases 1&2 (ERK1/2) with U0126 prevented the CNTF-induced ubiquitination of TH and the associated decrease in protein half-life. Likewise, inhibiting ERK1/2 activation blunted the cytokine-stimulated loss of TH protein in sympathetic neurons, despite *enhancing* the loss of TH mRNA. These data suggest that gp130 cytokines stimulate proteasomal degradation of TH through an ERK1/2 dependent pathway, and may have important implications for local regulation of neurotransmission at sites of inflammation.

Introduction

Inflammatory cytokines acting through the gp130 receptor suppress noradrenergic function in a subset of sympathetic neurons during development (Stanke *et al.* 2006), and more broadly in adult sympathetic neurons after nerve injury (Pellegrino *et al.* 2011;Rao *et al.* 1993;Zigmond *et al.* 1996). Activation of gp130 decreases the expression of genes involved in noradrenergic transmission in sympathetic neurons, including that of tyrosine hydroxylase (TH), the rate-limiting enzyme for norepinephrine (NE) synthesis (Fann and Patterson 1993;Li *et al.* 2003;Nawa *et al.* 1991). Similar changes have been modeled *in vitro* by treating cultured sympathetic neurons with gp130 cytokines such as ciliary neurotrophic factor (CNTF) or leukemia inhibitory factor (LIF) (Li *et al.* 2003;Nawa *et al.* 1991;Patterson and Chun 1977;Saadat *et al.* 1989;Yamamori *et al.* 1989)

Several gp130 cytokines are elevated in the left ventricle after myocardial infarction (Aoyama *et al.* 2000;Frangogiannis *et al.* 2002;Gwechenberger *et al.* 1999;Kreusser *et al.* 2008), and activation of gp130 results in the loss of TH in the peri-infarct region of the left ventricle (Parrish *et al.* 2010). Suppression of the TH gene cannot explain the selective loss of TH enzyme in peri-infarct neurons, because activation of cardiac sympathetic nerves after myocardial infarction increases TH mRNA (Parrish *et al.* 2008). Furthermore, TH protein content is normal in cardiac sympathetic axons farther away from the site of damage (Li *et*

al. 2004;Parrish *et al.* 2008). This raises the possibility that cytokines have direct effects on TH degradation in addition to their well-characterized effects on TH gene expression and protein synthesis.

Targeted degradation of proteins occurs primarily through the ubiquitin-proteasome system (Ciechanover 2005). Tyrosine hydroxylase is a substrate for degradation by the ubiquitin-proteasome system (Doskeland and Flatmark 2002;Nakashima *et al.* 2011), and its ubiquitination degradation can be stimulated by angiotensin (1-7) (Lopez Verrilli *et al.* 2009). We tested the hypothesis that gp130 cytokines stimulate the ubiquitination and proteasomal degradation of TH using cultured sympathetic neurons and M17 neuroblastoma cells. Our results support the notion that cytokine activation of gp130 stimulates proteasomal degradation of TH in sympathetic neurons.

Experimental procedures:

Animal

Pregnant adult Sprague Dawley rats were obtained from Charles River. Wild-type C57BL/6J mice were obtained from Jackson Laboratories (Sacramento, CA, USA). The $gp130^{DBH\text{-}Cre/lox}$ mice were generated as previously described (Stanke *et al.* 2006). All animals were housed individually with a 12 hr:12 hr light dark cycle and *ad libitum* access to food and water. All procedures were approved by

the Institutional Animal Care and Use Committee, and comply with the Guide for the Care and Use of Laboratory Animals published by the US National Institutes of Health (NIH publication No. 85-23, revised 1996).

Cell culture

Cells were grown under sterile conditions in a humidified 5% CO_2 incubator at 37°C. Superior cervical ganglia (SCG) from newborn rats or mice (P0-P1) were dissociated and grown in cell culture as previously described (Dziennis and Habecker 2003;Li *et al.* 2003) using C2 medium supplemented with 50 ng/mL nerve growth factor (NGF, BD Bioscience, Bedford, MA, USA), and 3% fetal bovine serum (ATCC)(Pellegrino *et al.* 2011). Sympathetic neurons were grown in 12, 24, or 96-well plates pre-coated with 100 µg/mL poly-L-lysine (Sigma, St. Louis, MO, USA) and 10 µg/mL collagen (BD bioscience). Non-neuronal cells were eliminated by treating the cultures with the anti-mitotic agent cytosine arabinoside (Ara C, 1 µM, Sigma) for 2 days. SK-N-BE(2)M17 human neuroblastoma cells (M17 cells) were grown in Dulbecco's modified Eagle's medium (Gibco, Rockville, MD, USA) supplemented with 10% fetal bovine serum. M17 cells were plated at 1 X 10^5 cells per well in 12-well plates.

Cytokines and other reagents were diluted in culture medium before addition to the culture plates. Cells were treated with 100 ng/ml CNTF or LIF (Pepro Tech, Rocky Hill, NJ, USA), 100 nM MG-132 (Calbiochem, San Diego, CA, USA), 20 µM STAT3i V (STAT3 Inhibitor V, Calbiochem), 10 µM U0126 (Sigma), and 2 µM

Janus tyrosine kinase (JAK) inhibitor (Calbiochem). The duration and timing of treatments is noted for each experiment. All conditions were assayed in triplicate and experiments repeated at least 3 times.

Immunoblot Analysis

Cells were washed with ice-cold phosphate-buffer saline (PBS) and lysed at 4°C in RIPA lysis buffer (1% Triton-X100, 1% sodium deoxycholate, 0.2% SDS, 125 mM NaCl, 50 mM Tris pH 8.0, 10% glycerol, 25 mM β-glycerolphosphate, 1 mM EDTA, 25 mM NaF, protease inhibitor cocktail (Roche) and 1 mM sodium orthvanadate). Lysates were fractionated on SDS-polyacrylamide gels and transferred to nitrocellulose membranes. Blots were incubated in 5% low fat milk in Tris-buffered saline (pH 7.4) containing 0.1% tween-20 at 25°C. Membranes were subsequently incubated at 4°C overnight with rabbit anti-TH (1:5000, Millipore Corporation, Bedford, MA, USA), mouse anti-ubiquitin (1:500, Santa Cruz, Biotechnology, Santa Cruz, CA, USA), rabbit anti-pERK1/2 (phospho-extracellular signal-regulated kinases 1 and 2, 1:1000, Cell Signaling, Technology, Beverly, MA, USA), rabbit anti-total ERK (1:1000, Cell Signaling), rabbit anti-pSTAT3 (phospho-Tyr705 Signal Transducer and Activator of Transcription 3, 1:1000, Cell Signaling), or rabbit anti-total STAT3 (1:1000, Cell Signaling) antibodies. The immunoblots were incubated with horseradish peroxidase - conjugated secondary antibody immune-complexes were visualized

by chemiluminescence (Super Signal Dura, Pierce, Rockford, IL, USA) and quantified using Labworks software.

Immunoprecipitation

After treatment, neurons were washed with ice-cold PBS and lysed at 4°C in RIPA lysis buffer. Aliquots of cell lysates (150 µg total protein) were incubated with Protein G-Sepharose conjugated beads (Invitrogen, Carlsbad, CA, USA) for 2 hr to eliminate non-specific binding. Pre-cleared cell lysates were incubated with a saturating amount of primary antibody (1.5 µg rabbit anti-TH per condition) overnight at 4°C. Protein G beads were added in excess to each sample and incubated for 2 hr. After incubation, beads were washed with ice-cold PBS 5 times to remove non-specific binding. Proteins were released from immune-complexes by incubation with SDS sample buffer (Dziennis and Habecker 2003) at 95° C for 5 min then analyzed by western blot.

Estimation of TH half-life

Pulse Chase. Neurons were cultured as described above, and 5 days after plating metabolic labeling was carried out using an approach similar to that previously used to determined TH half-life (Franklin and Johnson 1998;Wu and Cepko 1994). Prior to labeling, neurons were incubated for 1 hr at 37° C in culture medium without L-methionine and L-cysteine supplemented with 5% fetal bovine serum. To label newly synthesized protein, [^{35} S] methionine/cysteine (20 µCi/mL, 73% L-methionine, 22% L-cysteine, Perkin Elmer, Waltham, MA, USA)

was added for 1 hr. Cells were washed with PBS to remove unincorporated isotope and chase medium (DMEM) with methionine supplemented to 150 mg/L was added to stop labeling. Cultures were lysed in RIPA lysis buffer with Triton-X100 at 0, 4, 8, 16, 24 hr later. TH was immunoprecipitated from samples and immune complexes were resolved by SDS-PAGE gel electrophoresis. Labeled TH was quantified using a Bio-Rad Phosphoimager (Bio-Rad laboratories, Hercules, CA, USA).

Protein synthesis inhibition. M17 neuroblastoma cells were treated with 20 µg/mL cycloheximide with or without 100 ng/mL CNTF or 0.1% ethanol vehicle. For inhibition of MEK/ERK signaling, M17 cells were pretreated with vehicle or 10 µM U0126 for 30min, and then incubated with 20 µg/mL cycloheximide in the presence or absence of CNTF. 0.1 % dimethylsulfoxide (DMSO) and 0.1% ethanol were added as vehicle controls. Cells were lysed at 0, 8, 12, and 24 hours, and 8 µg aliquots were assayed for TH content by western blot.

For half-life calculation, TH levels were plotted as the percentage of TH remaining, normalized to initial TH levels, on a natural log scale versus time. The data were fitted to a first-order decay function to estimate the degradation rate constant (k_d), which then was used to calculate a half-life ($t_{1/2}$). TH half-life was calculated from $t_{1/2} = \ln 2 / k_d$.

Real Time PCR

Neurons were harvested using the Cells-to-cDNA II kit from Ambion. Cell lysates were treated with DNase and reverse transcribed. Real-time PCR was performed with the ABI TaqMan Universal PCR Master Mix in the ABI 7500, using ABI pre-validated TaqMan gene expression assays for TH and GAPDH. For the PCR amplification, 2 µl of RT reactions were used in a total volume of 20 µl, and each sample was assayed in triplicate. Standard curves were generated with known amounts of RNA (0.5 ng – 100 ng) and TH mRNA was normalized to GAPDH mRNA in the same sample.

Transient Transfection and Reporter Assays

DNA used for transfection was purified using the Qiagen Maxiprep kit (Qiagen, Valencia, CA, USA). M17 cells were plated at a density of 1.0×10^5 cells per well in 6-well plates and immediately treated with 100 ng/mL CNTF. 48 hours after plating, media were removed and cells were transfected using the $CaPO_4$ method. Cells were transfected with 1 µg of 4.5TH-fLuc, or 1 µg empty pcDNA3 vector. 100 ng pRL-null was used as a control for transfection efficiency. After 4 hour incubation with DNA, cells were shocked with 15% glycerol/PBS, washed with PBS, and placed back into culture media containing CNTF. Firefly luciferase activity from promoter luciferase constructs and *Renilla* luciferase activity from the pRL-null internal control were assayed 48 hours after transfection using the

Dual-Luciferase Reporter Assay system. Firefly luciferase values were normalized to *Renilla* luciferase values.

Statistical analyses

Data are presented as mean values± SEM. Significant differences were assessed by one-way analysis of variance (ANOVA) using GraphPad Prism 5 (GraphPad Software, Inc.). Tukey's post hoc test was used to compare to all conditions. P values <0.05 were considered significant.

Results:

To investigate the mechanisms that underlie the gp130-dependent loss of tyrosine hydroxylase in the left ventricle after myocardial infarction (Parrish *et al.* 2010), we first confirmed that similar changes occurred in cell culture. Treatment of wild-type sympathetic neurons with the cytokine CNTF decreased TH content and stimulated phosphorylation of ERK1/2 and STAT3 (Fig. 2. 1). In contrast, CNTF did not decrease TH or increase phosphorylation of ERK1/2 or STAT3 in sympathetic neurons lacking gp130 (Fig. 2.1). To determine if CNTF had an effect on TH protein turnover, we carried out pulse chase experiments in wild type sympathetic neurons. CNTF was added during the "chase" phase, and samples were collected over 24 hours after CNTF addition. CNTF decreased TH

half-life by approximately 50% compared to control neurons (control 28.3 ± 0.7 hr vs. CNTF 12.8 ± 2.2 hr, n=3 experiments, $p<0.05$) (Fig. 2. 2B). Additional experiments confirmed that TH mRNA was unchanged 24 hr after CNTF treatment (Fig. 2.2A), consistent with a normal level of TH synthesis.

Although primary cultures of sympathetic neurons faithfully reproduce neurotransmitter changes that are observed *in vivo*, the large number of cells required for half-life experiments led us to establish a cell line model system for further investigation of mechanisms. We previously found that CNTF and LIF activate the same signaling pathways and suppress dopamine beta hydroxylase expression in M17 neuroblastoma cells and sympathetic neurons (Dziennis and Habecker 2003). Therefore, we examined TH expression in M17 cells to determine if they would provide a suitable model for half-life experiments. Treatment of M17 cells with CNTF or LIF stimulated STAT3 phosphorylation (Fig. 2. 3A), inhibited TH gene transcription (Fig.2. 3B), and decreased TH protein content (Fig. 2. 3C). We then used M17 cells to determine if cytokines altered TH protein stability by measuring the effect of CNTF on TH half-life. We were unable to attain equilibrium using the pulse-chase method, and therefore inhibited protein synthesis in order to obtain the degradation rate for TH. The estimated half-life for TH in control cells was 36.8 ±1.9 hr (k_d= 0.021 h^{-1}; n=3) while the estimated half-life after CNTF treatment was 15.8 ±1.7 hr (k_d = 0.046 $h^{-1;}$ n=3) (Fig. 2. 4). CNTF decreased TH protein half-life by approximately 50%, similar to the change we observed in sympathetic neurons.

The half-life data suggest that CNTF stimulates TH degradation. TH can be broken down by the ubiquitin-proteasome system (Doskeland and Flatmark 2002;Lopez Verrilli *et al.* 2009), so we asked if CNTF stimulated the ubiquitination and proteasomal degradation of TH. Sympathetic neurons or neuroblastoma cells were treated for 30 minutes with vehicle or CNTF, and TH was immunoprecipitated (IP) with an anti-TH antibody. Samples were then fractionated and blotted with an anti-ubiquitin antibody. Ubiquitin conjugated TH was detected as a high molecular weight smear and was increased after CNTF exposure in neurons and neuroblastoma cells (Fig.2.5A, B). To confirm that CNTF-stimulated TH ubiquitination was a direct effect of CNTF activating its receptor, we examined ubiquitinated TH in neurons lacking the gp130 receptor. CNTF did not increase the accumulation of ubiquitinated TH in neurons lacking gp130, although TH was abundant in the immunoprecipitated samples, and absent in the post-IP lysates (Fig. 2.5C). Many ubiquitin-conjugated proteins were detected in the post-IP lysates present on the same blot (Fig. 2.5C). To determine if TH ubiquitination was associated with increased proteasomal degradation, neurons were treated with vehicle or CNTF for 4 days. During the last 2 days, cells were treated with the proteasome inhibitors MG-132 (100 nM; Fig. 2.5D) or lactacystin (100 nM; Fig.2.5E), or 0.1% DMSO as a vehicle control. The cytokine-induced loss of TH was prevented by both proteasome inhibitors but not the DMSO control treatment, consistent with proteasomal degradation. Cell death was monitored in sister cultures and no significant cell death was

observed with 2 day MG-132 and lactacystin treatment compared to control (data not shown). These data suggest that cytokines stimulate TH turnover in sympathetic neurons by targeting the enzyme for proteasomal degradation.

In order to determine which signaling pathways were involved in cytokine-stimulated ubiquitination of TH, we used a pharmacological approach to inhibit key signaling pathways. Cytokine activation of gp130 stimulates phosphorylation of JAK kinases and the downstream signaling molecules ERK1/2 and STAT3 (Dziennis and Habecker 2003;Fischer and Hilfiker-Kleiner 2008). We first examined the role of ERK1/2, and found that the MEK (MAPK/ERK kinase) inhibitor U0126 prevented both ERK1/2 phosphorylation and CNTF-stimulated TH ubiquitination (Fig.2.6). We then treated sympathetic neurons with CNTF in the presence or absence of drugs that blocked activation of Jak, ERK1/2, or STAT3. Once again, blocking ERK phosphorylation prevented CNTF-stimulated ubiquitination of TH. Likewise, blocking JAK prevented phosphorylation of both ERK1/2 and STAT3, and inhibited cytokine-stimulated TH ubiquitination (Fig.2.7). In contrast, treating neurons with STAT3iV blocked STAT3 phosphorylation but increased TH ubiquitination independent of CNTF (Fig.2.7). The STAT3 inhibitor AG490 did not inhibit STAT3 phosphorylation at concentrations consistent with cell survival (data not shown).

CNTF decreased the half-life of TH, and our ubiquitination experiments suggested that ERK1/2 signaling was required for cytokine-induced TH

degradation. However, the time course for ubiquitination was 30 minutes, and several days of cytokine exposure were required to observe a significant proteasome-dependent loss of TH. To determine if cytokines stimulated degradation of TH via an ERK1/2-dependent pathway, we measured the half-life of TH in control and in CNTF-treated M17cells with or without U0126 to prevent ERK activation. CNTF decreased TH half-life by approximately 50%, consistent with our previous results, but the decrease in half-life was blocked by U0126 (CON 33.3 ± 3.6 hr, UO 28.3 ± 2.4 hr, CNTF 16 ± 0.5 hr*, CNTF+UO 27.0 ± 3.5 hr, n=3 experiments, *p<0.05 vs. CON) (Fig. 2.8). Thus, ERK1/2 activation is required for the cytokine-induced degradation of TH.

As ERK1/2 was involved in cytokine-stimulated TH degradation, we tested if inhibiting ERK1/2 activation could prevent the loss of TH protein in CNTF-treated neurons. Neurons were treated with CNTF for 5 days with or without U0126, and assayed for either TH protein or TH mRNA. Blocking ERK1/2 activation in CNTF-treated cells partially rescued TH protein levels, but exacerbated the loss of TH mRNA (Fig. 2.9). To ensure that ERK-dependent TH degradation was a general effect of gp130 activation and was not specific to CNTF, we repeated these experiments with the cytokine LIF and the MEK inhibitor PD98059, and obtained similar results. LIF decreased TH protein and mRNA in sympathetic neurons, as expected. Blocking ERK activation blunted the loss of TH protein while exacerbating the loss of TH mRNA (data not shown).

Discussion

It is well established that inflammatory cytokines such as CNTF and LIF suppress sympathetic noradrenergic neurotransmission (Patterson and Chun 1977;Saadat *et al.* 1989;Yamamori *et al.* 1989). This suppression was thought to be mediated by reducing the expression of noradrenergic genes (Fann and Patterson 1993;Li *et al.* 2003;Nawa *et al.* 1991;Pellegrino *et al.* 2011). Recently, however, we found that TH content was reduced locally in sympathetic axons in the damaged left ventricle after cardiac ischemia-reperfusion, but not in axon branches projecting to unaffected regions of the heart (Parrish *et al.* 2008). Moreover, TH mRNA was actually increased in the cell bodies of sympathetic neurons projecting to the heart following myocardial infarction (Parrish *et al.* 2008). Cytokine activation of gp130 receptors triggered the local loss of TH (Parrish *et al.* 2010), suggesting that cytokines might directly affect the stability of TH in a portion of the target field of these sympathetic neurons.

TH is a substrate for ubiquitination (Doskeland and Flatmark 2002;Lopez Verrilli *et al.* 2009;Nakashima *et al.* 2011) which targets cells for degradation through the proteasome, the major protein degradation pathway in mammalian cells (Ciechanover 2005). Cytokines stimulate the ubiquitin-proteasome system after nerve injury (Jho *et al.* 2004) making this system an ideal candidate for triggering the loss of TH in the peri-infarct left ventricle. We found that cytokine activation of gp130 increased the ubiquitination of TH in cultured sympathetic

neurons and neuroblastoma cells. In addition, the proteasome inhibitors MG-132 and lactacystin prevented the loss of TH in CNTF-treated cells, while the lysosome inhibitor chloroquine did not (data not shown). Together our data suggest that gp130 cytokines stimulate degradation of TH through the ubiquitin-proteasome system in sympathetic neurons.

The cytokine CNTF stimulated ubiquitination of TH within 30 minutes, consistent with targeting the enzyme for proteasomal degradation. However, significant decreases in TH enzyme levels were not observed until 4 days after cytokine addition. TH is a stable protein with reported half-life ranging from 17 hr to 34 hr in various catecholamine-producing cells (Fernandez and Craviso 1999;Tank *et al.* 1986;Wu and Cepko 1994), and a half-life of several days in adrenal gland (Chuang *et al.* 1975;Mueller *et al.* 1969). The long half-life is consistent with a relatively long lag time to observe the loss of TH protein in cultured neurons. Cytokines also decrease TH mRNA, and ultimately protein synthesis, in sympathetic neurons (Fann and Patterson 1993;Li *et al.* 2003;Nawa *et al.* 1991). However, TH mRNA levels were not significantly decreased until 48 hours after CNTF addition, also consistent with the delay in decreased neuronal TH content. Thus, CNTF stimulates ubiquitination of TH within minutes and decreases enzyme half-life within hours, but depletion of neuronal TH stores is not apparent until several days after exposure.

Our experiments generated half-life values for TH in control cells ranging from 28 to 37 hours, which is consistent with previous reports. Cycloheximide can stabilize TH protein in some cell types (Fernandez and Craviso 1999), but our use of cycloheximide resulted in half-life values consistent with those obtained using other methods. A limitation of our half-life experiments is that we were unable to measure TH levels beyond 24 hours due to cell viability issues. We believe the data are reliable because the resulting half-life values are in line with values in the literature, similar results were obtained using pulse-chase and protein synthesis inhibitors, and CNTF decreased the half-life by a similar amount in both neurons and neuroblastoma cells.

Cytokines such as CNTF activate two primary signaling pathways in sympathetic neurons: JAK/STAT3 and ERK1/2. Activation of both STAT3 and ERK1/2 can regulate protein degradation through the ubiquitin-proteasome system (Niu *et al.* 1998;Ozawa *et al.* 2008). We found that cytokine activation of ERK1/2 was required for both TH ubiquitination and subsequent degradation. Blockade of ERK1/2 activation was sufficient to prevent CNTF-stimulated ubiquitination and degradation of TH as measured by protein half-life. However, inhibiting ERK1/2 activation provided only a partial rescue of TH protein during 5 days of CNTF or LIF treatment, despite completely rescuing TH half-life. CNTF and LIF suppress TH gene expression in addition to their effect on protein turnover, and inhibiting ERK1/2 activation *enhanced* the loss of TH mRNA. Thus, decreased synthesis of new enzyme likely offset the absence of protein

degradation, resulting in a partial rescue of TH protein in cytokine treated cells. In contrast to the clear role for ERK1/2 revealed by our experiments, it is difficult to draw any specific conclusions about the role of STAT3 phosphorylation in TH ubiquitination and degradation. The STAT3 inhibitor STAT3iV increased TH ubiquitination and ERK1/2 phosphorylation (Fig. 2.7), but that effect was independent of CNTF. Other putative STAT3 inhibitors we tested did not prevent phosphorylation of STAT3. Together our data identify a clear role for ERK signaling, but cannot rule out a role for STAT3.

This study revealed that inflammatory cytokines acting through gp130 target TH for proteasomal degradation, leading to the loss of neurotransmitter production in affected neurons. This has important implications for pathologies that involve inflammation and increased production of gp130 inflammatory cytokines. For example, cytokines are elevated in the heart after myocardial infarction (Aoyama *et al.* 2000;Frangogiannis *et al.* 2002;Gwechenberger *et al.* 1999) where they cause local depletion of TH and NE in the left ventricle (Parrish *et al.* 2010). This results in heterogeneity of sympathetic transmission that contribute to development of arrhythmias and sudden cardiac death (Rubart and Zipes 2005). Diet-induced obesity and metabolic dysfunction also result in peripheral inflammation (Elmarakby and Imig 2010;Hotamisligil 2006), which may be tied to the sympathetic dysfunction that occurs in those diseases (Grassi *et al.* 2010;Morgan and Rahmouni 2010). Inflammatory cytokines including IL-6 are also elevated in Parkinson's disease, which is characterized by the loss of TH

(Ciesielska *et al.* 2007). Recent studies indicate that dysfunction in the ubiquitin-proteasome system contributes to dopaminergic neuron degeneration in Parkinson's disease and inhibiting proteasome activity is protective for dopaminergic neurons (McNaught *et al.* 2006;Oshikawa *et al.* 2009). Thus, our study provides an important link between inflammation and the loss of TH in disease states.

In summary, gp130 cytokines increase the degradation of TH through the ubiquitin-proteasome system via an ERK-dependent signaling pathway. Our findings suggest that local effects of inflammatory cytokines on TH stability may modulate neurotransmitter synthesis in a variety of pathological conditions.

Acknowledgements: This work was supported by National Institutes of Health Grant HL068231 (to B. A. H.) and a Tartar Trust Fellowship (to X. S.). The authors have no financial conflict of interest. The authors thank Drs. Philip Stork, Dennis Koop, and William Woodward for helpful discussions, Dr. Suzan Dziennis for technical assistance, Dr. Kwang-Soo Kim (McLean Hospital/Harvard Medical School, Waltham, MA) for SK-N-BE(2)M17 human neuroblastoma cells, and Dr. Dona Chikaraishi (Duke University Medical Center, Durham, NC) for the 4.5TH-fLuc TH promoter construct.

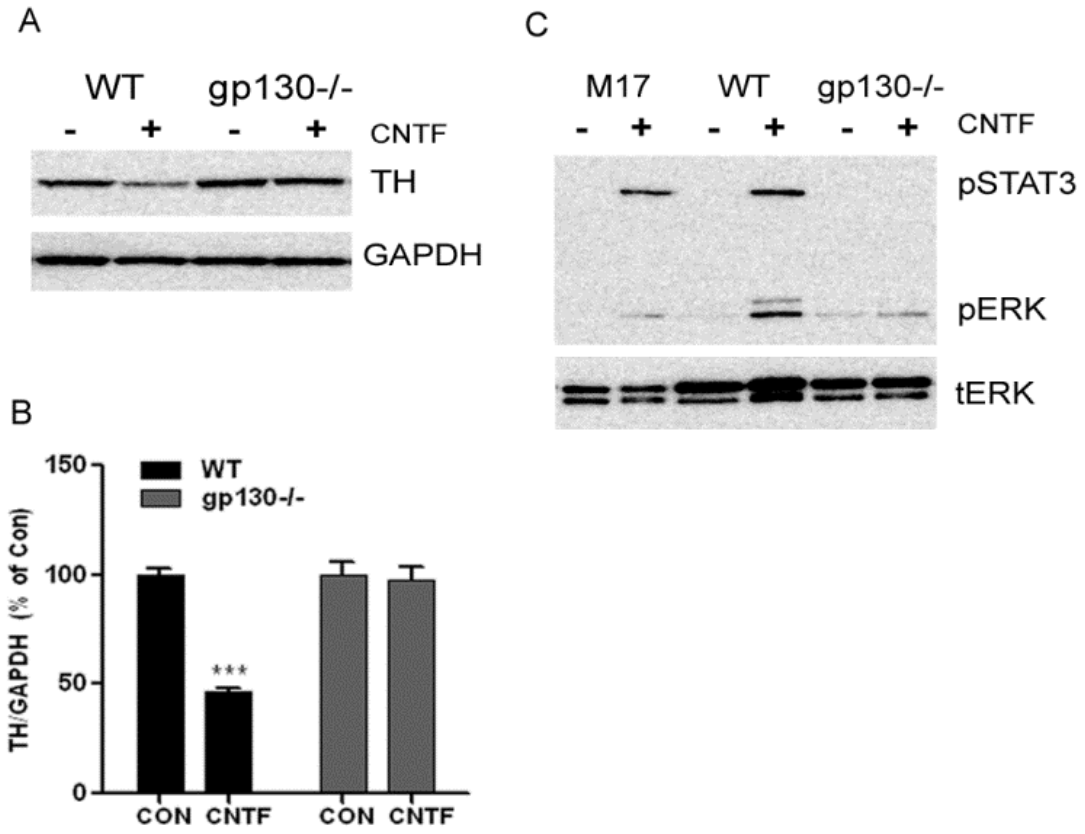

Figure 2.1 CNTF suppresses TH via gp130.

A. A representative western blot showing TH content in wild-type (WT) and gp130-/- sympathetic neurons following 5 days in 100ng/ml CNTF. The blot was stripped and re-blotted for GAPDH to control for protein loading. **B**. Quantification of TH content assayed in triplicate by immunoblot. TH was decreased in WT but not gp130-/- neurons. Data are mean ± SEM, averaged from 3 independent experiments; ***p<0.001. **C**. Phospho-ERK1/2 (p-ERK1/2) and phospho-STAT3 (p-STAT3) were identified by immunoblot in M17 neuroblastoma cells, WT

mouse neurons and gp130-/- neurons treated with CNTF for 15 minutes. Membranes were stripped and re-probed for total ERK (tERK) as a control. Data shown are representative of three experiments assayed in triplicate.

A

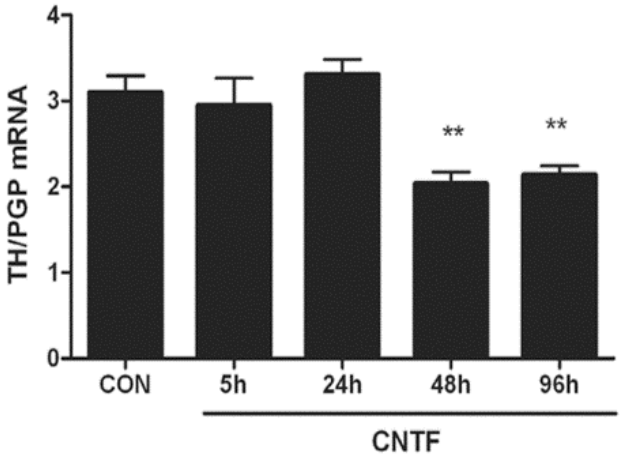

B

Half-life	
CON	28.3 ± 0.7 h
CNTF	12.8 ± 2.2 h **

Figure 2.2 CNTF decreases TH mRNA and protein half-life in sympathetic neurons.

A. Time course of TH mRNA changes following treatment with vehicle (CON) or CNTF. TH mRNA was normalized to the pan-neuronal marker PGP. Data are mean ± SEM, n=3, and are representative of 3 experiments (** $p<0.01$ vs. CON). **B**. TH half-life was quantified by pulse-chase analysis in neurons treated with vehicle (CON) or CNTF. Data are the mean ± SEM averaged from 3 experiments (** $p<0.01$ vs. CON).

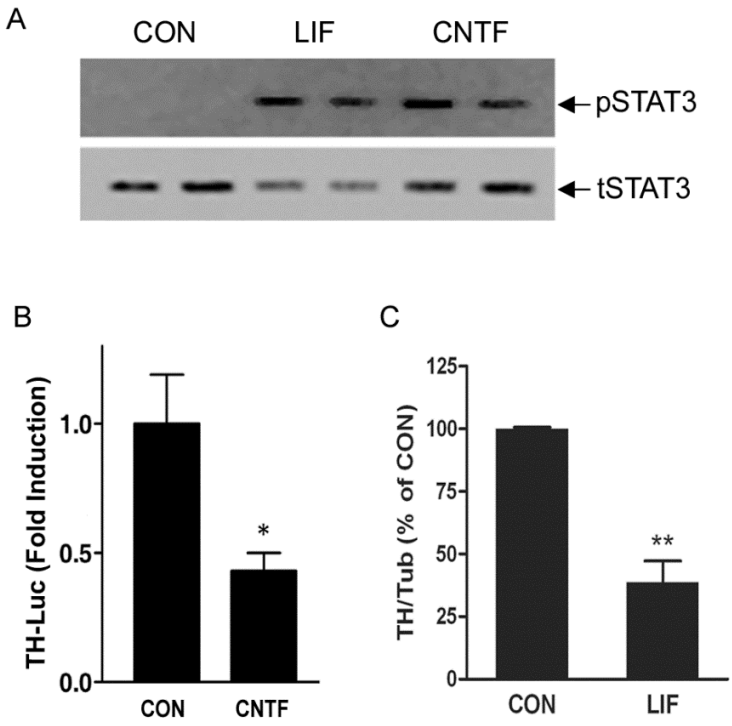

Figure 2.3 CNTF and LIF suppress TH in M17 neuroblastoma cells.

A. Representative blot of phospho-STAT3 (pSTAT3) and total STAT3 (tSTAT3) in M17 cells treated with LIF or CNTF for 15 minutes. **B.** TH transcription was assessed by transfecting (CON) or CNTF-treated M17 cells with the 4.5TH-fLuc reporter construct and pRL-null internal control. Cells were maintained for 2 more days in vehicle or CNTF prior to analysis of luciferase. Data are a ratio of firefly luciferase/renilla luciferase, and are mean ± SEM, n=3 (representative of 3 independent experiments, *p <0.05). C. TH content was quantified in control (CON) and LIF-treated M17 cells by immunoblot and normalized to tubulin. Data are mean ± SEM, averaged from 3 independent experiments (** p<0.01).

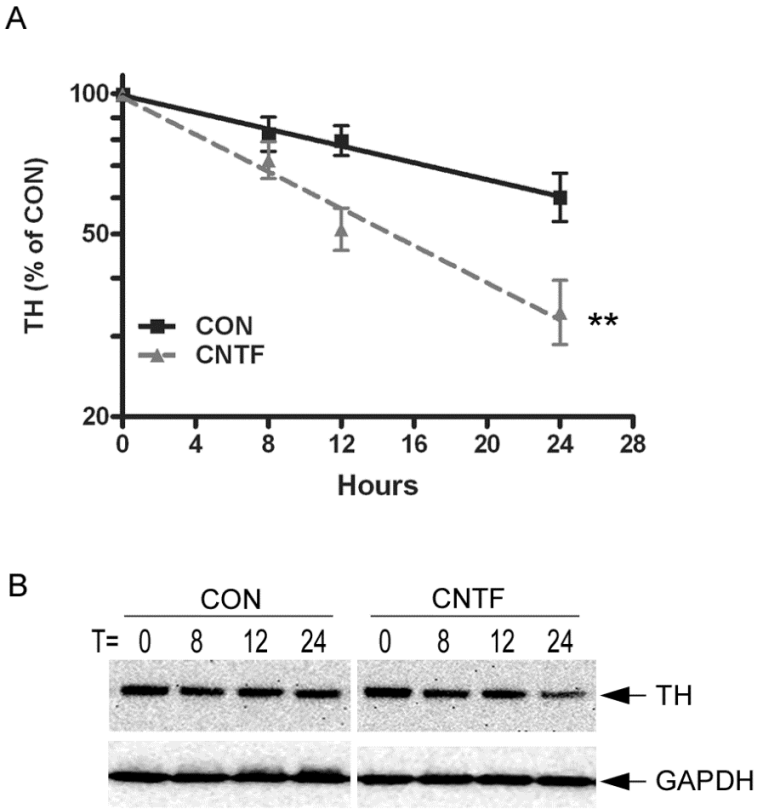

Figure 2.4 CNTF decreases TH half-life.

A. Natural log plot of TH content in control and CNTF treated M17 cells, graphed as percentage of the TH present at time 0. Data shown are the mean of 3 independent experiments ± SEM; ** $p<0.01$. **B**. A representative blot showing TH content at different time points. The blot was stripped and re-probed for GAPDH as a control for protein loading. One replicate is shown, but each time point was assayed in triplicate.

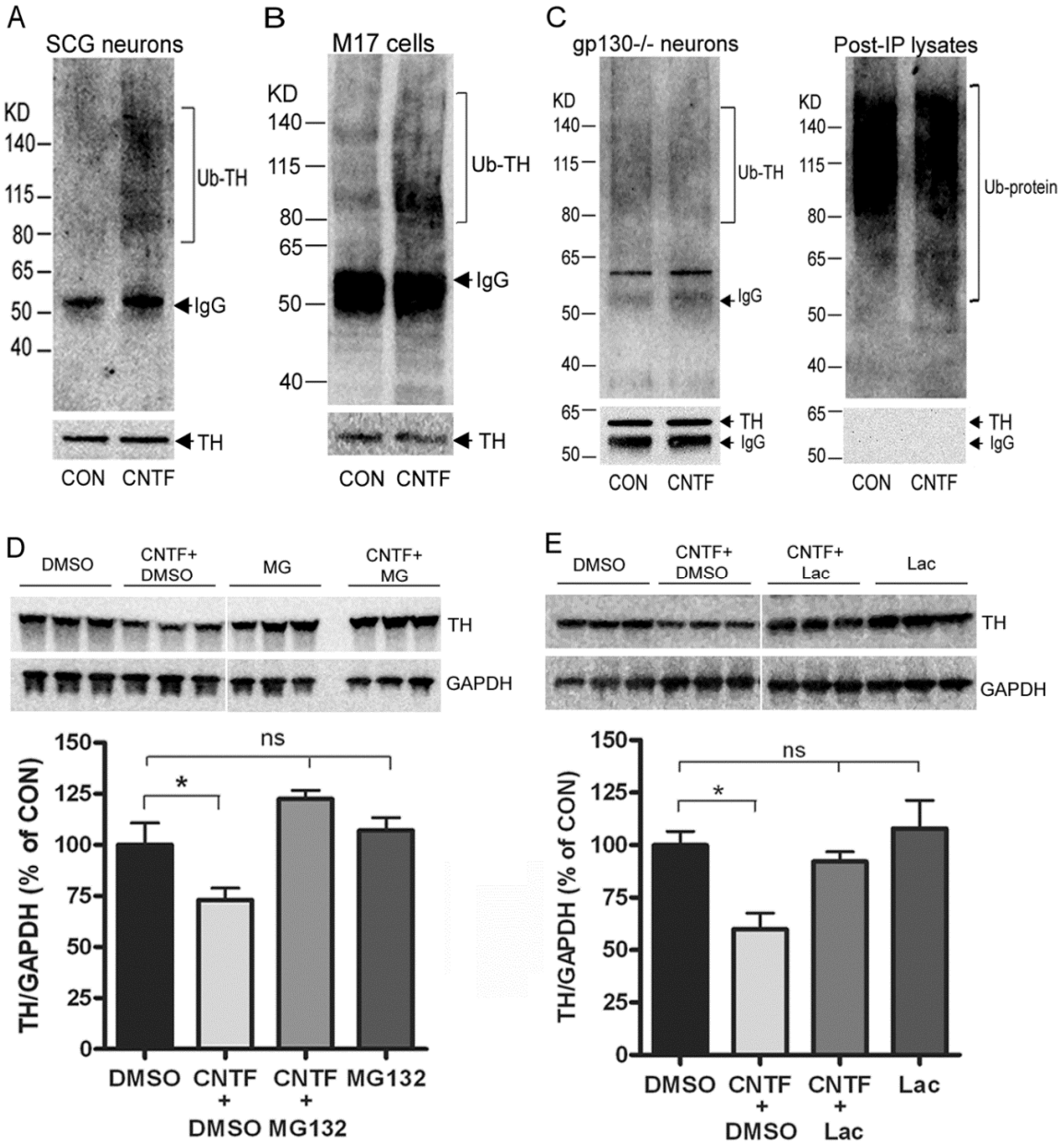
A
SCG neurons
KD
140
115
80
65
50
40
Ub-TH
IgG
TH
CON CNTF
B
M17 cells
KD
140
115
80
65
50
40
Ub-TH
IgG
TH
CON CNTF
C
gp130-/- neurons
KD
140
115
80
65
50
40
Ub-TH
IgG
65
50
TH
IgG
CON CNTF
Post-IP lysates
KD
140
115
80
65
50
40
Ub-protein
65
50
TH
IgG
CON CNTF
D
DMSO
CNTF+ DMSO
MG
CNTF+ MG
TH
GAPDH
TH/GAPDH (% of CON)
150
125
100
75
50
25
0
ns
*
DMSO
CNTF + DMSO
CNTF + MG132
MG132
E
DMSO
CNTF+ DMSO
CNTF+ Lac
Lac
TH
GAPDH
TH/GAPDH (% of CON)
150
125
100
75
50
25
0
ns
*
DMSO
CNTF + DMSO
CNTF + Lac
Lac

Figure 2.5 CNTF stimulates ubiquitination and proteasomal degradation of TH.

A-C. Ubiquitinated TH in wild type sympathetic neurons (**A**, SCG), M17 neuroblastoma cells (**B**, M17 cells), and sympathetic neurons lacking gp130 (**C**, gp130-/- neurons). All cells were treated for 30 min with 100 ng/ml CNTF. TH was immunoprecipitated and blotted with an anti-ubiquitin antibody. Blotting for total TH confirmed similar amounts of TH protein pulled down in the different treatment conditions, while no TH was detected in the post-IP lysate. Ubiquitin-conjugated TH is increased in wild type neurons and M17 cells, but not gp130-/- neurons. **D, E**. Sympathetic neurons were treated with 100 ng/mL CNTF for 4 days. During the last 2 days cells were also treated with 0.1% DMSO vehicle or the proteasome inhibitor (**D**) MG-132 (100 nM) or (**E**) lactacystin (Lac, 100 nM). TH was quantified in triplicate by western blot and the membrane stripped and blotted for GAPDH. Representative blots are shown along with their quantification (mean ± SEM, n=3, *$p<0.05$). Each inhibitor was tested in at least 3 independent experiments.

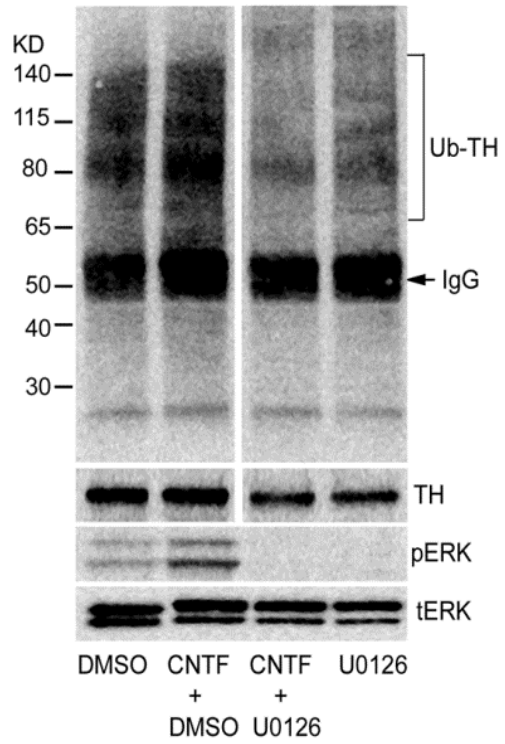

Figure 2.6 ERK1/2 activation is required for CNTF stimulated TH ubiquitination.

Sympathetic neurons were treated with CNTF for 30 min, with or without 10 μM U0126 to prevent ERK1/2 activation. TH was immunoprecipitated and immunoblotted with anti-ubiquitin antibody. Total TH levels were identified by immunoblot as a control. CNTF-induced phosphorylation of ERK1/2 was blocked by U0126, but total ERK1/2 was unchanged. Representative of at least 3 independent experiments.

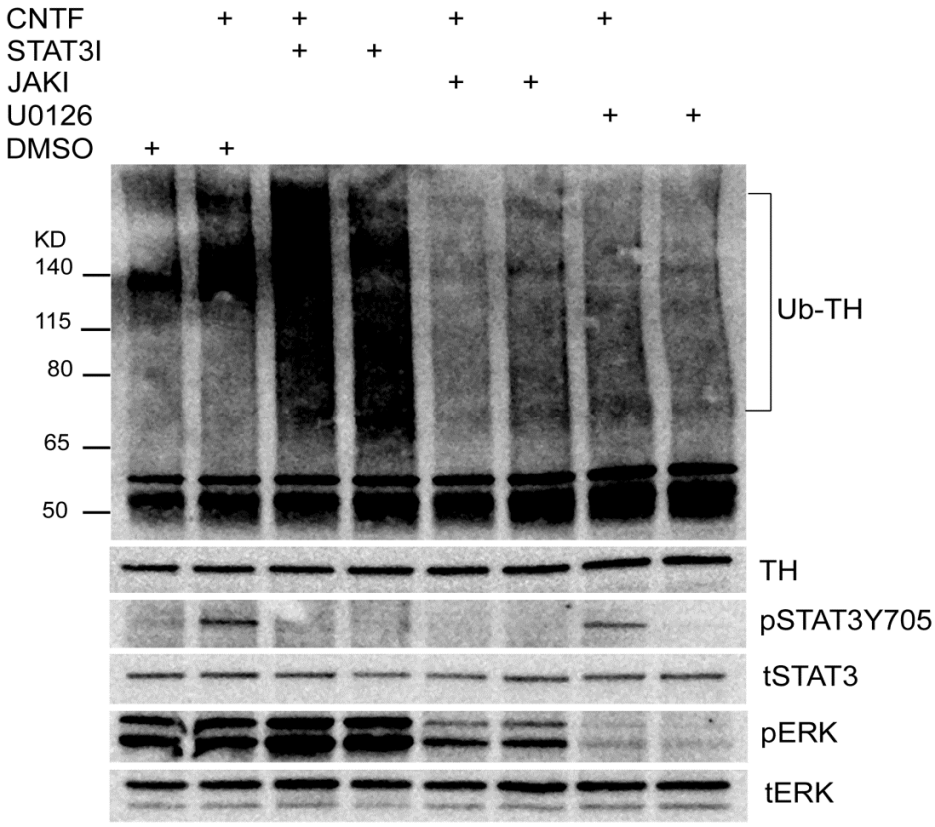

Figure 2.7 Intracellular signaling involved in TH ubiquitination.

Cultured sympathetic neurons were treated with CNTF for 30 min in the presence or absence of JAK inhibitor (JAKI, 2 μM), U0126 (10 μM, UO), or STAT3I (20 μM) to block phosphorylation of STAT3. TH was immunoprecipitated and blotted with an anti-ubiquitin antibody. Additional aliquots from the same cells were blotted for phospho-STAT (pSTAT3Y705) and phospho-ERK1/2 (pERK). Total TH, ERK1/2, and STAT3 were blotted to control for protein loading. Data shown are representative of at least 3 independent experiments.

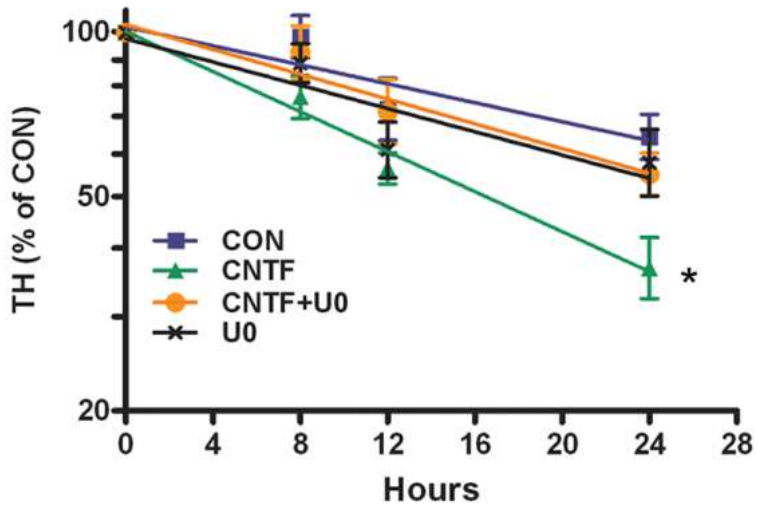

Figure 2.8 ERK1/2 activation is required for cytokine-induced TH protein turnover.

The natural log plot of TH content in M17 cells, graphed as percentage of the TH present at time 0, is shown. Data are the mean of 3 independent experiments ± SEM; * $p<0.05$ vs. control. Each condition was assayed in triplicate for each experiment. Calculated half-life: Control 33.3 ± 3.6 hr, CNTF 16.3 ± 0.5* hr, CNTF+U0 27.0 ± 3.5 hr, U0 28.3 ± 2.4 hr, n=3 experiments.

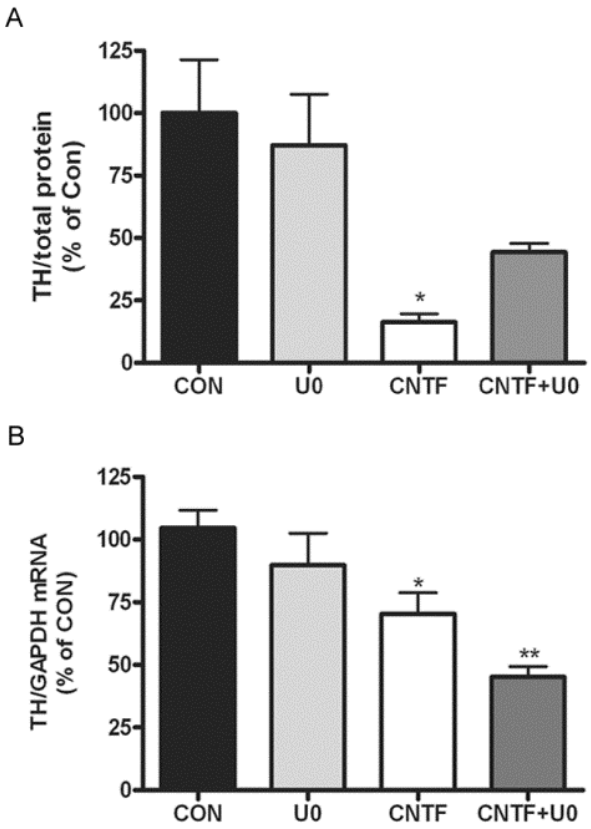

Figure 2.9 Blocking ERK activation blunts CNTF suppression of TH protein but exacerbates loss of TH mRNA.

Sympathetic neurons were treated with 100 ng/ml CNTF for 5 days with or without U0126 (10 μM). **A**. TH protein was quantified by immunoblot and normalized to total protein. Data are from a representative experiment, mean ± SEM, n=3, * $p<0.05$ vs. control. **B**. TH mRNA was quantified by real-time PCR and normalized to GAPDH mRNA. Data are from a representative experiment, mean ± SEM, n=3, ** $p<0.01$, * $p<0.05$. All data are representative of three independent experiments.

Chapter 3

Ciliary neurotrophic factor stimulates tyrosine hydroxylase activity

Xiao Shi, William R. Woodward, and Beth A. Habecker

Department of Physiology and Pharmacology, Oregon Health & Science University, Portland, OR, 97239, USA

Corresponding Author: Beth A. Habecker, PhD,

Chapter 3 is a manuscript that appears as it was published in:

Journal of Neurochemistry, 2012, Volume 121, p. 700-704

Abstract

Tyrosine hydroxylase (TH) is the rate limiting enzyme in norepinephrine synthesis, and its expression and activity are regulated by many factors in sympathetic neurons. Cytokines that act through gp130, such as CNTF (ciliary neurotrophic factor) decrease norepinephrine production in sympathetic neurons by suppressing TH mRNA and stimulating degradation of TH protein, leading to the loss of enzyme. Their effect on the activity of TH is unclear, but recent *in vivo* observations suggest that cytokines may stimulate TH activity. We investigated this issue by quantifying TH protein levels and activity in cultured sympathetic neurons. We also examined the state of TH phosphorylation on Serine 31 and 40, sites known to affect TH activity and degradation. We found that CNTF, acting through gp130, stimulated the rate of L-DOPA (L-3, 4-dihydroxyphenylalanine) production while at the same time decreasing TH enzyme levels, thereby increasing the specific activity of the enzyme. We also found that phosphorylation of TH on Ser31 was increased, and phosphorylation on Ser40 was decreased, after four days of CNTF exposure. Our data are consistent with previous findings that Ser31 phosphorylation stimulates TH activity, whereas Ser40 phosphorylation can target TH for proteasomal degradation.

Introduction

Tyrosine hydroxylase (TH), the rate limiting enzyme in norepinephrine synthesis, catalyzes the hydroxylation of L-tyrosine to form L-3, 4-dihydroxyphenylalanine (L-DOPA). Many factors are known to regulate both the activity and expression of this enzyme including nerve activity, catecholamines, neurotrophins, and inflammatory cytokines (Dunkley *et al.* 2004;Landis 1996;Lewis-Tuffin *et al.* 2004). For example, acute stimulation of sympathetic nerves or depolarization of PC12 cells increases TH activity via phosphorylation (Salvatore *et al.* 2001;Zigmond *et al.* 1989), while chronic nerve stimulation or cell depolarization increases TH mRNA and protein levels (Lewis-Tuffin *et al.* 2004;Zigmond 1980;Zigmond 1988).

In contrast to the stimulatory effects of nerve activity, inflammatory cytokines that act through gp130, such as LIF (leukemia inhibitory factor) and CNTF (ciliary neurotrophic factor), decrease TH content and catecholamine production in sympathetic neurons (Saadat *et al.* 1989;Yamamori *et al.* 1989). These cytokines decrease TH mRNA (Lewis *et al.* 1994;Nawa *et al.* 1991) and stimulate the proteasomal degradation of TH protein (Shi and Habecker 2012), leading to the loss of enzyme. Their effect on TH activity is unclear, but recent *in vivo* observations suggest that cytokines may stimulate TH activity. TH enzyme levels in the peri-infarct region of the left ventricle, corrected for neuronal loss, are reduced by ~70-80% following myocardial infarction (Li *et al.* 2004;Parrish *et*

al. 2008;Parrish *et al.* 2009). The loss of peri-infarct TH is triggered by cytokines, and is absent in mice whose sympathetic neurons lack the gp130 receptor (Parrish *et al.* 2008). However, peri-infarct NE levels are similar in wild type and gp130 knockout mice (Parrish *et al.* 2009), despite the depletion of TH in wild type neurons. These data suggest the possibility that inflammatory cytokines influence TH enzyme activity in addition to their effect on enzyme levels.

We examined this issue by treating cultured sympathetic neurons with recombinant CNTF, and measuring TH protein levels by western blot analysis and TH activity using an HPLC method to measure L-DOPA production. We also examined the state of TH phosphorylation on Ser31 and Ser40, sites that are thought to affect TH activity (Daubner *et al.* 2011;Dunkley *et al.* 2004) and TH turnover (Nakashima *et al.* 2011).

Methods:

Animals

Pregnant adult Sprague Dawley rats were obtained from Charles River. Wildtype C57BL/6J mice were obtained from Jackson Laboratories. The $gp130^{DBH\text{-}Cre/lox}$ mice, whose sympathetic neurons lack gp130, were generated as previously described (Stanke *et al.* 2006). All animals were housed individually with a 12 hr:12 hr light dark cycle with *ad libitum* access to food and water. All procedures

were approved by the Institutional Animal Care and Use Committee, and comply with the Guide for the Care and Use of Laboratory Animals published by the US National Institutes of Health (NIH publication No. 85-23, revised 1996).

Primary Cell culture

Superior cervical ganglia (SCG) from newborn rats or mice (P0-P1) were dissociated and grown in cell culture as previously described (Dziennis and Habecker 2003;Shi and Habecker 2012) using C2 medium supplemented with 50 ng/mL nerve growth factor (NGF, BD Bioscience), and 3% fetal bovine serum (ATCC)(Pellegrino *et al.* 2011). Neurons were grown under sterile conditions in a humidified 5% CO_2 incubator at 37°C. Sympathetic neurons were grown in 24-well plates pre-coated with 100 µg/mL poly-L-lysine (Sigma) and 10 µg/mL collagen (BD bioscience). Non-neuronal cells were eliminated by treating the cultures with the anti-mitotic agent, cytosine arabinoside (Ara C, 1 µM, Sigma) for 2 days.

Recombinant CNTF (100 ng/mL, Pepro Tech) was diluted in culture medium before addition to the culture plates. Neurons were maintained in 100 ng/mL CNTF for 4 days because previous studies showed that TH content was reliably

decreased by this treatment paradigm (Shi and Habecker 2012), mimicking the cytokine-induced loss of enzyme *in vivo* (Parrish *et al.* 2010).

In vitro TH enzyme activity assay

Cultures of sympathetic neurons (20,000 cells/sample for rat cultures or 12,000 cells/sample for mouse) were homogenized in 150 µL of 5 mM Tris-acetate buffer (pH 6.0) containing 0.1% Triton X-100, protease inhibitor cocktail (Roche) and sodium orthovanadate (1 mM). TH enzyme activity was determined by measuring the initial rate of L-DOPA production from L-tyrosine under standardized conditions (Acheson *et al.* 1984). A 60 µL aliquot of the homogenate was combined with an equal volume of reaction buffer and assayed for TH activity under the following conditions: 120 mM Tris-acetate buffer (pH 6.0), 3 mM 6-methyl-5, 6, 7, 8 tetrahydropterin HCl (BH4), 10 mM 2-mercaptoethanol, catalase (200,000 U/mL), 100 µM L-tyrosine, and the internal standard, 1.0 µM 3,4-dihydroxybenzylamine (DHBA). The reaction mixtures were incubated at 37°C. Aliquots (20 µL) of the reaction mixture were removed at regular intervals (every 3 min. for rat cultures and every 4 min. for mouse cultures) and added to 1 mL of a chilled solution containing 0.5 M Tris-acetate buffer (pH 8.0), 0.1 M EDTA, and 15 mg of alumina to stop the reaction. The L-DOPA and DHBA were purified by an alumina extraction procedure described previously (Li *et al.* 2004), and the

production of L-DOPA was measured by HPLC using electrochemical detection as previously described (Li *et al.* 2004).

Immunoblot Analysis

Cells were washed with ice-cold PBS and lysed at 4°C in homogenization buffer as described above. Lysates were fractionated on SDS-polyacrylamide gels and transferred to nitrocellulose membranes. Blots were incubated in 5% low fat milk in Tris-buffered saline (pH 7.4) containing 0.1% tween-20 at room temperature. Membranes were subsequently incubated at 4°C overnight with rabbit anti-TH (1:5000, Millipore), rabbit anti-pTH Ser31 (1:1000, Cell Signaling), or rabbit anti-pTH Ser40 (1:1000, Cell Signaling). The immunoblots were incubated with horseradish peroxidase HRP - conjugated secondary antibody and immune complexes were visualized by chemiluminescence (Super Signal Dura, Pierce). Band intensity was recorded by a -40ºC CCD camera and analyzed using LabWorks software (UVP, Upland, CA), quantifying only sub-saturating exposures. To quantify TH phosphorylation levels, the band density obtained for phospho-specific TH was normalized to the total TH protein in that sample. Total and mean band density gave similar results.

Statistical analyses

Data are presented as mean values± SEM. Significant differences were assessed by one-way analysis of variance (ANOVA) using GraphPad Prism 5 (GraphPad Software, Inc.). Tukey's post hoc test was used to compare to all conditions. P values <0.05 were considered significant.

Results:

In order to determine if cytokines alter neurotransmitter production in sympathetic neurons, we treated sympathetic neuron cultures with 100 ng/mL CNTF for 4 days, and then measured TH activity in cell homogenates. Cytokines significantly decreased TH protein levels after 4 days (Fig. 3.1A & B). TH activity was quantified by measuring the initial rate of L-DOPA formation under standardized conditions (Acheson *et al.* 1984) by a sensitive HPLC method using electrochemical detection (Li *et al.* 2004). Under these conditions, L-DOPA production in control cells was linear with respect to protein concentration and time (Fig. 3.1C). We normalized the rate of L-DOPA formation in each condition to the total amount of TH protein present, as determined by western blotting. The rate of L-DOPA production, corrected for TH protein levels, was significantly increased by CNTF treatment (Fig. 3.1D). In order to rule out the possibility L-DOPA was further converted to dopamine by aromatic amino acid decarboxylase under our assay conditions, we examined the reaction mixture for the presence of dopamine by HPLC but were unable to detect it. Moreover, the present or

absence of carbidopa, an aromatic amino acid decarboxylase inhibitor, in the reaction mixture did not alter the rate of L-DOPA formation (data not shown).

Cytokine suppression of TH content requires activation of the gp130 receptor. Therefore, we asked whether the CNTF-stimulated increase in TH activity was gp130-dependent. Cultures of neurons from wild type mice and from mice whose sympathetic neurons lack gp130 were treated with CNTF for 4 days, and TH activity was assayed. CNTF increased the specific activity of TH in wild type neurons as previously shown in rat sympathetic neurons, but had no effect on TH activity in neurons lacking gp130 signaling (Fig. 3.2). This confirms that CNTF influences TH activity through the gp130 receptor, and that similar changes occur in neurons derived from rat and mouse.

Changes in the phosphorylation of TH can regulate TH activity and catecholamine production. To determine if the CNTF-induced changes in TH activity correlated with changes in TH phosphorylation, we used western blots to assess the phosphorylation of two key sites, Ser31 and Ser40, thought to be involved in the regulation of TH activity (Fig. 3.3 A). In untreated control neurons, the ratio of phospho-Ser31 (pSer31) to total TH averaged 0.8 ± 0.1 (mean ± sem, n=3 experiments) while the ratio of pSer40 to total TH averaged 2.0 ± 0.5 (mean ± sem, average of 3 experiments). One day of CNTF treatment increased the portion of TH that was phosphorylated on Ser31 (165 ± 11% of control; mean ± sem, n=3 experiments) and decreased the fraction of TH phosphorylated on

Ser40 (57 ± 14 % of control; mean ± sem, n=3 experiments). These changes were maintained through four days of CNTF treatment, with more TH phosphorylated on Ser31 and less phosphorylated on Ser40 compared to control cells (Fig.3.3). Data from a representative experiment are graphed in Figure 3.3 (B, C) as the ratio of phospho TH/total TH rather than percent of control.

Discussion

Following myocardial infarction, cytokines acting through the gp130 receptor reduce the levels of TH enzyme in sympathetic neurons in the peri-infarct region of the left ventricle. Myocardial infarction studies in mice whose sympathetic neurons lack the gp130 receptor suggested that cytokines might cause a compensatory increase in the activity of TH that at least partially counteracts the loss of enzyme (Parrish *et al.* 2010). We confirmed that prediction in the present study. The specific activity of TH in sympathetic neurons treated with CNTF is ~80% greater than that in untreated neurons. Furthermore, in neurons lacking gp130 signaling, the specific activity of TH and level of TH protein in CNTF treated cells was the same as that in untreated neurons. These results suggest that CNTF, acting through the gp130 receptor complex, influences not only the level TH protein but also the activity of the enzyme.

In order to compare the activity of TH enzyme in cultured sympathetic neurons, we developed an HPLC assay to measure the initial rate of L-DOPA production under standardized conditions in which the substrates, L-tyrosine and BH4, were present in saturating concentrations (Acheson *et al.* 1984). We have shown that under our assay conditions L-DOPA production is linear for at least 16 minutes and increased with increasing volume of homogenate. Our assays attempted to control factors that could potentially affect our comparisons of TH activity. For example, we ruled out further metabolism of L-DOPA by showing that carbidopa, a decarboxylase inhibitor, had no effect on the rate of L-DOPA production and that dopamine was undetectable even at reaction times as long as 60 minutes.

Our observation that CNTF stimulates TH enzyme activity conflicts with earlier reports that TH activity was either unchanged or decreased in neurons treated with inflammatory cytokines (Iacovitti *et al.* 1981;Swerts *et al.* 1983;Wolinsky and Patterson 1983). Several factors could account for the discrepancy between our results and those of the earlier studies with respect to the effect of cytokines on TH activity. First, previous studies used conditioned media and tissue extracts which are mixtures of cytokines and other factors that may influence TH activity (Iacovitti *et al.* 1981;Swerts *et al.* 1983;Wolinsky and Patterson 1983), whereas we used recombinant CNTF. Second, we treated the neurons for 4 days while other studies treated cultured neurons for several weeks and maintained the cultures in different media and growth factor conditions. Finally, we quantified L-DOPA production using HPLC with

electrochemical detection, a more sensitive assay of TH activity than measuring the accumulation of labeled catecholamines. For these reasons, we have confidence that CNTF and related cytokines increase the activity of TH in addition to decreasing TH levels.

The mechanism of how CNTF influences TH activity is not entirely clear and needs additional investigation. One possibility is that CNTF affects TH activity by a post-translational modification, such as altering the phosphorylation state of the enzyme. TH is phosphorylated at several serine residues: Ser8, Ser19, Ser31, and Ser40 (Daubner *et al.* 2011;Dunkley *et al.* 2004). Phosphorylation of Ser31 and Ser40 are clearly associated with stimulation of TH activity (Bobrovskaya *et al.* 1998), with less evidence for Ser8 or 19 playing a direct role in stimulating TH catalytic activity (Daubner *et al.* 2011;Dunkley *et al.* 2004). We investigated the effect of CNTF treatment on pSer31 and pSer40, and found that chronic treatment with CNTF increased the fraction of TH phosphorylated on Ser31 while decreasing the fraction of TH phosphorylated on Ser40. The increased phosphorylation at Ser31 may contribute to the stimulation of TH activity observed in our study. This is consistent with studies of depolarization-induced stimulation of TH, where phosphorylation of Ser31 stimulated TH activity while increases in Ser40 phosphorylation had no effect on catecholamine production (Salvatore *et al.* 2001). The major kinases that phosphorylate TH on Ser31 are ERK1/2 (Dunkley *et al.* 2004). CNTF stimulates ERK1/2 activation in sympathetic neurons (Dziennis and Habecker 2003;Shi and

Habecker 2012), suggesting that CNTF stimulation of ERK 1/2 activity is responsible for the increase in Ser31 phosphorylation. Ser31 (and Ser40) phosphorylation can increase TH activity by altering the binding affinity of TH for its cofactor, BH_4. However, BH_4 is present in saturating concentrations under our assay conditions, so the specific mechanism by which CNTF increases TH activity in our study remains unknown.

Phosphorylation of TH affects enzyme stability in addition to altering catalytic activity (Mockus *et al.* 1997;Moy and Tsai 2004;Nakashima *et al.* 2011). The observation that phosphorylation at Ser40 targets TH for degradation by the ubiquitin-proteasome system is of particular interest (Nakashima *et al.* 2011). CNTF increases proteasomal degradation of TH in sympathetic neurons (Shi and Habecker 2012), contributing to the loss of enzyme observed in our experiments. Thus, the decrease in Ser40 phosphorylated TH our studies may result from degradation of that pool of enzyme rather than changes in kinase or phosphatase activity. Our results, taken together with previous studies of TH phosphorylation, suggest that CNTF-stimulated Ser31 phosphorylation contributes to the increase in TH activity, whereas Ser40 phosphorylation may target TH for proteasomal degradation. These contradictory effects of inflammatory cytokines on TH have interesting implications for neurodegenerative diseases, where cytokines may promote the loss of TH protein while at the same time increasing the catalytic activity of remaining enzyme.

Acknowledgements: This work was supported by NIH R01 HL068231. The authors have no financial conflict of interest.

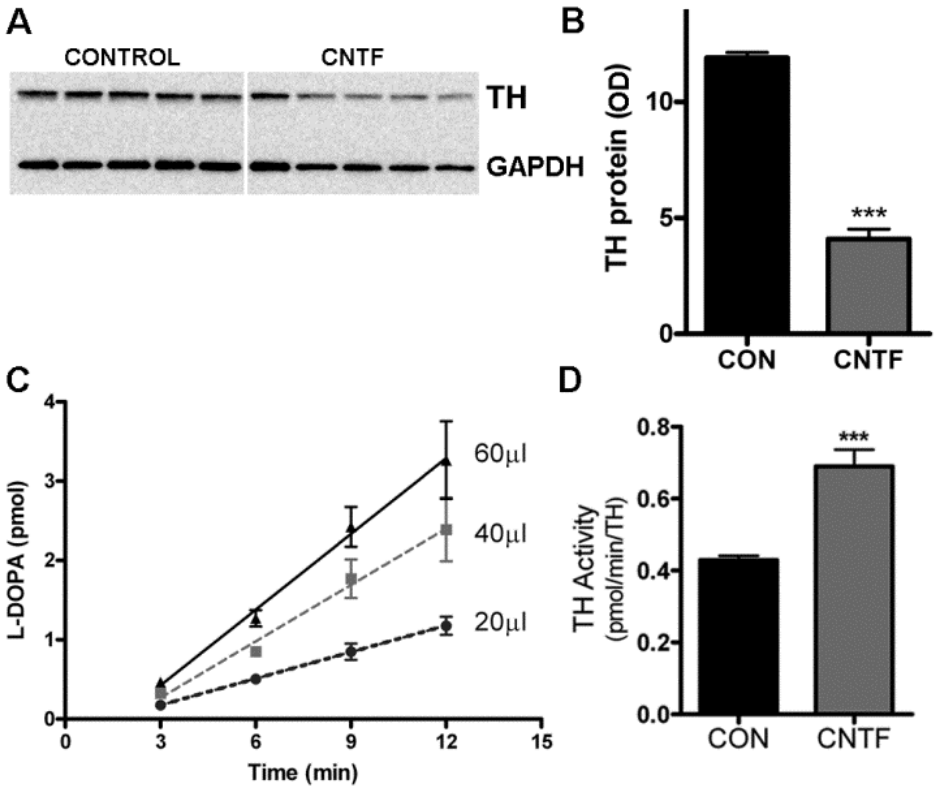

Figure 3.1 CNTF increases TH activity while decreasing TH levels.

A&B) TH content was assayed by western blot. A representative blot identifying TH and GAPDH in 5 control and 5 CNTF-treated samples is shown in **(A)**, with quantification of TH by optical density units (OD) shown in **(B)**. Data are mean±sem, n=5 samples, ***p<0.001, and are representative of results from 3 independent experiments. **C)** TH activity was quantified by measuring the initial rate L-DOPA synthesis. L-DOPA production in control cells was linear with respect to protein concentration and time. Slopes for 20, 40, and 60 µL samples were 0.1 ± 0.01, 0.2 ± 0.03, and 0.3 ± 0.04 pmol L-DOPA/min, respectively. **D)** TH specific activity in neurons treated with control media (CON) or 100 ng/ml

CNTF for 4 days (mean±sem, n=5 samples, ***p<0.001). Data are representative of 3 independent experiments. Activity was calculated as the rate of L-DOPA production normalized to TH content in the cell (pmol L-DOPA/min/OD unit of TH).

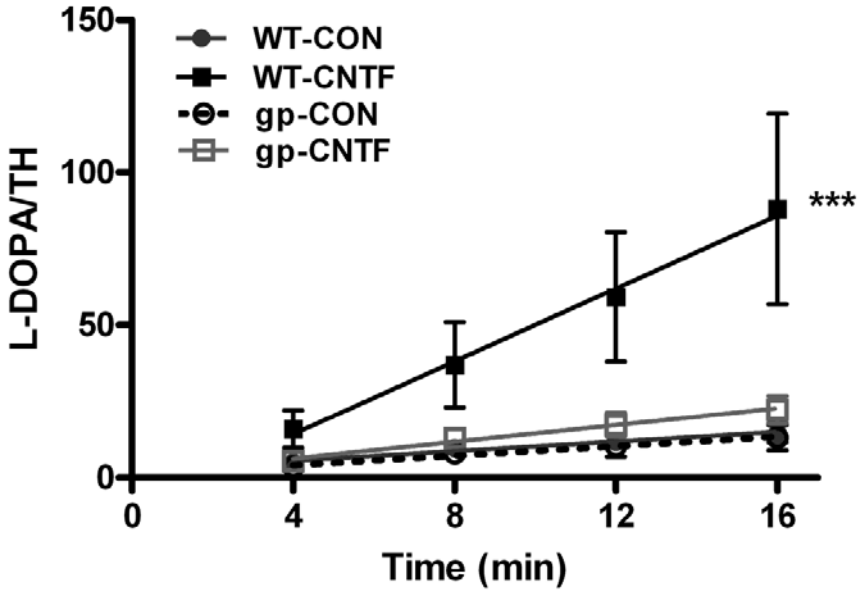

Figure 3.2 CNTF stimulates TH activity via gp130.

Wild type (WT) sympathetic neurons and neurons lacking gp130 (gp) were maintained for four days in control media (CON) or in media supplemented with 100 ng/ml CNTF. TH activity was quantified by measuring the rate of L-DOPA formation (pmol) normalized to TH content (OD units). Data are mean±sem, n=3 samples, ***p<0.005, and are representative of 2 independent experiments.

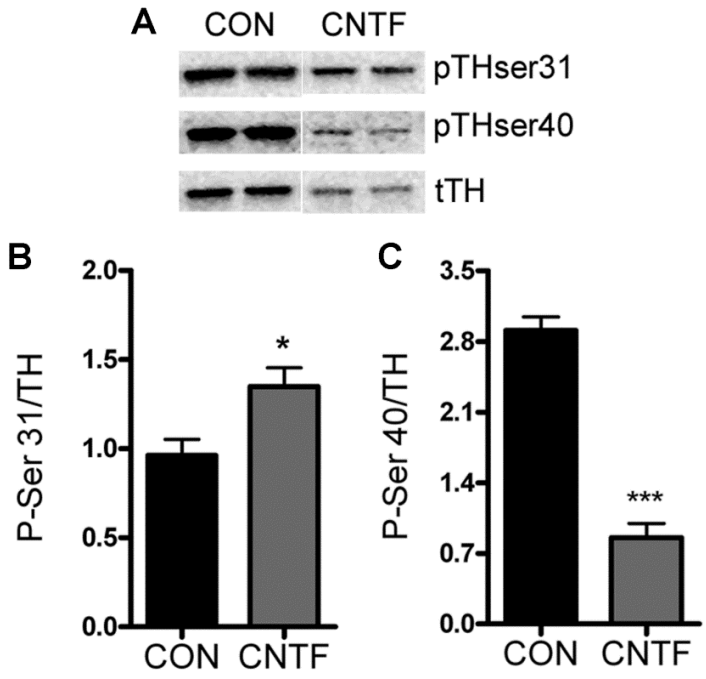

Figure 3.3 TH phosphorylation.

Neurons were treated for four days with control media (CON) or media supplemented with 100 ng/ml CNTF and blotted for total and phosphorylated TH. A) Sample western blot showing total TH (tTH), TH phosphorylated on Ser31 (pTHser31), and TH phosphorylated on Ser40 (pTHser40) in the same samples. B) Quantification of Ser31 phosphorylated TH normalized to total TH. Data are mean±sem, n=4-5 samples, *$p<0.05$. C) Quantification of Ser40 phosphorylated TH normalized to total TH. Data are mean±sem, n=5 samples, ***$p<0.0001$. These data are representative of results from 3 independent experiments.

Chapter 4 Discussion and Future Directions

4.1 Summary of the results

Cytokines suppress TH during development and nerve injury (Rao *et al.* 1993;Stanke *et al.* 2006;Sun *et al.* 1996). Suppression of TH mRNA was thought to be the mechanism, but the studies presented in this dissertation showed that cytokines have a direct effect on TH protein in addition to suppressing TH mRNA. At the same time, cytokines stimulated a compensatory increase in TH activity (Fig. 4.1). Cultured sympathetic neurons and SK-N-BE (2) M17 neuroblastoma cell line were used to investigate the molecular mechanism of cytokine suppression of TH. The studies in Chapter 2 showed for the first time that inflammatory cytokines can stimulate proteasomal degradation of TH in catecholaminergic neurons. I showed that gp130 cytokines, such as CNTF, decreased TH half-life in sympathetic neurons and neuroblastoma cells, suggesting an increase TH protein turnover. CNTF induced TH ubiquitination and stimulated TH proteasomal degradation. ERK1/2 was required for CNTF-induced TH ubiquitination and the associated decrease in TH half-life. In chapter 3, I showed that CNTF increased TH specific activity, which partially offsets the depletion of enzyme in neurons exposed to cytokines. Increased phosphorylation of TH at Ser31 after four days CNTF treatment was associated with stimulation of TH activity. Decreased phosphorylation at Ser40 was detected and may contribute to increase TH proteasomal degradation. Thus, cytokines influence not

only the level of TH protein, but also the activity of the enzyme. These studies have important implications for local regulation of neurotransmission at the site of inflammation and contribute to understanding the dysfunction and degeneration of catecholaminergic neurons in neurologic diseases which are affected by inflammatory cytokines.

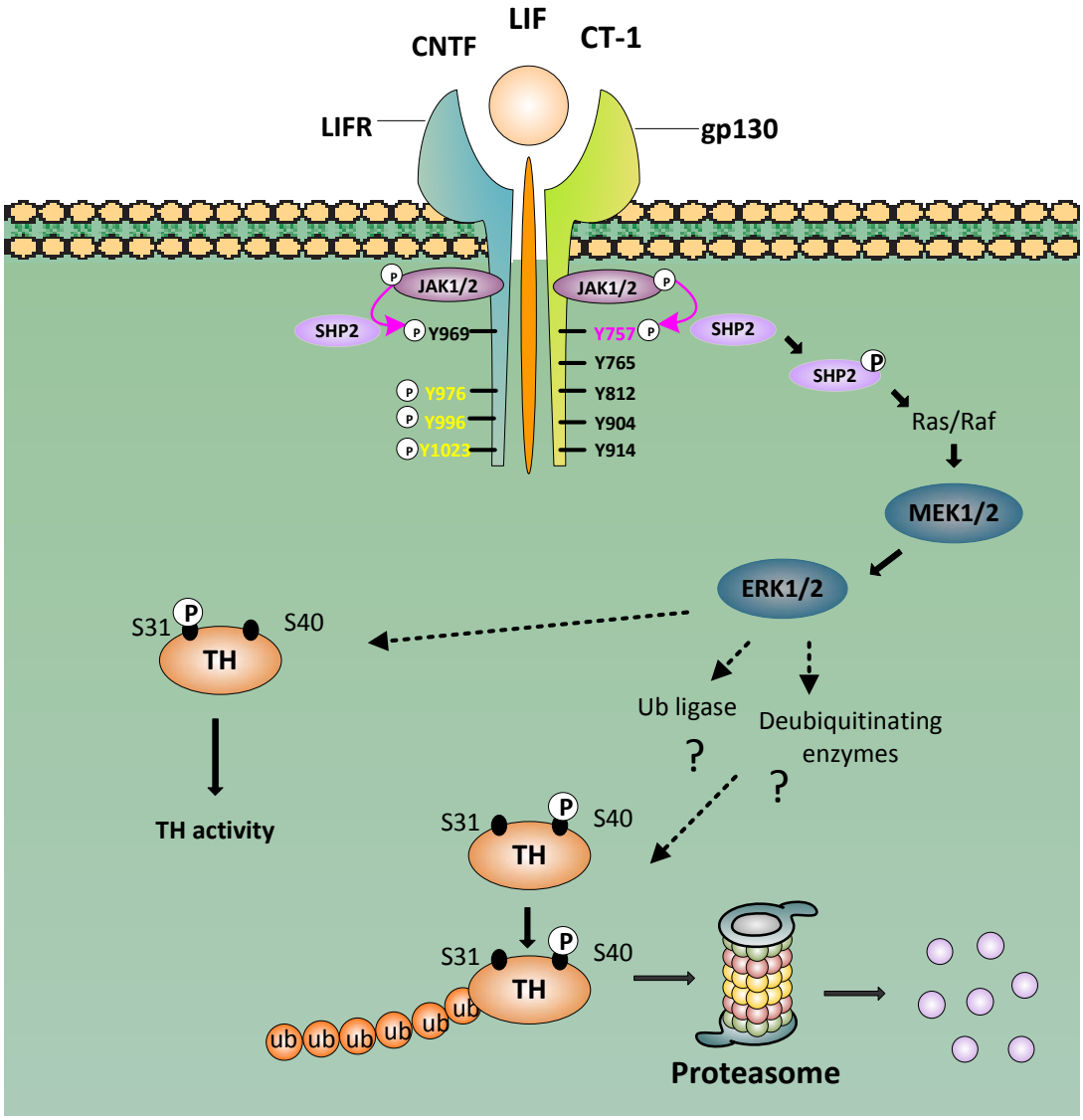

Figure 4.1 Schematic diagram showing the action of cytokines on TH degradation and activity.

4.2 The mechanism of cytokine suppression of TH

4.2.1 Cytokines induce TH degradation

In vivo studies indicated that TH protein levels were depleted in the peri-infarct left ventricle after myocardial infarction, while TH mRNA was elevated in the sympathetic neurons innervating the heart (Parrish *et al.* 2008;Parrish *et al.* 2010). This suggested that cytokines had a local effect in TH protein stability in the axon. Increased TH protein degradation would lead to decreased TH protein levels despite increased TH mRNA in the cell body. TH can be degraded through the ubiquitin-proteasome system (Doskeland and Flatmark 2002;Lopez Verrilli *et al.* 2009), and TH ubiquitination can be regulated by extracellular stimuli (Lopez Verrilli *et al.* 2009), making the ubiquitin-proteasome pathway a good candidate for the loss of TH in the heart. Therefore, I hypothesized that gp130 cytokines stimulated TH proteasomal degradation in sympathetic neurons (Chapter 2). The data in chapter 2 support my hypothesis that cytokines stimulate TH turnover.

Cytokines induced TH ubiquitination in sympathetic neurons within 30 to 60 minutes. However, it took four to five days to detect decreased TH protein levels. One explanation is that TH is a long half-life protein, with reported half-life of about 17-30 hours in PC-12 cells and chromaffin cells (Chuang *et al.* 1975;Mueller *et al.* 1969;Tank *et al.* 1986;Wu and Cepko 1994). In my study, TH half-life was about 28 hours in sympathetic neurons and 36 hours in the SK-N-BE

(M17) neuroblastoma cell line. TH mRNA was not affected by cytokines until two days later (chapter 2). Taking continuing synthesis and slow degradation together, it takes days to see an actual drop in TH protein even through it gets ubiquitinated in such a short amount of time.

Deubiquitinating enzymes, which remove ubiquitin, also can regulate the level of ubiquitinated proteins (Zhao *et al.* 2011). MAPKs can regulate deubiquitinating enzyme (Liang *et al.* 2011) suggesting that deubiquitinating enzymes might be activated by cytokine treatment. This could remove ubiquitin from TH and lead to slower protein degradation. Thus, cytokine-induced changes in deubiquitinating enzymes could explain why ubiquitinated TH was only elevated within 30 to 60 min when the ubiquitination process was initiated.

Another possibility is that degradation of the different pools of phosphorylated TH may cause the time delay in the detection of total TH protein loss. Phosphorylation at the N- terminus of TH triggers TH proteasomal degradation (Nakashima *et al.* 2011). Phosphorylation at different sites results in different effects. TH phosphorylation at Ser31is associated with an increase in TH activity (Moy and Tsai 2004), while TH phosphorylated at Ser40 residue is reported to be prone to protein degradation (Kawahata *et al.* 2009). Inhibiting proteasome activity causes the accumulation of TH phosphorylated at Ser40, but not TH phosphorylated at Ser31 (Kawahata *et al.* 2009). Therefore, phosphorylation at Ser40 might be a signal to target TH for ubiquitination and

degradation. Thus, the pool of TH phosphorylated at Ser40 may be ubiquitinated and degraded through ubiquitin proteasome system after cytokine stimulation, but not the pool of TH phosphorylated at Ser31. In my study, TH phosphorylation at Ser40 was significantly decreased with chronic cytokine treatment. This is consistent with the pool of Ser40 phosphorylated TH being degraded after four days of cytokine treatment (Chapter 3).

Degradation of TH at different locations within the neuron might also contribute to the delay in the loss of TH protein after cytokine treatment. Phosphorylation of TH at its N-terminus is thought to actively occur in the nerve terminals (Ugrumov *et al.* 2011). In a short time frame, TH phosphorylated at Ser40 by cytokines in the axon might be ubiquitinated and degraded, but not the large pool of unphosphorylated TH at the cell body.

4.2.2 Signaling pathways involved in TH ubiquitination

Clearly, ERK1/2 is required for cytokine-induced TH ubiquitination and degradation. Interestingly, inhibiting STAT3 activation with STAT3iV also increased ERK1/2 phosphorylation (Chapter 2). Testing the role of the Akt pathway was complicated by the fact that the PI3K inhibitor, LY294002 also blunted ERK1/2 phosphorylation (Appendices, Fig. A.1). Treatment with LY294002 decreased TH ubiquitination (Appendices, Fig. A.1), but it may be due to the off-target effects of inhibiting ERK1/2 phosphorylation. The STAT inhibitor, which strongly stimulated TH ubiquitination, also inhibited Akt phosphorylation.

Thus, two different drugs inhibit Akt phosphorylation: the STAT3 inhibitor which stimulated TH ubiquitination and the PI3K inhibitor which blocked TH ubiquitination. All of our data point to ERK1/2 as the key regulator of TH ubiquitination since the drugs inhibiting ERK activation decreased TH ubiquitination, while drugs enhancing ERK phosphorylation increased TH ubiquitination.

Jak/STAT3 is another major signaling pathway which is activated by cytokines. To identify the role of this pathway in TH degradation, I treated sympathetic neurons with STAT3iV which blocks STAT3 phosphorylation. Inhibiting cytokine-induced STAT3 activation increased TH ubiquitination, and enhanced cytokine activation of ERK1/2. Activation of STAT3 leads to expression of SOSC3 (Appendices, Fig. A.2), which serves as a negative feedback inhibitor of STAT3 signaling. SOCS3 competes with SHP2 for binding to tyrosine 757 in the gp130 cytokine receptor, and the competition for binding attenuates ERK signaling. Thus, inhibiting STAT3 activation prevents SOSC3 induction, increasing cytokine activation of ERK1/2 and subsequent ubiquitination of TH. However, the STAT3 inhibitor also increased TH ubiquitination independent of cytokines, suggesting a direct effect of the drug on TH ubiquitination.

Activation of ERK1/2 is required for TH ubiquitination and the associated protein degradation (Chapter 2). Inhibiting proteasome activity with MG-132 caused the accumulation of ubiquitinated TH without cytokine treatment,

suggesting that there is a basal TH turnover which is not related to cytokine treatment (Appendices, Fig. A.3). Cytokine treatment increased TH ubiquitination through an ERK1/2 dependent pathway (Chapter2). Interestingly, blocking ERK1/2 activation by U0126 did not affect the level of ubiquitinated TH or total ubiquitinated protein when proteasome activity was inhibited (Appendices, Fig. A.4).This suggests that the basal and stimulated TH turnover use different mechanisms and ERK1/2 is not required for basal TH turnover.

However, little is known about the mechanism of ERK1/2 regulating TH degradation. MAPKs can stimulate E3 ubiquitin ligase expression to regulate protein stability (Li *et al.* 2005;Yamashita *et al.* 2005), so activation of ERK1/2 by cytokines might phosphorylate E3 ubiquitin ligase which leads to increase TH ubiquitination. MAPKs also can regulate the expression of deubiquitinating enzymes (Liang *et al.* 2011). Targeting deubiquitinating enzyme might be another potential way to regulate the level of ubiquitinated TH.

4.2.3 Cytokines stimulate TH activity

Neuronal depletion of the gp130 cytokine receptor prevents the loss of TH in the peri-infarct left ventricle but did not restore NE levels (Parrish *et al.* 2010), suggesting other mechanisms may also contribute to decreased NE content in the nerve terminals. The NE content in the nerve terminal is regulated by synthesis, release and uptake. Studies in chapter 3 showed that cytokines stimulated TH activity in sympathetic neurons despite suppressing TH protein

levels. Furthermore, NE transporter activity is decreased and the NE release is increased in neuronal gp130 KO animals (Hasan *et al.* 2012;Parrish *et al.* 2010). Decreased TH activity coupled with increased NE release and impaired uptake all contribute to low NE levels in neuronal gp130 KO mice, despite restoration of normal TH enzyme levels.

Chronic cytokine treatment increased TH specific activity (Chapter 3). The mechanism is not entirely clear. Cytokines could affect TH activity by altering phosphorylation states. Data in chapter 3 showed CNTF increased the fraction of Ser31 phosphorylated TH while decreasing the fraction of Ser40 phosphorylated TH. Increased TH Ser31 phosphorylation is associated with an increase in TH activity (Dunkley *et al.* 2004;Kumer and Vrana 1996;Moy and Tsai 2004), which might be due to CNTF stimulated ERK1/2 activation, since ERK1/2 are the major kinases phosphorylating TH on Ser31(Dunkley *et al.* 2004). Increased Ser40 phosphorylation can also lead to increased TH activity by increasing the binding affinity for BH_4 (Daubner *et al.* 1992;McCulloch *et al.* 2001). However, BH_4 is at a saturating concentration in the activity assay and is not a limiting factor for the assay. Phosphorylated at Ser40 can target TH for proteasomal degradation, and may be involved in CNTF-stimulated TH degradation through the ubiquitin-proteasome system (Chapter 2). Therefore, the decrease in Ser40 phosphorylated TH after chronic treatment may be due to increased degradation of the pool of TH phosphorylated at Ser40 by cytokines. The mechanism of how cytokines affect TH activity needs additional investigation.

4.3 Medical implications

The studies presented in this thesis have important implications for pathologies including inflammation and neural dysfunction. Inflammation plays an important role in many chronic disorders that are associated with neural dysfunction such as cardiovascular diseases, Parkinson's disease (PD), diabetes and obesity. For example, cytokines are elevated in the heart after myocardial infarction (Aoyama *et al.* 2000;Frangogiannis *et al.* 2002;Gwechenberger *et al.* 1999;Kreusser *et al.* 2008). The elevated cytokines lead to local depletion of TH and NE content (Parrish *et al.* 2010). This results in heterogeneity of sympathetic transmission, which contributes to the development of arrhythmias and sudden cardiac death (Rubart and Zipes 2005). Sympathetic dysfunction also occurs in the diet-induced obesity and metabolic dysfunction, which involve inflammation (Elmarakby and Imig 2010;Grassi *et al.* 2010;Hotamisligil 2006;Morgan and Rahmouni 2010). Inflammatory cytokines including IL-6 are elevated in PD (Ciesielska *et al.* 2007), and my studies are particularly relevant to the pathology and treatment of PD.

TH plays an important role in PD since it is the rate-limiting enzyme in dopamine biosynthesis. PD is a movement disorder which is characterized as selective loss of dopaminergic neurons in the Substantia Nigra, and the elevation of inflammatory cytokines, including IL-6 (Ciesielska *et al.* 2007). Studies

revealed that dysfunction of the ubiquitin-proteasome system contributes to the degeneration of the dopaminergic neurons (McNaught *et al.* 2002;McNaught *et al.* 2006;McNaught *et al.* 2010). Thus, regulation of TH degradation might be an important piece in PD. In this thesis, I showed that inflammatory cytokines related to IL-6 can stimulate TH degradation through the ubiquitin-proteasome system. This suggests that inflammatory cytokines might down-regulate TH by the ubiquitin-proteasome pathway in PD, and that proteasome inhibitors may be a treatment strategy for Parkinson's disease (Lin *et al.* 2012).

Dysregulation of TH activity also contributes to decrease in dopamine production during PD. Accumulation of α-synuclein in lewy bodies, which is cytotoxic to dopaminergic neurons and can induce dopaminergic neuron apoptosis, is a hallmark of PD. α-synuclein can bind to TH and regulate TH activity by preventing its phosphorylation (Peng *et al.* 2005;Perez *et al.* 2002). TH content and activity are both decreased in PD. However, TH specific activity (activity/ enzyme protein) is increased in the striatum in both the MPTP (1-methyl-4-phenyl-1, 2, 3, 6-tetrahydropyridine) -induced PD model and in postmortem brains from PD patients (Khakimova *et al.* 2011;Nakashima *et al.* 2012). Inflammatory cytokines stimulate TH specific activity in cultured sympathetic neurons (Chapter 3) and this type of compensatory increase in enzyme activity by cytokines might play a role in PD.

4.4 Future directions and limitations

The studies in this thesis revealed the mechanism by which cytokines suppress TH in sympathetic neurons, providing a better understanding of how neurotransmission is regulated at sites of inflammation. However, several limitations exist. One limitation of the study in chapter 2 is the method used to detect the interaction of TH and ubiquitin. The interaction of TH and ubiquitin was detected by co-immunoprecipitation which probed for ubiquitin from immunoprecipitated endogenous TH. In contrast, TH was not detected after immunoprecipitating all ubiquitinated proteins from cultured sympathetic neurons. This might be due to the sensitivity of the method, since ubiquitinated TH might be a small fraction of the large pool of total ubiquitinated protein, and the quality of anti-ubiquitin antibody may not be sufficient. An alternative method could be used to confirm the interaction between these two proteins. This could be done by co-immunoprecipitating TH and ubiquitin in M17 neuroblastoma cells which over-express HA-tagged ubiquitin. Using this method, we could confirm the interaction of TH and ubiquitin. The other limitation is using pharmacological methods to study the role of signaling pathways involved in cytokine suppression of TH. These drugs may have off-target effects despite using concentrations that are specific to the designated targets. A genetic approach is a good alternative method that could be used to investigate the role of different signaling pathways in cytokine-induced TH degradation.

Several questions also remain unanswered. The action of STAT3 in TH ubiquitination and degradation remains unclear because the STAT inhibitor STATiV causes the accumulation of ubiquitinated TH independent of cytokine treatment. To determine the role of STAT3 in cytokine-induced changes in TH expression and regulation, conditional STAT3 knockout animals which do not have STAT3 expression in sympathetic neurons would be a good model. TH could be immunoprecipitated from cultured sympathetic neurons from wild-type or conditional STAT3 knockout animals in the presence or absence of cytokine treatment. I expect cytokine treatment will increase ERK1/2 activation and TH ubiquitination in neurons from STAT3 knockout animals compared to wild-type. If decreased ubiquitinated TH were detected in neurons from STAT3 knockout compared to wild-type animals, this suggests that STAT3 may play a role in TH ubiquitination as well.

SOCS3 is a potential mediator between the Jak/STAT and MEK/ERK pathway. Cytokines increase SOCS3 mRNA in cultured sympathetic neurons (Appendices, Fig. A.2). To directly test the role of SOCS3 in cross-talk between those two pathways and TH degradation, knocking down SOCS3 levels in cultured sympathetic neurons would be a useful strategy to investigate cross-talk. I expect cytokine treatment will increase ERK1/2 activation after knocking down SOCS3, which completes with SHP2 for docking sites on gp130, compared to control. Increased activation of ERK1/2 could result in increasing the level of ubiquitinated TH. Pretreated with U0126 should block this effect. Removing

SOCS3 will increase STAT3 level. To rule out the role of STAT3 in changes in TH ubiquitination, one could carry out an experiment to examine cytokine-stimulated TH ubiquitination in neurons from WT or STAT3 knockout animals with SOCS3 knock down.

Phosphorylated TH at Ser40 is prone to proteasomal degradation (Kawahata *et al.* 2009;Nakashima *et al.* 2011). Chronic cytokine treatment actually decreased the TH Ser40 levels despite cytokines increasing TH enzyme activity. To determine if the pool of Ser40 phosphorylated TH is degraded after cytokine treatment, the level of TH phosphorylated at Ser40 could be examined after blocking proteasome activity. I expect that cytokines cause the accumulation of Ser40 phosphorylated TH after blocking proteasome activity.

4.5 Conclusion

In conclusion, gp130 cytokines stimulate TH degradation through the ubiquitin-proteasome pathway. ERK1/2 is required for cytokine-induced TH degradation. Cytokines also increase TH activity. These finding indicate that cytokines can directly affect TH protein stability which may modulate neurotransmitter synthesis at site of inflammation. These have important implications in neurodegenerative diseases, where cytokines induce the loss of TH protein and increase the activity of the remaining enzyme.

Chapter 5 Methods

Detailed Methods

Animals

Pregnant adult Sprague-Dawley rats were obtained from Charles River. Wild-type C57BL/6J mice were obtained from Jackson Laboratories. The $gp130^{DBH\text{-}Cre/lox}$ mice were generated as described by Stanke et al. (Stanke *et al.* 2006). The $gp130^{DBH\text{-}Cre/lox}$ mice were genotyped upon arrival. Additional genotyping was performed on the first two litters from all breeding pairs. The primers and thermocyler protocol are list below.

gp130-flox: 5'-GGCTTTTCCTCTGGTTCTTG-3' (Forward primer)

5'-CAGGAACATTAGGCCAGATG-3' (Reverse primer)

Thermocycle	Time	
94°C	5min	
94°C	1min	
58°C	1min	40 cycles
72°C	2min	
72°C	5min	

DBH-CRE: 5’-GCGTCAGAGATTTGTTGGAGGAC-3’

5’-CACAGCATTGGAGTCAGAAGGG-3’

Thermocycle	Time	
95°C	3min	
95°C	45sec	
59°C	1min	35 cycles
72°C	1min	
72°C	10min	

All animals were housed individually with a 12 hr: 12 hr light dark cycle with *ad libitum* access to food and water. All procedures were approved by the Institutional Animal Care and Use Committee, and comply with the Guide for the Care and Use of Laboratory Animals published by the US National Institutes of Health (NIH publication No. 85-23, revised 1996).

Cell culture

1) Primary neuron culture: Superior cervical ganglia (SCG, Fig. 5.1) were dissected from newborn rats or mice (P0-P1). The SCG were digested with Hanks balanced salt solution (Invitrogen) containing 5 mg/mL dispase (Boehringer) and 1mg/mL collagenase (Worthington). The ganglia were digested

for 45 min (mice) or 75 min (rats) in an incubator at 37°C. After digestion, ganglia were triturated to disperse cells using a fire-polished glass pipette. Then neurons were washed with Dulbecco's modified Eagle's medium (DMEM) containing 10% serum 3 times and grown in C2 medium (DMEM/F12 1:1 (Gibco), 0.5 mg/mL BSA (Sigma), 1.4 mM L-glutamine (Gibco), 30 nM Selenium, 10 µg/mL Transferrin, and 10 µg/mL insulin (ITS-X 100X, Gibco)) supplemented with 100 U/mL Penicillin G (Gibco), 100 µg/mL streptomycin sulfate (Gibco), 50 ng/mL nerve growth factor (NGF, BD bioscience), and 3% fetal bovine serum (ATCC) (Li *et al.* 2003;Pellegrino *et al.* 2011). Sympathetic neurons were grown in 12, 24, or 96-well plates pre-coated with 100 µg/mL poly-L-lysine (Sigma) and 10 µg/mL collagen (BD bioscience). Cells were grown under sterile conditions in a humidified 5% CO_2 incubator at 37°C. Non-neuronal cells were eliminated by treating the cultures with the anti-mitotic agent cytosine arabinoside (Ara C, 1 µM, Sigma) for the first 2 days. Half of the culture medium was replaced every other day.

2) Neuroblastoma cell culture: SK-N-BE (2) M17 human neuroblastoma cells (M17 cells) were grown in DMEM (Gibco) supplemented with 100 U/mL Penicillin G (Gibco), 100 µg/mL streptomycin sulfate (Gibco) and 10% fetal bovine serum (ATCC). M17 cells were plated at 1 X 10^5 cells per well in 6-well plates. Cells were grown under sterile conditions in a humidified 5% CO_2 incubator at 37°C.

Cytokines and other reagents were diluted in culture medium before addition to the culture plates. Cells were treated with 100 ng/ml CNTF or LIF (Pepro Tech), 100 nM MG-132 (Calbiochem), 20 μM STAT3i V (STAT3 Inhibitor V, Calbiochem), 10 μM U0126 (Sigma), and 2 μM JAK (Janus tyrosine kinase) inhibitor (Calbiochem). The duration and timing of treatment is noted for each experiment. All conditions were assayed in triplicate and experiments repeated at least 3 times.

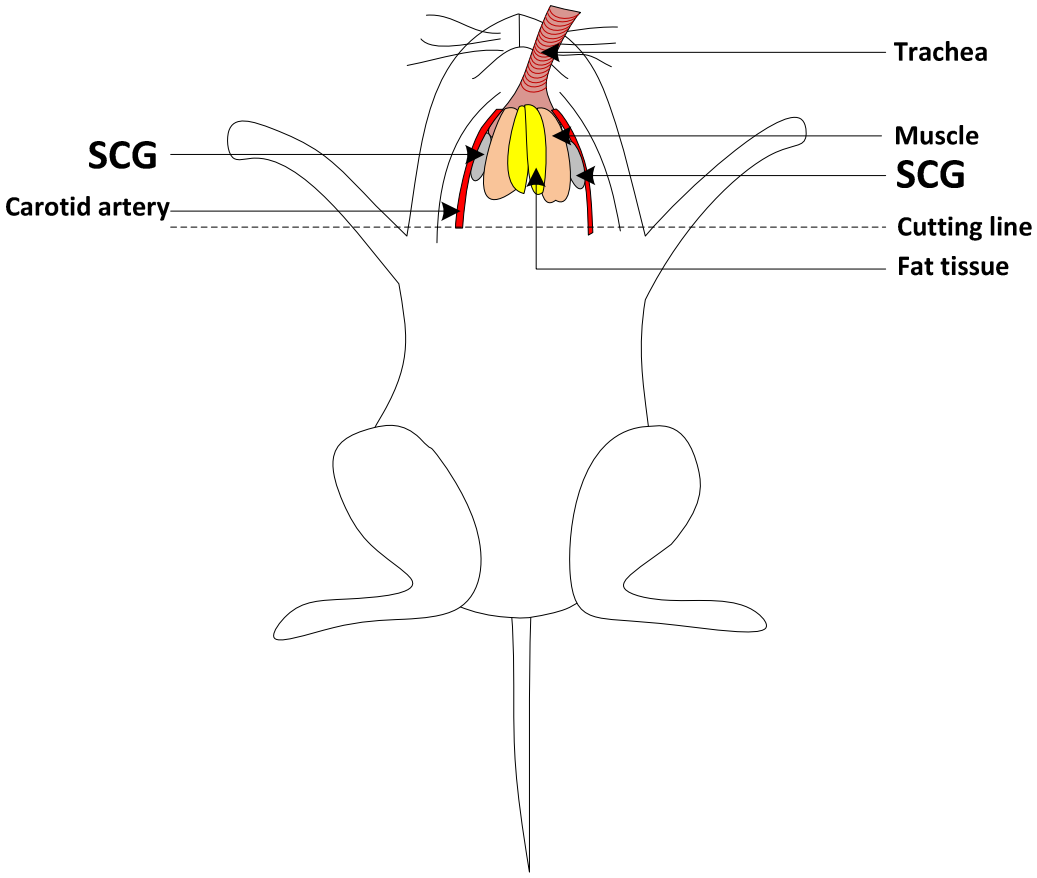

Figure 5.1 Schematic diagram showing location of SCGs in rodent (ventral side).

After anesthesia, rats or mice were decapitated right above the shoulder (cutting line). The rodent heads were pinned down on a dissection pad. The skin and muscles were cleaned away until the trachea was visible. The trachea was pulled

up using forceps. Doing this exposed a pair of muscles and fat running almost parallel to each other on both sides underneath the trachea. The ganglia were attached to the carotid arteries on both sides.

Immunoblot Analysis

Cells were washed with ice-cold PBS and lysed at 4°C in RIPA lysis buffer containing 1% Triton-X100, 1% sodium deoxycholate, 0.2% sodium dodecyl sulfate (SDS), 125 mM NaCl, 50 mM Tris pH 8.0, 10% glycerol, 25 mM β-glycerolphosphate, 1 mM EDTA, 25 mM NaF, protease inhibitor cocktail (Roche, 1 tablet / 50 mL lysis buffer) and 1 mM sodium orthvanadate. Protein concentration was quantified using the bicinchoninic acid (BCA) protein assay kit (Pierce). Lysates containing 20 µg of total protein were mixed with 5X SDS sample buffer (300 mM Tris-HCl, PH 6.8, 50% glycerol (v/v), 10% SDS (w/v), 10% β-Mercaptoethanol (v/v) and 0.02% Bromophenol Blue) and heated at 95˚C for 5 min. Lysates were fractionated on 4-12% SDS-polyacrylamide gels (Bio-rad) at 200V for 50-60 minutes. Then protein was transferred from the gels to nitrocellulose membranes (Schleicher & Schuell, Germany), which were pre-soaked in transfer buffer (40 mM glycine, 50 mM Tris-base, 0.04% SDS (w/v) and 20% methanol (v/v)), and transferred at 25V for 30 min by semi-dry transfer apparatus (Bio-rad). Blots were washed 3 times with TBST (100 mM NaCl, 10 mM Tris pH 7.4, 0.1% tween-20) and blocked in 5% non-fat dry milk in TBST at room temperature for 30 min. Membranes were subsequently incubated at 4°C overnight with primary antibodies diluted in 5% non-fat dry milk in TBST (Table 5.1). Blots were washed 3 times with TBST after incubation with primary antibodies. The immunoblots were then incubated with horseradish peroxidase (HRP) - conjugated secondary antibodies for 1 hour at room temperature in

TBST with 5% non-fat dry milk (goat anti-rabbit-HRP IgG, 1:10,000; Pierce Cat #: 32460), goat anti-mouse-HRP IgG (Santa Cruz, Cat #: sc-2005; 1:1,000 for the mouse anti-ubiquitin (Santa Cruz) antibody, 1:10,000 for the rest primary antibodies). Immune-complexes were visualized by chemiluminescence (Super Signal Dura, Pierce) and quantified using Labworks software (UVP, upland CA). TH protein is normalized to GAPDH protein.

To probe for a second protein as a loading control, blots were stripped for 30min in a 50˚C water bath in stripping buffer containing 62.5 mM Tris (pH 6.8), 2% SDS, and 0.7 %(v/v) β-mercaptoethanol. Blots were washed extensively in TBST and blocked with 5% non-fat dry milk in TBST at room temperature for 30 min. The blot was then incubated with primary antibody at 4˚C overnight. The rest of the procedure is as described above.

Table 5.1 Primary antibodies used in immunoblot and immunoprecipitation analysis

Antibody	Dilution	Company	Catalog #
Rabbit anti-TH IgG	1:5000	Millipore	AB-152
Rabbit anti-pTHser31 IgG	1:1000	Cell signaling	3370
Rabbit anti-pTHser40 IgG	1:1000	Cell signaling	2791
Mouse anti-ubiquitin IgG	1:500	Santa Cruz	Sc-8017
	1:1000	Cell signaling	3936
Mouse anti-GAPDH IgG	1:5000	Affinity BioReagent	MA1-16757
Rabbit anti-pERK1/2 IgG	1:1000	Cell signaling	9101L
Rabbit anti-total ERK1/2 IgG	1:1000	Cell signaling	9102L
Rabbit anti-pSTAT3 IgG (Phosph-Tyr705)	1:1000	Cell signaling	9131
Rabbit anti-total STAT3 IgG	1:1000	Cell signaling	9132
Rabbit anti-pAKT IgG (Phosph-Ser473)	1:1000	Cell signaling	9271
Rabbit anti-total AKT IgG	1:1000	Cell signaling	9271

Immunoprecipitation

Neurons were plated in 12-well plates with 10,000 cells per well. M17 cells were plated in 6-well plates with 1 X 10^5 cells per well. After treatment with or without CNTF or other inhibitors for 30 min, neurons or M17 neuroblastoma cells were washed with ice-cold PBS and lysed at 4°C in RIPA lysis buffer (150 µl/well in a 12-well plate). To get enough protein from primary cultured neurons, lysates from 3 wells were pooled together for each treatment condition. Protein concentration was quantified using the bicinchoninic acid protein assay kit (Pierce). Aliquots of cell lysates (150 µg total protein for M17 neuroblastoma cells, 30 µg total protein for neurons) were incubated with Protein G-Sepharose conjugated beads (Invitrogen) for 2 h at 4°C to eliminate non-specific binding. Pre-cleared cell lysates were incubated with a saturating amount of primary antibody (1.5 µg rabbit anti-TH (Millipore) per condition for both M17 cells and neurons) overnight at 4°C. 30 µl protein G beads slurry were added to each sample and incubated for 2 hr at 4°C. After incubation, samples were spun down briefly for 1 min at 4°C with 1.3 × 10^4g to collect beads. The beads were then washed with ice-cold PBS 5 times to remove non-specific binding. Proteins were released from immune-complexes by incubation with 50 µl 2×SDS sample buffer at 95° C for 5 min then analyzed by western bot.

Estimation of TH half-life

1) Pulse Chase: Neurons were cultured as described above, and 5 days after plating, metabolic labeling was carried out using an approach similar to that previously used to determine TH half-life (Franklin and Johnson 1998;Wu and Cepko 1994). Neurons were plated at 10,000 cells per well in a 12-well plate. Prior to labeling, neurons were incubated for 1 hr at 37° C in culture medium DMEM without L-methionine and L-cysteine (MP biomedicals) supplemented with 5% fetal bovine serum (ATCC). To label newly synthesized protein, 20 µCi/mL [^{35}S] methionine/cysteine (73% L-methionine, 22% L-cysteine, Perkin Elmer) was added for 1 hr. Cells were washed 3 times with PBS to remove unincorporated isotope, and chase medium (C2 medium with or without CNTF) with methionine supplemented to 150 mg/L was added to stop labeling. Cultures were lysed in RIPA lysis buffer with Triton-X100 at 0, 4, 8, 16, 24 hours later. TH was immunoprecipitated from samples as described above. The immune complexes were eluted with 50 µl 2×SDS sample buffer and then resolved by 10% SDS-PAGE gel electrophoresis. The gels were then soaked in fix buffer containing10% acetic acid and 20% isopropanol for 10-15 min and dried for 5 hours on a gel dryer. The dried gels were exposed on pre-clear phosphoimager plates for 2-7 days depending on intensity of the signal. Intensity of labeled TH was quantified using a Bio-Rad Phospho-imager system.

2) Protein synthesis inhibition: M17 neuroblastoma cells were plated at 1×10^5 cells per well in 6-well plates. Cells were treated with 20 µg/mL cycloheximide with or without 100 ng/mL CNTF or 0.1% ethanol vehicle. For inhibition of MEK/ERK signaling, M17 cells were pretreated with 0.1% DMSO or 10 µM U0126 for 30min, and then incubated with 20 µg/mL cycloheximide in the presence or absence of CNTF. 0.1 % DMSO and 0.1% ethanol were added as vehicle controls. Cells were lysed at 0, 8, 12, and 24 hours in 500 µl per well RIPA lysis buffer with protease inhibitor (Roche, 1 tablet / 50 mL lysis buffer) on ice. Protein concentration was quantified using the bicinchoninic acid protein assay kit (Pierce). 8 µg total proteins were assayed for TH content and GAPDH by western blot as described above. Intensity of TH and GAPDH bands was quantified using the UVP system. TH levels were plotted as the percentage of TH remaining, normalized to initial TH levels.

3) Half-life calculation: TH levels quantified from either the phosphor-imager system or UVP system were plotted on a natural log scale versus time. The data were fitted to a first-order decay function to estimate the degradation rate constant (k_d), which then was used to calculate a half-life ($t_{1/2}$). TH half-life was calculated from $t_{1/2}= \ln 2/ k_d$.

Transient Transfection and Reporter Assays

DNA used for transfection was purified using the Qiagen Maxiprep kit. M17 cells were plated at a density of 1.0 x 10^5 cells per well in 6-well plates and immediately treated with vehicle or 100ng/mL CNTF. 48 hours after plating, media was removed and cells were transfected using the $CaPO_4$ method (Dziennis and Habecker 2003). Cells were transfected with 1 µg of 4.5TH-fLuc and 100 ng pRL-null constructs as a control for transfection efficiency. After 4 hour incubation with DNA, cells were shocked with 15% glycerol in PBS. M17 cells were then washed 3 times with PBS, and placed back into culture media containing media alone or media with CNTF. Firefly luciferase activity from 4.5TH-fLuc and *Renilla* luciferase activity from the pRL-null internal control were assayed 48 hours after transfection using the Dual-Luciferase Reporter Assay system (Promega). Firefly luciferase values were normalized to *Renilla* luciferase values.

Real-Time PCR

Neurons were plated at 2,000 cells per well in 96-well plates. Cells were harvested using the Cells-to-cDNA II kit from Ambion. Cell lysates were treated with DNase and reverse transcribed (42 ° C for 1 hour followed by 95° C for 5 min to kill the enzyme). An RNA alone control or a water alone control were included to test for genomic DNA contamination. Real-time PCR was performed with the ABI TaqMan Universal PCR Master Mix in the ABI 7500, using ABI pre-

validated TaqMan gene expression assays for TH and GAPDH. For the PCR amplification, 2 µl of reverse transcription reactions were used in a total volume of 20 µl, and each sample was assayed in triplicate. Standard curves were generated with known amounts of rat SCG RNA ranging from 0.5 ng – 100 ng. TH mRNA was normalized to GAPDH mRNA in the same sample.

In vitro TH enzyme activity assay

Cultures of sympathetic neurons were plated at ~20,000 cells per well in 24-well plates. Neurons were homogenized in 150 µL homogenization buffer containing 5 mM Tris-acetate buffer (pH 6.0), 0.1% Triton X-100, protease inhibitor cocktail (Roche; 1 tablet/ 50 mL lysis buffer) and 1 mM sodium orthovanadate. TH enzyme activity was determined by measuring the initial rate of L-dihydroxyphenylalanine (L-DOPA) production from L-tyrosine under standardized conditions (Acheson *et al.* 1984). A 60 µL aliquot of the homogenate from each treatment group was combined with an equal volume of reaction buffer and assayed for TH activity under the following conditions: 120 mM Tris-acetate buffer (pH 6.0), 3 mM 6-methyl-5, 6, 7, 8-tetrahydropterin HCl (Sigma), 10 mM 2-mercaptoethanol (Sigma), catalase (200,000 U/mL, Sigma), 100 µM L-tyrosine (Sigma), and the internal standard, 1.0 µM dihydroxybezylamine (DHBA), to correct for sample recovery. The reaction mixtures were incubated at 37°C. Aliquots (20 µL) of the reaction mixture were removed at 4, 8, 12, and 16 minutes and added to 1 mL of a chilled solution containing 0.5 M Tris-acetate buffer (pH

8.0), 0.1 M EDTA and 15 mg alumina to stop the reaction. The L-DOPA and DHBA were purified by an alumina extraction procedure. The alumina was washed 3 times with mqH_2O and the catechols were eluted with 150 µl 0.1M perchloric acid. L-DOPA standards (0.2 µM) were processed similarly. The production of L-DOPA was measured by HPLC using electrochemical detection.

HPLC

L-DOPA and DA were measured by high-performance liquid chromatography (HPLC) with electrochemical detection. 70 µl of eluted sample was injected onto the HPLC and the catechols were fractionated by reverse- phase HPLC on a C18 column (5 µm, 4.5 mm × 1.5 cm) using a mobile phase that consisted of 75 mM $NaH_2PO_4 \cdot H_2O$, 1.7 mM sodium octane sulfonate, and 5% acetonitrile , pH 3.0. A coulometric electrochemical detector was used (Coulochem III, ESA) with an electrode voltage set at 180 mV, full scale 200 nA. The detection limits for L-DOPA were 0.01 pmol with recoveries from the alumina extraction > 60%.

Statistical analyses

Data are presented as mean values± SEM. Student's t test was used for a single comparison between two groups. One-way analysis of variance (ANOVA) with a Tukey's post hoc test was used to compare across treatment groups. The

statistics were carried out using GraphPad Prism 5 (GraphPad Software, Inc.). P values <0.05 were considered significant.

Chapter 6 Appendices

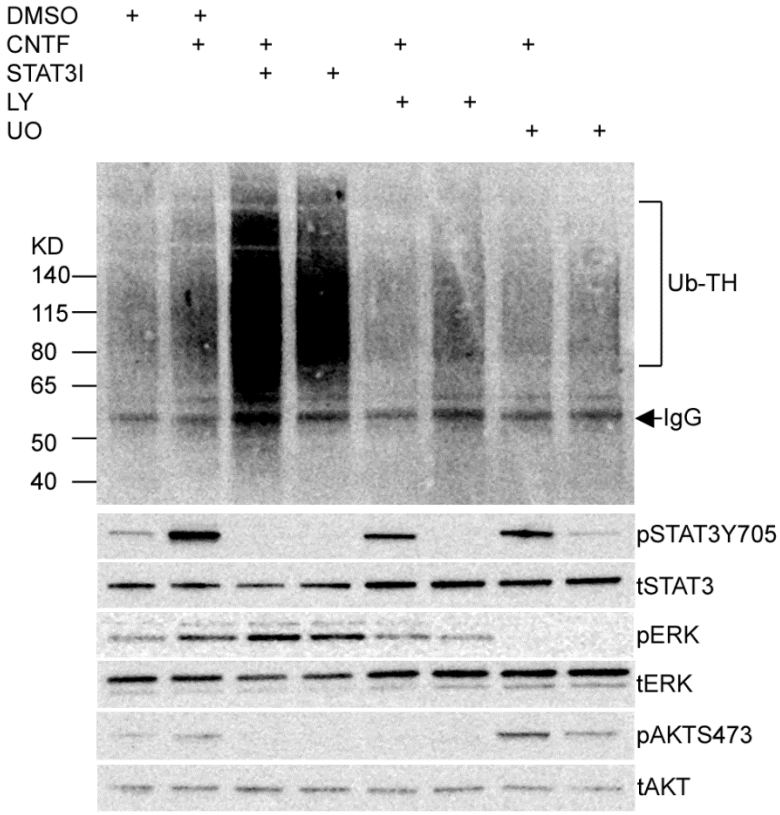

Figure A.1 CNTF stimulation of TH ubiquitination does not required AKT activation.

Cultured sympathetic neurons were treated with CNTF for 30 min, with or without 10 µM U0126 (U0) to prevent ERK1/2 phosphorylation, 20 µM STAT3 inhibitor (STAT3I) to block phosphorylation of STAT3, or 20 µM LY294002 to prevent phosphorylation of Akt. TH was immunoprecipitated and immunoblotted with

anti-ubiquitin antibody. CNTF stimulated phosphorylation of STAT3 (pSTAT3Y705), ERK1/2 (pERK), and Akt (pAktS473), and the actions of CNTF were blocked by the various antagonists. Total STAT3 (tSTAT3), ERK (tERK), and Akt (tAKT) levels were unchanged by CNTF or the other drug treatments. Inhibition of Akt phosphorylation by LY294002 inhibited the accumulation of Ub-TH, but the inhibition of Akt by STAT3I enhanced buildup of Ub-TH.

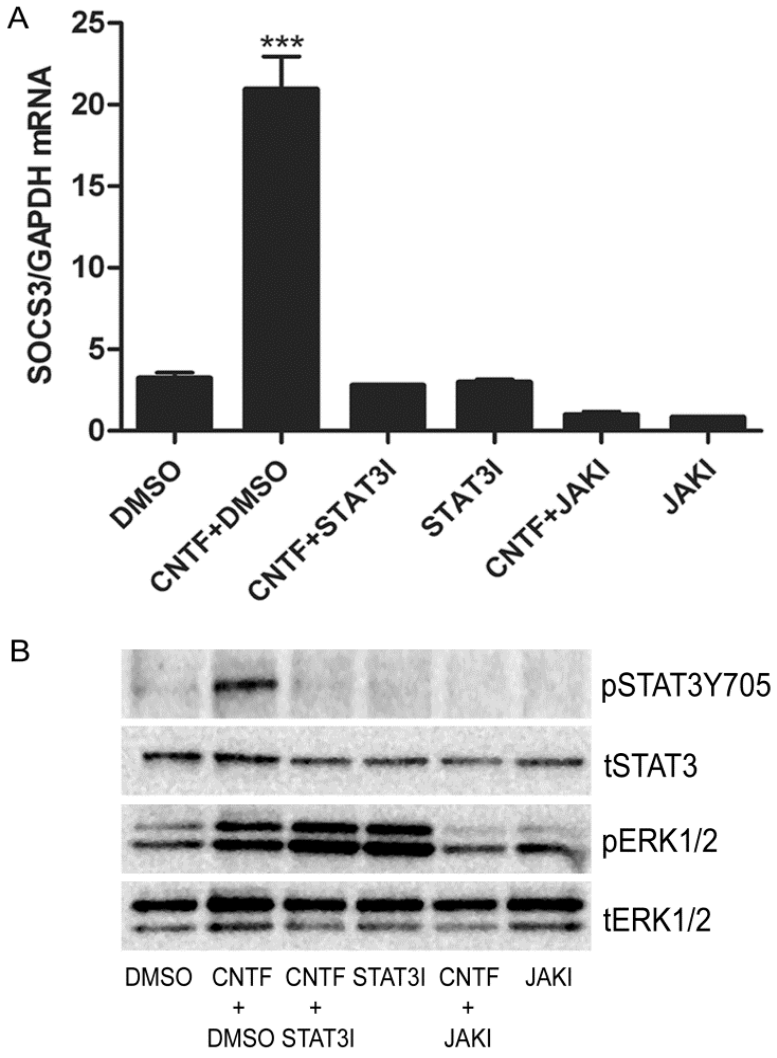

Figure A.2 Blocking STAT3 activation decreased SOCS3 mRNA and stimulated ERK phosphorylation in sympathetic neurons.

(A) Sympathetic neurons were stimulated with CNTF, with or without STAT3 inhibitor (STAT3I) or JAK inhibitor (JAKI) for 30 min. SOCS3 mRNA was

quantified by real-time PCR and normalized to GAPDH mRNA. Data are expressed as the mean ± SEM, n=3, *** $p<0.001$ compared with control. Data shown are representative of three independent experiments. **(B)** Sister cultures were treated as above, and phospho-ERK and STAT3 were assessed by western blot. CNTF stimulates phosphorylation of ERK and STAT3, and inhibition of STAT3 leads to increased ERK phosphorylation (pERK1/2) without changing total ERK (tERK1/2).

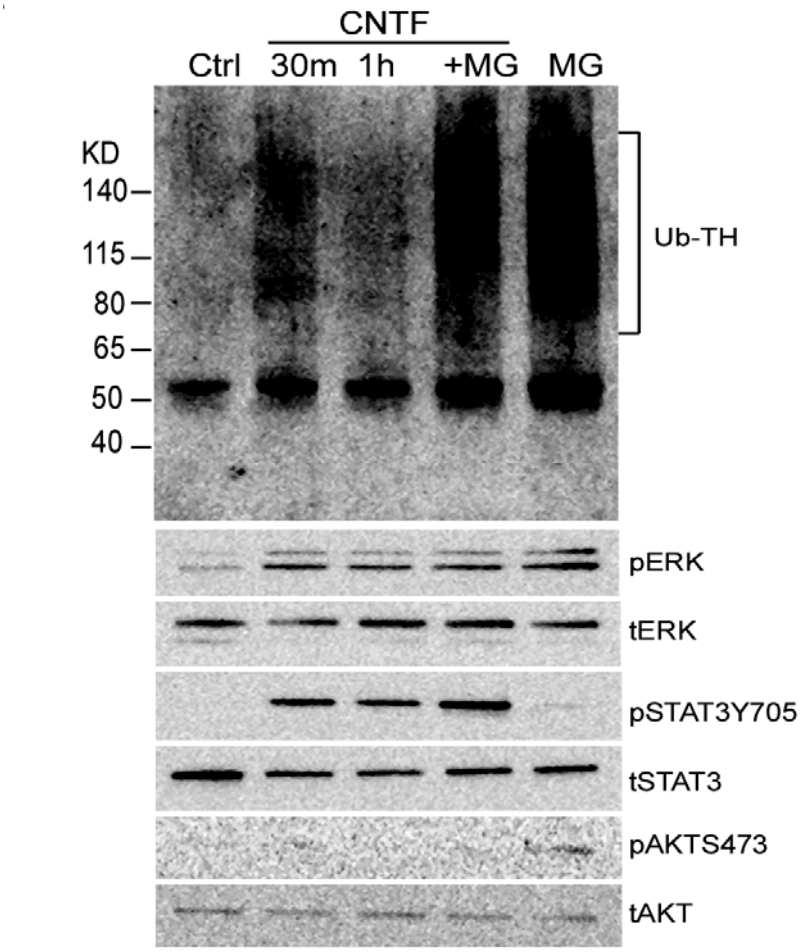

Figure A.3 Blocking proteasome activity caused the accumulation of ubquitinated TH.

Cultured sympathetic neurons were treated with 10 µM MG-132 for 1 hr with or without CNTF. Cells were also treated with CNTF as a positive control. TH was immunoprecipitated and immunoblotted with an anti-ubiquitin antibody. CNTF stimulated phosphorylation of STAT3 (pSTAT3Y705), ERK1/2 (pERK), and Akt

(pAktS473, minor extent). Total STAT3 (tSTAT3), ERK (tERK), and Akt (tAKT) levels were unchanged by CNTF or the other drug treatments.

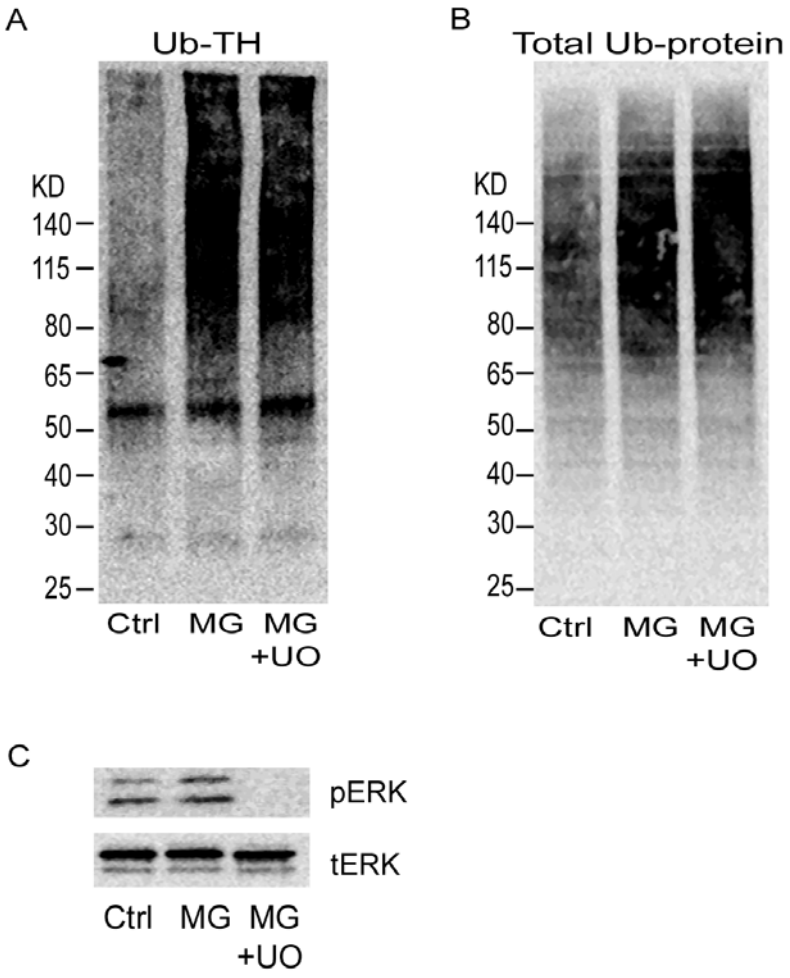

Figure A.4. ERK activation is not required for basal TH ubiquitination. Sympathetic neurons were stimulated with MG-132 (10 µM), with or without U0126 (10 µM) for 30 min. TH was immunoprecipitated out, and the TH fraction (A) and supernatant containing non-TH proteins (B) were blotted for ubiquitin. U0126 treatment blocked ERK1/2 phosphorylation (C) but did not affect the accumulation of Ub-TH (A) or total ubiquitinated proteins (B).

References

Acheson A. L., Naujoks K. and Thoenen H. (1984) Nerve growth factor-mediated enzyme induction in primary cultures of bovine adrenal chromaffin cells: specificity and level of regulation. *J. Neurosci.* **4,** 1771-1780.

Amerik A. Y. and Hochstrasser M. (2004) Mechanism and function of deubiquitinating enzymes. *Biochim. Biophys. Acta* **1695,** 189-207.

Aoyama T., Takimoto Y., Pennica D., Inoue R., Shinoda E., Hattori R., Yui Y. and Sasayama S. (2000) Augmented expression of cardiotrophin-1 and its receptor component, gp130, in both left and right ventricles after myocardial infarction in the rat. *J. Mol. Cell Cardiol.* **32,** 1821-1830.

Blum A. and Miller H. (1998) Role of cytokines in heart failure. *Am. Heart J.* **135,** 181-186.

Bobrovskaya L., Cheah T. B., Bunn S. J. and Dunkley P. R. (1998) Tyrosine hydroxylase in bovine adrenal chromaffin cells: angiotensin II-stimulated activity and phosphorylation of Ser19, Ser31, and Ser40. *J. Neurochem.* **70,** 2565-2573.

Bullock A. N., Debreczeni J. E., Edwards A. M., Sundstrom M. and Knapp S. (2006) Crystal structure of the SOCS2-elongin C-elongin B complex defines a

prototypical SOCS box ubiquitin ligase. *Proc. Natl. Acad. Sci. U. S. A* **103,** 7637-7642.

Chuang D., Zsilla G. and Costa E. (1975) Turnover rate of tyrosine hydroxylase during Trans-synaptic induction. *Mol. Pharmacol.* **11,** 784-794.

Ciechanover A. (2005) Proteolysis: from the lysosome to ubiquitin and the proteasome. *Nat. Rev. Mol. Cell Biol.* **6,** 79-87.

Ciechanover A., Orian A. and Schwartz A. L. (2000) The ubiquitin-mediated proteolytic pathway: mode of action and clinical implications. *J. Cell Biochem. Suppl* **34,** 40-51.

Ciesielska A., Joniec I., Kurkowska-Jastrzebska I., Przybylkowski A., Gromadzka G., Czlonkowska A. and Czlonkowski A. (2007) Influence of age and gender on cytokine expression in a murine model of Parkinson's disease. *Neuroimmunomodulation.* **14,** 255-265.

Daubner S. C., Lauriano C., Haycock J. W. and Fitzpatrick P. F. (1992) Site-directed mutagenesis of serine 40 of rat tyrosine hydroxylase. Effects of dopamine and cAMP-dependent phosphorylation on enzyme activity. *J. Biol. Chem.* **267,** 12639-12646.

Daubner S. C., Le T. and Wang S. (2011) Tyrosine hydroxylase and regulation of dopamine synthesis. *Arch. Biochem. Biophys.* **508,** 1-12.

Doskeland A. P. and Flatmark T. (2002) Ubiquitination of soluble and membrane-bound tyrosine hydroxylase and degradation of the soluble form. *Eur. J. Biochem.* **269,** 1561-1569.

Dunkley P. R., Bobrovskaya L., Graham M. E., von Nagy-Felsobuki E. I. and Dickson P. W. (2004) Tyrosine hydroxylase phosphorylation: regulation and consequences. *J. Neurochem.* **91,** 1025-1043.

Dziennis S. and Habecker B. A. (2003) Cytokine suppression of dopamine-beta-hydroxylase by extracellular signal-regulated kinase-dependent and -independent pathways. *J. Biol. Chem.* **278,** 15897-15904.

Elmarakby A. A. and Imig J. D. (2010) Obesity is the major contributor to vascular dysfunction and inflammation in high-fat diet hypertensive rats. *Clin. Sci. (Lond)* **118,** 291-301.

Fann M. J. and Patterson P. H. (1993) A novel approach to screen for cytokine effects on neuronal gene expression. *J. Neurochem.* **61,** 1349-1355.

Fernandez E. and Craviso G. L. (1999) Protein synthesis blockade differentially affects the degradation of constitutive and nicotinic receptor-induced tyrosine hydroxylase protein level in isolated bovine chromaffin cells. *J. Neurochem.* **73,** 169-178.

Fischer P. and Hilfiker-Kleiner D. (2008) Role of gp130-mediated signalling pathways in the heart and its impact on potential therapeutic aspects. *Br. J. Pharmacol.* **153 Suppl 1,** S414-S427.

Fossom L. H., Sterling C. R. and Tank A. W. (1992) Regulation of tyrosine hydroxylase gene transcription rate and tyrosine hydroxylase mRNA stability by cyclic AMP and glucocorticoid. *Mol. Pharmacol.* **42,** 898-908.

Frangogiannis N. G., Smith C. W. and Entman M. L. (2002) The inflammatory response in myocardial infarction. *Cardiovasc. Res.* **53,** 31-47.

Franklin J. L. and Johnson E. M. (1998) Control of neuronal size homeostasis by trophic factor-mediated coupling of protein degradation to protein synthesis. *J. Cell Biol.* **142,** 1313-1324.

Furshpan E. J., MacLeish P. R., O'Lague P. H. and Potter D. D. (1976) Chemical transmission between rat sympathetic neurons and cardiac myocytes developing in microcultures: evidence for cholinergic, adrenergic, and dual-function neurons. *Proc. Natl. Acad. Sci. U. S. A* **73,** 4225-4229.

Grassi G., Seravalle G. and Dell'oro R. (2010) Sympathetic activation in obesity: a noninnocent bystander. *Hypertension* **56,** 338-340.

Gwechenberger M., Mendoza L. H., Youker K. A., Frangogiannis N. G., Smith C. W., Michael L. H. and Entman M. L. (1999) Cardiac myocytes produce

interleukin-6 in culture and in viable border zone of reperfused infarctions. *Circulation* **99,** 546-551.

Habecker B. A., Sachs H. H., Rohrer H. and Zigmond R. E. (2009) The dependence on gp130 cytokines of axotomy induced neuropeptide expression in adult sympathetic neurons. *Dev. Neurobiol.* **69,** 392-400.

Haglund K., Sigismund S., Polo S., Szymkiewicz I., Di Fiore P. P. and Dikic I. (2003) Multiple monoubiquitination of RTKs is sufficient for their endocytosis and degradation. *Nat. Cell Biol.* **5,** 461-466.

Hasan W., Woodward W. R. and Habecker B. A. (2012) Altered atrial neurotransmitter release in transgenic p75(-/-) and gp130 KO mice. *Neurosci. Lett.* **529,** 55-59.

Haycock J. W. (2002) Species differences in the expression of multiple tyrosine hydroxylase protein isoforms. *J. Neurochem.* **81,** 947-953.

Heinrich P. C., Behrmann I., Haan S., Hermanns H. M., Muller-Newen G. and Schaper F. (2003) Principles of interleukin (IL)-6-type cytokine signalling and its regulation. *Biochem. J.* **374,** 1-20.

Heinrich P. C., Behrmann I., Muller-Newen G., Schaper F. and Graeve L. (1998) Interleukin-6-type cytokine signalling through the gp130/Jak/STAT pathway. *Biochem. J.* **334 (Pt 2),** 297-314.

Hotamisligil G. S. (2006) Inflammation and metabolic disorders. *Nature* **444,** 860-867.

Iacovitti L., Joh T. H., Park D. H. and Bunge R. P. (1981) Dual expression of neurotransmitter synthesis in cultured autonomic neurons. *J. Neurosci.* **1,** 685-690.

Jho D. H., Engelhard H. H., Gandhi R., Chao J., Babcock T., Ong E. and Espat N. J. (2004) Ciliary neurotrophic factor upregulates ubiquitin-proteasome components in a rat model of neuronal injury. *Cytokine* **27,** 142-151.

Kamura T., Sato S., Haque D., Liu L., Kaelin W. G., Jr., Conaway R. C. and Conaway J. W. (1998) The Elongin BC complex interacts with the conserved SOCS-box motif present in members of the SOCS, ras, WD-40 repeat, and ankyrin repeat families. *Genes Dev.* **12,** 3872-3881.

Kanazawa H., Ieda M., Kimura K., Arai T., Kawaguchi-Manabe H., Matsuhashi T., Endo J., Sano M., Kawakami T., Kimura T., Monkawa T., Hayashi M., Iwanami A., Okano H., Okada Y., Ishibashi-Ueda H., Ogawa S. and Fukuda K. (2010) Heart failure causes cholinergic transdifferentiation of cardiac sympathetic nerves via gp130-signaling cytokines in rodents. *J. Clin. Invest* **120,** 408-421.

Kawahata I., Tokuoka H., Parvez H. and Ichinose H. (2009) Accumulation of phosphorylated tyrosine hydroxylase into insoluble protein aggregates by

inhibition of an ubiquitin-proteasome system in PC12D cells. *J. Neural Transm.* **116,** 1571-1578.

Khakimova G. R., Kozina E. A., Sapronova A. Y. and Ugrumov M. V. (2011) Dopamine synthesis in the nigrostriatal system at the presymptomatic and early symptomatic stages in parkinsonian mice. *Dokl. Biol. Sci.* **440,** 284-286.

Kreusser M. M., Buss S. J., Krebs J., Kinscherf R., Metz J., Katus H. A., Haass M. and Backs J. (2008) Differential expression of cardiac neurotrophic factors and sympathetic nerve ending abnormalities within the failing heart. *J. Mol. Cell Cardiol.* **44,** 380-387.

Kumer S. C. and Vrana K. E. (1996) Intricate regulation of tyrosine hydroxylase activity and gene expression. *J. Neurochem.* **67,** 443-462.

Landis S. C. (1983) Development of cholinergic sympathetic neurons: evidence for transmitter plasticity in vivo. *Fed. Proc.* **42,** 1633-1638.

Landis S. C. (1996) The development of cholinergic sympathetic neurons: a role for neuropoietic cytokines? *Perspect. Dev. Neurobiol.* **4,** 53-63.

Landis S. C. and Keefe D. (1983) Evidence for neurotransmitter plasticity in vivo: developmental changes in properties of cholinergic sympathetic neurons. *Dev. Biol.* **98,** 349-372.

Lehmann I. T., Bobrovskaya L., Gordon S. L., Dunkley P. R. and Dickson P. W. (2006) Differential regulation of the human tyrosine hydroxylase isoforms via hierarchical phosphorylation. *J. Biol. Chem.* **281,** 17644-17651.

Lehmann U., Schmitz J., Weissenbach M., Sobota R. M., Hortner M., Friederichs K., Behrmann I., Tsiaris W., Sasaki A., Schneider-Mergener J., Yoshimura A., Neel B. G., Heinrich P. C. and Schaper F. (2003) SHP2 and SOCS3 contribute to Tyr-759-dependent attenuation of interleukin-6 signaling through gp130. *J. Biol. Chem.* **278,** 661-671.

Lewis S. E., Rao M. S., Symes A. J., Dauer W. T., Fink J. S., Landis S. C. and Hyman S. E. (1994) Coordinate regulation of choline acetyltransferase, tyrosine hydroxylase, and neuropeptide mRNAs by ciliary neurotrophic factor and leukemia inhibitory factor in cultured sympathetic neurons. *J. Neurochem.* **63,** 429-438.

Lewis-Tuffin L. J., Quinn P. G. and Chikaraishi D. M. (2004) Tyrosine hydroxylase transcription depends primarily on cAMP response element activity, regardless of the type of inducing stimulus. *Mol. Cell Neurosci.* **25,** 536-547.

Li W., Knowlton D., Van Winkle D. M. and Habecker B. A. (2004) Infarction alters both the distribution and noradrenergic properties of cardiac sympathetic neurons. *Am. J. Physiol Heart Circ. Physiol* **286,** H2229-H2236.

Li W., Knowlton D., Woodward W. R. and Habecker B. A. (2003) Regulation of noradrenergic function by inflammatory cytokines and depolarization. *J. Neurochem.* **86,** 774-783.

Li Y. P., Chen Y., John J., Moylan J., Jin B., Mann D. L. and Reid M. B. (2005) TNF-alpha acts via p38 MAPK to stimulate expression of the ubiquitin ligase atrogin1/MAFbx in skeletal muscle. *FASEB J.* **19,** 362-370.

Liang G., Ahlqvist K., Pannem R., Posern G. and Massoumi R. (2011) Serum response factor controls CYLD expression via MAPK signaling pathway. *PLoS. One.* **6,** e19613.

Lin X., Parisiadou L., Sgobio C., Liu G., Yu J., Sun L., Shim H., Gu X. L., Luo J., Long C. X., Ding J., Mateo Y., Sullivan P. H., Wu L. G., Goldstein D. S., Lovinger D. and Cai H. (2012) Conditional expression of Parkinson's disease-related mutant alpha-synuclein in the midbrain dopaminergic neurons causes progressive neurodegeneration and degradation of transcription factor nuclear receptor related 1. *J. Neurosci.* **32,** 9248-9264.

Lopez Verrilli M. A., Pirola C. J., Pascual M. M., Dominici F. P., Turyn D. and Gironacci M. M. (2009) Angiotensin-(1-7) through AT receptors mediates tyrosine hydroxylase degradation via the ubiquitin-proteasome pathway. *J. Neurochem.* **109,** 326-335.

McCulloch R. I., Daubner S. C. and Fitzpatrick P. F. (2001) Effects of substitution at serine 40 of tyrosine hydroxylase on catecholamine binding. *Biochemistry* **40,** 7273-7278.

McNaught K. S., Jackson T., JnoBaptiste R., Kapustin A. and Olanow C. W. (2006) Proteasomal dysfunction in sporadic Parkinson's disease. *Neurology* **66,** S37-S49.

McNaught K. S., JnoBaptiste R., Jackson T. and Jengelley T. A. (2010) The pattern of neuronal loss and survival may reflect differential expression of proteasome activators in Parkinson's disease. *Synapse* **64,** 241-250.

McNaught K. S., Mytilineou C., JnoBaptiste R., Yabut J., Shashidharan P., Jennert P. and Olanow C. W. (2002) Impairment of the ubiquitin-proteasome system causes dopaminergic cell death and inclusion body formation in ventral mesencephalic cultures. *J. Neurochem.* **81,** 301-306.

Mockus S. M., Kumer S. C. and Vrana K. E. (1997) A chimeric tyrosine/tryptophan hydroxylase. The tyrosine hydroxylase regulatory domain serves to stabilize enzyme activity. *J. Mol. Neurosci.* **9,** 35-48.

Morgan D. A. and Rahmouni K. (2010) Differential effects of insulin on sympathetic nerve activity in agouti obese mice. *J. Hypertens.* **28,** 1913-1919.

Moy L. Y. and Tsai L. H. (2004) Cyclin-dependent kinase 5 phosphorylates serine 31 of tyrosine hydroxylase and regulates its stability. *J. Biol. Chem.* **279,** 54487-54493.

Mueller R. A., Thoenen H. and Axelrod J. (1969) Inhibition of trans-synaptically increased tyrosine hydroxylase activity by cycloheximide and actinomycin D. *Mol. Pharmacol.* **5,** 463-469.

Muller F. and Rohrer H. (2002) Molecular control of ciliary neuron development: BMPs and downstream transcriptional control in the parasympathetic lineage. *Development* **129,** 5707-5717.

Myung J., Kim K. B. and Crews C. M. (2001) The ubiquitin-proteasome pathway and proteasome inhibitors. *Med. Res. Rev.* **21,** 245-273.

Nagamoto-Combs K., Piech K. M., Best J. A., Sun B. and Tank A. W. (1997) Tyrosine hydroxylase gene promoter activity is regulated by both cyclic AMP-responsive element and AP1 sites following calcium influx. Evidence for cyclic amp-responsive element binding protein-independent regulation. *J. Biol. Chem.* **272,** 6051-6058.

Nagatsu T. and Ichinose H. (1991) Comparative studies on the structure of human tyrosine hydroxylase with those of the enzyme of various mammals. *Comp Biochem. Physiol C.* **98,** 203-210.

Nakashima A., Mori K., Kaneko Y. S., Hayashi N., Nagatsu T. and Ota A. (2011) Phosphorylation of the N-terminal portion of tyrosine hydroxylase triggers proteasomal digestion of the enzyme. *Biochem. Biophys. Res. Commun.* **407,** 343-347.

Nakashima A., Ota A., Kaneko Y. S., Mori K., Nagasaki H. and Nagatsu T. (2012) A possible pathophysiological role of tyrosine hydroxylase in Parkinson's disease suggested by postmortem brain biochemistry: a contribution for the special 70th birthday symposium in honor of Prof. Peter Riederer. *J. Neural Transm.*

Nawa H., Nakanishi S. and Patterson P. H. (1991) Recombinant cholinergic differentiation factor (leukemia inhibitory factor) regulates sympathetic neuron phenotype by alterations in the size and amounts of neuropeptide mRNAs. *J. Neurochem.* **56,** 2147-2150.

Niu H., Ye B. H. and la-Favera R. (1998) Antigen receptor signaling induces MAP kinase-mediated phosphorylation and degradation of the BCL-6 transcription factor. *Genes Dev.* **12,** 1953-1961.

Ohtani T., Ishihara K., Atsumi T., Nishida K., Kaneko Y., Miyata T., Itoh S., Narimatsu M., Maeda H., Fukada T., Itoh M., Okano H., Hibi M. and Hirano T. (2000) Dissection of signaling cascades through gp130 in vivo: reciprocal roles for S. *Immunity.* **12,** 95-105.

Oshikawa T., Kuroiwa H., Yano R., Yokoyama H., Kadoguchi N., Kato H. and Araki T. (2009) Systemic administration of proteasome inhibitor protects against MPTP neurotoxicity in mice. *Cell Mol. Neurobiol.* **29,** 769-777.

Ozawa Y., Nakao K., Kurihara T., Shimazaki T., Shimmura S., Ishida S., Yoshimura A., Tsubota K. and Okano H. (2008) Roles of STAT3/SOCS3 pathway in regulating the visual function and ubiquitin-proteasome-dependent degradation of rhodopsin during retinal inflammation. *J. Biol. Chem.* **283,** 24561-24570.

Palmer D. C. and Restifo N. P. (2009) Suppressors of cytokine signaling (SOCS) in T cell differentiation, maturation, and function. *Trends Immunol.* **30,** 592-602.

Parrish D. C., Alston E. N., Rohrer H., Hermes S. M., Aicher S. A., Nkadi P., Woodward W. R., Stubbusch J., Gardner R. T. and Habecker B. A. (2009) Absence of gp130 in dopamine beta-hydroxylase-expressing neurons leads to autonomic imbalance and increased reperfusion arrhythmias. *Am. J. Physiol Heart Circ. Physiol* **297,** H960-H967.

Parrish D. C., Alston E. N., Rohrer H., Nkadi P., Woodward W. R., Schutz G. and Habecker B. A. (2010) Infarction-induced cytokines cause local depletion of tyrosine hydroxylase in cardiac sympathetic nerves. *Exp. Physiol* **95,** 304-314.

Parrish D. C., Gritman K., Van Winkle D. M., Woodward W. R., Bader M. and Habecker B. A. (2008) Postinfarct sympathetic hyperactivity differentially

stimulates expression of tyrosine hydroxylase and norepinephrine transporter. *Am. J. Physiol Heart Circ. Physiol* **294,** H99-H106.

Patterson P. H. and Chun L. L. (1977) The induction of acetylcholine synthesis in primary cultures of dissociated rat sympathetic neurons. I. Effects of conditioned medium. *Dev. Biol.* **56,** 263-280.

Pellegrino M. J., Parrish D. C., Zigmond R. E. and Habecker B. A. (2011) Cytokines inhibit norepinephrine transporter expression by decreasing Hand2. *Mol. Cell Neurosci.* **46,** 671-680.

Peng X., Tehranian R., Dietrich P., Stefanis L. and Perez R. G. (2005) Alpha-synuclein activation of protein phosphatase 2A reduces tyrosine hydroxylase phosphorylation in dopaminergic cells. *J. Cell Sci.* **118,** 3523-3530.

Perez R. G., Waymire J. C., Lin E., Liu J. J., Guo F. and Zigmond M. J. (2002) A role for alpha-synuclein in the regulation of dopamine biosynthesis. *J. Neurosci.* **22,** 3090-3099.

Piech-Dumas K. M. and Tank A. W. (1999) CREB mediates the cAMP-responsiveness of the tyrosine hydroxylase gene: use of an antisense RNA strategy to produce CREB-deficient PC12 cell lines. *Brain Res. Mol. Brain Res.* **70,** 219-230.

Powell S. R. (2006) The ubiquitin-proteasome system in cardiac physiology and pathology. *Am. J. Physiol Heart Circ. Physiol* **291,** H1-H19.

Rao M. S., Sun Y., Escary J. L., Perreau J., Tresser S., Patterson P. H., Zigmond R. E., Brulet P. and Landis S. C. (1993) Leukemia inhibitory factor mediates an injury response but not a target-directed developmental transmitter switch in sympathetic neurons. *Neuron* **11,** 1175-1185.

Rubart M. and Zipes D. P. (2005) Mechanisms of sudden cardiac death. *J. Clin. Invest* **115,** 2305-2315.

Saadat S., Sendtner M. and Rohrer H. (1989) Ciliary neurotrophic factor induces cholinergic differentiation of rat sympathetic neurons in culture. *J. Cell Biol.* **108,** 1807-1816.

Salvatore M. F., Waymire J. C. and Haycock J. W. (2001) Depolarization-stimulated catecholamine biosynthesis: involvement of protein kinases and tyrosine hydroxylase phosphorylation sites in situ. *J. Neurochem.* **79,** 349-360.

Sarkar A. A. and Howard M. J. (2006) Perspectives on integration of cell extrinsic and cell intrinsic pathways of signaling required for differentiation of noradrenergic sympathetic ganglion neurons. *Auton. Neurosci.* **126-127,** 225-231.

Schotzinger R. J. and Landis S. C. (1988) Cholinergic phenotype developed by noradrenergic sympathetic neurons after innervation of a novel cholinergic target in vivo. *Nature* **335,** 637-639.

Shi X. and Habecker B. A. (2012) gp130 cytokines stimulate proteasomal degradation of tyrosine hydroxylase via extracellular signal regulated kinases 1 and 2. *J. Neurochem.* **120,** 239-247.

Stanke M., Duong C. V., Pape M., Geissen M., Burbach G., Deller T., Gascan H., Otto C., Parlato R., Schutz G. and Rohrer H. (2006) Target-dependent specification of the neurotransmitter phenotype: cholinergic differentiation of sympathetic neurons is mediated in vivo by gp 130 signaling. *Development* **133,** 141-150.

Sun Y., Landis S. C. and Zigmond R. E. (1996) Signals triggering the induction of leukemia inhibitory factor in sympathetic superior cervical ganglia and their nerve trunks after axonal injury. *Mol. Cell Neurosci.* **7,** 152-163.

Sutherland C., Alterio J., Campbell D. G., Le B. B., Mallet J., Haavik J. and Cohen P. (1993) Phosphorylation and activation of human tyrosine hydroxylase in vitro by mitogen-activated protein (MAP) kinase and MAP-kinase-activated kinases 1 and 2. *Eur. J. Biochem.* **217,** 715-722.

Swerts J. P., Le Van T. A., Vigny A. and Weber M. J. (1983) Regulation of enzymes responsible for neurotransmitter synthesis and degradation in cultured rat sympathetic neurons. I. Effects of muscle-conditioned medium. *Dev. Biol.* **100,** 1-11.

Tan J. M., Wong E. S., Kirkpatrick D. S., Pletnikova O., Ko H. S., Tay S. P., Ho M. W., Troncoso J., Gygi S. P., Lee M. K., Dawson V. L., Dawson T. M. and Lim K. L. (2008) Lysine 63-linked ubiquitination promotes the formation and autophagic clearance of protein inclusions associated with neurodegenerative diseases. *Hum. Mol. Genet.* **17,** 431-439.

Tank A. W., Ham L. and Curella P. (1986) Induction of tyrosine hydroxylase by cyclic AMP and glucocorticoids in a rat pheochromocytoma cell line: effect of the inducing agents alone or in combination on the enzyme levels and rate of synthesis of tyrosine hydroxylase. *Mol. Pharmacol.* **30,** 486-496.

Ugrumov M. V., Khaindrava V. G., Kozina E. A., Kucheryanu V. G., Bocharov E. V., Kryzhanovsky G. N., Kudrin V. S., Narkevich V. B., Klodt P. M., Rayevsky K. S. and Pronina T. S. (2011) Modeling of presymptomatic and symptomatic stages of parkinsonism in mice. *Neuroscience* **181,** 175-188.

Wen R., Li J., Xu X., Cui Z. and Xiao W. (2012) Zebrafish Mms2 promotes K63-linked polyubiquitination and is involved in p53-mediated DNA-damage response. *DNA Repair (Amst)* **11,** 157-166.

Wolinsky E. and Patterson P. H. (1983) Tyrosine hydroxylase activity decreases with induction of cholinergic properties in cultured sympathetic neurons. *J. Neurosci.* **3,** 1495-1500.

Wu D. K. and Cepko C. L. (1994) The stability of endogenous tyrosine hydroxylase protein in PC-12 cells differs from that expressed in mouse fibroblasts by gene transfer. *J. Neurochem.* **62,** 863-872.

Yamamori T., Fukada K., Aebersold R., Korsching S., Fann M. J. and Patterson P. H. (1989) The cholinergic neuronal differentiation factor from heart cells is identical to leukemia inhibitory factor. *Science* **246,** 1412-1416.

Yamashita M., Shinnakasu R., Asou H., Kimura M., Hasegawa A., Hashimoto K., Hatano N., Ogata M. and Nakayama T. (2005) Ras-ERK MAPK cascade regulates GATA3 stability and Th2 differentiation through ubiquitin-proteasome pathway. *J. Biol. Chem.* **280,** 29409-29419.

Yu C., Kastin A. J., Tu H. and Pan W. (2007) Opposing effects of proteasomes and lysosomes on LIFR: modulation by TNF. *J. Mol. Neurosci.* **32,** 80-89.

Zhang J. G., Metcalf D., Rakar S., Asimakis M., Greenhalgh C. J., Willson T. A., Starr R., Nicholson S. E., Carter W., Alexander W. S., Hilton D. J. and Nicola N. A. (2001) The SOCS box of suppressor of cytokine signaling-1 is important for inhibition of cytokine action in vivo. *Proc. Natl. Acad. Sci. U. S. A* **98,** 13261-13265.

Zhao X., Fiske B., Kawakami A., Li J. and Fisher D. E. (2011) Regulation of MITF stability by the USP13 deubiquitinase. *Nat. Commun.* **2,** 414.

Zigmond R. E. (1980) The long-term regulation of ganglionic tyrosine hydroxylase by preganglionic nerve activity. *Fed. Proc.* **39,** 3003-3008.

Zigmond R. E. (1988) A comparison of the long-term and short-term regulations of tyrosine hydroxylase activity. *J. Physiol (Paris)* **83,** 267-271.

Zigmond R. E., Hyatt-Sachs H., Mohney R. P., Schreiber R. C., Shadiack A. M., Sun Y. and Vaccariello S. A. (1996) Changes in neuropeptide phenotype after axotomy of adult peripheral neurons and the role of leukemia inhibitory factor. *Perspect. Dev. Neurobiol.* **4,** 75-90.

Zigmond R. E., Schwarzschild M. A. and Rittenhouse A. R. (1989) Acute regulation of tyrosine hydroxylase by nerve activity and by neurotransmitters via phosphorylation. *Annu. Rev. Neurosci.* **12,** 415-461.